Evaluation of Expression Systems of Recombinant Human Interferon Gamma

Thesis submitted by

Ali Razaghi

MSc, (SLU, Uppsala, Sweden)

Submitted in 2017

for the degree of Doctor of Philosophy (PhD)

College of Science & Engineering,

James Cook University (JCU)

Townsville, Australia

Acknowledgements

My interest in science and nature rooted from the early childhood and forged when I watched a movie about young Thomas Edison who established a lab in his basement, so I did the same at ten years old, then at 16 years old, I was one of the finalists in national practical chemistry Olympiad in Iran. Thereafter, I walked a long way, and my motivation was evolved from chemistry to microbial biology and up to this point in medical biotechnology and cancer therapeutics.

I acknowledge project support by the Advanced Manufacturing Cooperative Research Centre (AMCRC), funded through the Australian Government's Cooperative Research Centre Scheme and the JCU Postgraduate Research Scholarship (JCUPRS) which was granted by Graduate Research School.

I particularly appreciate my primary advisor, A/Prof. Kirsten Heimann for providing me the opportunity to follow my genuine desire in research in medical biotechnology and cancer biology/therapeutic and secondary advisor A/Prof. Leigh Owens for his bright idea to work with human interferon gamma which shaped my thesis during this research.

I am thankful to Dr Roger Heurlimann for mentoring me as a friend with many laboratory techniques from qPCR to gel electrophoresis; he was an invaluable help during my work. To Dr Jose Domingos for sharing his knowledge with me for RNA extraction and analysis, to Mrs Narges Mashkour for training me with mammalian culturing techniques, to A/Prof. Patrick Schaeffer for permitting me to work at his laboratory and troubleshooting my protein analysis and to Dr Jennifer Elliman for training me with some instruments in the lab.

I acknowledge people at the NQAIF, MEEL and Virology Laboratories, especially, Dr Florian Berner, Dr Nick Von Alvensleben, Dr David Jones, Danilo Malara and Dr Samuel Cires for being nice friends to me.

Finally, I would like to especially thank my special mother and father, "Parvin" and "Rasoul" for their never-ending supports and kindness which was always present through my whole life. I would also like to remember my late grandmother "Aaliyah" herself from a scholar household, who believed that I would be a "doctor" one day!

Statement of the Contribution of Others

Funding of PhD

- The Advanced Manufacturing Cooperative Research Centre (AMCRC).
- Tuition fee waiver, James Cook University
- Doctoral completion Award, Graduate Research School, JCU
- JCU Postgraduate Research Scholarship (JCUPRS)

Funding of the project

- AMCRC-MBD Energy Ltd linkage grant
- JCU-HDR Rnhancement Scheme Grant for Research to Ali Razaghi
- Private funding by Ali Razaghi for cancer research
- NQAIF Culturing Facility, College of Science and Engineering, JCU
- Private funding by Stan Hudson and Kirsten Heimann for expression studies at the Protein Expression Facility at the University of Queensland
- Provision of consumables at the Virology Laboratory for mammalian culturing facility, College of Public Health, Medical & Vet Sciences, JCU

Intellectual contribution and data collection

Chapter 1. Ali Razaghi wrote a literature review. Kirsten Heimann and Leigh Owens provided the supervision and editorial assistance.

Chapter 2. Ali Razaghi, Kirsten Heimann, Obulisamy Parthiba Karthikeyan designed the experiments, collected the data, performed the data analysis and wrote the drafts. Kirsten Heimann and Leigh Owens provided the supervision and editorial assistance.

Chapter 3. Ali Razaghi designed the experiments in collaboration with Linda Lua and Kirsten Heimann, collected the data, performed the data analysis and wrote the draft. Obulisamy parthiba Karthikeyan and Emilyn Tan provided technical assistance. Kirsten Heimann and Leigh Owens provided the supervision and editorial assistance.

Chapter 4. Ali Razaghi designed the experiments, collected the data, performed the data analysis and wrote the draft. Roger Huerlimann provided technical assistance. Kirsten Heimann and Leigh Owens provided the supervision and editorial assistance.

Chapter 5. Ali Razaghi designed the experiments with cellular biology and signalling pathway input by Kirsten Heimann, collected the data, performed the data analysis and

wrote the draft. Kirsten Heimann and Leigh Owens provided the supervision and editorial assistance.

Chapter 6. Ali Razaghi wrote the draft. Kirsten Heimann provided the supervision and editorial assistance.

Abstract

Human interferon gamma (hIFNγ) is a cytokine belonging to a diverse group of interferons which have a crucial immunological function against mycobacteria and a wide variety of viral infections. Specifically, recombinant hIFNγ has been shown to be an effective biopharmaceutical, against a wide range of viral, immuno-suppressive diseases with promising prospects in cancer immunotherapy resulting in a strong increase in demand and price. To date, it has been approved for treatment of chronic granulomatous disease and malignant osteopetrosis. hIFNγ is commonly expressed in *Escherichia coli*, marketed as ACTIMMUNE®. However, the resulting product of the prokaryotic expression system is unglycosylated with a short half-life in the bloodstream; the purification process is tedious and makes the product costlier. To solve these limitations; recombinant hIFNγ, as a lucrative biopharmaceutical, has been engineered in different expression systems including prokaryotic, protozoan, fungal (yeasts), plant, insect, and mammalian cells. Other expression systems also did not show satisfactory results regarding yields, the biological activity of the protein or economic viability. This thesis aimed to 1) lower the cost of production by using cheap C1 carbon sources (*e.g.* methane) from agricultural activities (*e.g.* intensive dairy, piggeries, *etc*.) for the cultivation of transformed yeast and 2) to assess the therapeutic efficacy of recombinant hIFNγ in its glycosylated and non-glycosylated form from different expression systems against ovarian cancer cells. Chapter 1 of the thesis gives a comprehensive review of expression and production of recombinant hIFNγ leading to the aims of the research. The second chapter investigated the potential of *Rhodotorula glutinis*; a yeast once reported as a methane-oxidizing yeast, for growth on cheap C1 carbon sources (methane and methanol) to evaluate the species potential for lowering production costs of recombinant immuno-therapeutics. In contrast to previous reports, *R. glutinis* did not utilise any C1 carbon sources even under near-identical experimental conditions to those reported. It also failed to grow on intermediates of the methane oxidation pathway (methanol, formaldehyde and formate) and only grew on C2 or more complex carbon sources. It is therefore concluded that *R. glutinis* is neither a methanotrophic nor methylotrophic yeast and not suitable as a cheap carbon-sustained expression system. This result led the research to look for an alternative yeast species with a proven ability to utilise a C1 carbon source (*i.e.* methanol). Among these alternative expression systems, *Pichia pastoris* was chosen as a proven methylotrophic (*i.e.* methanol-utilising) heterologous expression system. Six months after choosing this expression system, efficient expression of hIFNγ was reported by Wang *et al* (2014). Therefore, the third chapter replicated hIFNγ expression in *P. pastoris* similar to the

previous study and expanded on it by using four different strains (X33: wild type; GS115: HIS-Mut+; KM71H: Arg+, Mut- and CBS7435: MutS) and three different vectors (pPICZαA, pPIC9, and pPpT4αS). In addition, the native sequence (NS) and two codon-optimised sequences (COS1 and COS2) for *P. pastoris* were used. Methanol induction yielded no expression/ secretion of hIFNγ in X33; highest levels were recorded for CBS7435: Mut^S (~16 μg L^{-1}). mRNA copy number calculations acquired from RT-qPCR for GS115-pPIC9-COS1 proved low abundance of mRNA. A 10-fold increase in expression of hIFNγ was achieved by lowering the minimal free energy of the mRNA and a 100-fold by using the Mut^S phenotypes, but yields were substantially lower than reported by Wang *et al* (2014). The results show that commercial production of low cost, eukaryotic recombinant hIFNγ is not an economically viable in *P. pastoris*. In the fouth chapter, the aim was to study how selective pressure on the Histidinol dehydrogenase gene (*HIS4*), using amino acid starvation, affects the level of expression and secretion of the adjacent *hIFNγ* in the transformed *P. pastoris* GS115 strain, a histidine-deficient mutant. *hIFNγ* was cloned into the pPIC9 vector adjacent to the *HIS4* gene, a gene essential for histidine biosynthesis, which was then transformed into *P. pastoris*. Under amino acid starvation, only successfully transformed cells (*hIFNγ –HIS4+*) can synthesise histidine and therefore thrive. As shown by ELISA, amino acid starvation-induced selective pressure on *HIS4* improved expression and secretion of the adjacent hIFNγ by 55% compared to unchallenged cells. RT-qPCR showed that there was also a positive correlation between duration of amino acid starvation and increased levels of the hIFNγ RNA transcripts. According to these results, it is suggested that these adjacent genes (*hIFNγ* and *HIS4*) in the transformed *P. pastoris* are transcriptionally co-regulated and their expression is synchronised. To the best of the knowledge of the authors; this is the first study demonstrating that amino acid starvation-induced selective pressure on *HIS4* can alter the regulation pattern of adjacent genes in $HIS4^+$ *P. pastoris* strains. The aim of the fifth chapter was to determine the effect of glycosylation and expression platform of hIFNγ on ovarian carcinoma cell lines; PEO1 & SKOV3. Additionally, signalling transduction pathway for cytostasis and cell death were explored. The results showed that hIFNγ affected both PEO1 and SKOV3, but the *E. coli*-derived product was not effective against SKOV3, while the mammalian expressed was effective against both cancer cell lines. The primary effect was through cytostasis by cell cycle arrest and to a lesser extent through cytotoxicity, whilst the cell death mechanism was not apoptotic. Mammalian expressed hIFNγ, particularly when expressed in HEK293 (human embryonic kidney 293), showed better cytostatic effectiveness for both cell lines and higher cytotoxicity towards SKOV3. Furthermore, deglycosylation only slightly

reduced the cytostatic and cytotoxic effects of the CHO-expressed hIFNγ. In general; mammalian expressed hIFNγ may be advantageous for inhibiting the growth of ovarian carcinomas more effectively, particularly for drug-resistant cell lines. We also suggested for the first time that upregulation of FADD in SKOV3 can be the reason of anti-apoptotic behaviour and drug resistance in this cell line, which may present a novel therapeutic target. In conclusion, expression of hIFNγ in C1 carbon utilising yeast yielded insufficient product to be commercially viable. I, therefore, recommend exploring different mammalian expression systems *e.g.* CHO, HEK293, PER.C6, and CAP/CAP-T for the production of this biopharmaceutical because these expression systems are highly productive, cost-efficient, possess human-like post-translation glycosylation outcomes which increase biological activity and half-life of the protein in the bloodstream. Achieving the milestone of improved quality and lowered costs can also facilitate uptake of mammalian-expressed recombinant hIFNγ for clinical trials particularly due to a strong potential in cancer immunotherapy.

.

Table of Contents

List of Tables

List of Figures

Abbreviations

3D, three dimensional

AGRF, Australian Genome Research Facility

AOX, alcohol oxidase

APCs, antigen-presenting cells

Atg5, autophagy protein 5

Bax, Bcl-2-associated X protein

Bid, BH3 interacting domain death agonist

BIIC, Baculovirus-infected insect cells

BMGY, buffered glycerol complex medium

BMMY, buffered methanol-complex medium

CASP1, 3, 7, 8, 9, Caspase1, 3, 7, 8, 9

CC, codon context

c-FLIP, cellular FLICE (FADD-like IL-1β-converting enzyme)-inhibitory protein

CHO, Chinese hamster ovary

CoG, cost of goods

COS1, codon-optimised sequence 1

COS2, codon-optimised sequence 2

CYT-C, Cytochrome-C

GHG, greenhouse gas

DCW, dry cell weight

DR, death receptor

FADD, Fas-Associated Death Domain Protein

Fas, cell surface death receptor

FasL, Fas Ligand

FBS, fetal bovine serum

FDA, Food and Drug Administration

GAS, Gamma interferon-activated sequence

GOI, gene of interest

HCDC, high cell density cultivation

HCV, hepatitis C virus

HEK293, human embryonic kidney 293

hIFNγ, human interferon gamma

***HIS4*,** histidinol dehydrogenase gene

hpi, hours post induction

HPLC, high-pressure liquid chromatography

ICU, individual codon usage

IFN, interferon

IFNAR, interferon-α/β receptor

IFNG, interferon gamma gene precursor

IFNGR, interferon gamma receptor

IFNGR-α, interferon gamma receptor alpha

IFNGR-β, interferon gamma receptor beta

IGRA, interferon gamma release assays

IRF-1, interferon regulatory factor 1

ISGs, IFN-stimulated genes

IU, international unit

JAK, Janus kinase

LC3, microtubule-associated protein 1 light chain 3

LTB, latent tuberculosis

MD, minimal Dextrose

MFE, minimum free energy

MGY, minimal glycerol medium

MM, minimal methanol medium

MMO, methane monooxygenases

MS, multiple sclerosis

Mut, methanol utilisation

Mut^{+}, methanol utilisation plus

Mut^{s}, slow methanol utilisation

NF-κB, nuclear factor kappa-light-chain-enhancer of activated B cells

NK cells, natural killer cells

NKT cells, natural killer T cells

NS, native sequence

PARP, poly (ADP-ribose) polymerase

PTM, post-translational modification

RIPK3, receptor-interacting kinase 3

STAT1, signal transducer & activator of transcription-1

STATs, signal transducers and activators of transcription

SVR sustained virological response

TAG, triacylglycerol

TB, tuberculosis

T_h1, T helper cell type 1

T_m, melting temperature

TM, transgenic mice

TNFα, tumour necrosis factor alpha

TRAIL, TNF-related apoptosis-inducing ligand

TT, transcription terminator

TUNEL, terminal deoxynucleotidyl transferase (TdT) dUTP Nick-End labelling assay

YMB, yeast malt broth

YNB, yeast nitrogen base

Chapter 1. General introduction

The following chapter is a collaborative effort of which each author's contribution has been detailed at the start of the thesis. The publication has been modified to fit the thesis format, and specific sections have been moved to the general discussion, as the information presented there was not available when the research and its approach was conceived. The scope was also broadened to introduce the motivation for the research.

Published: Razaghi Ali, Leigh Owens, and Kirsten Heimann. "Review of the recombinant human interferon gamma as an immunotherapeutic: Impacts of production platforms and glycosylation." *Journal of Biotechnology* 240 (2016): 48-60.

1.1 Abstract

Human interferon gamma is a cytokine belonging to a diverse group of interferons which have crucial immunological functions against mycobacteria and a wide variety of viral infections. To date, it has been approved for treatment of chronic granulomatous disease and malignant osteopetrosis, and its application as an immunotherapeutic agent against cancer is an increasing prospect. Recombinant human interferon gamma, as a lucrative biopharmaceutical, has been engineered in different expression systems including prokaryotic, protozoan, fungal (yeasts), plant, insect, and mammalian cells. Human interferon gamma is commonly expressed in *Escherichia coli*, marketed as ACTIMMUNE ®. However, the resulting product of the prokaryotic expression system is unglycosylated with a short half-life in the bloodstream; the purification process is tedious and makes the product costlier. Other expression systems also did not show satisfactory results in terms of yields, the biological activity of the protein or economic viability. Thus, the review aims to synthesise available information from previous studies on the production of human interferon gamma and its glycosylation patterns in different expression systems, to provide direction for future research in this field.

1.2 Preamble

Cancer and viral disease are a growing burden for health care systems. Among the various cancers, viral-induced liver cancers are of particular concern, globally. In 2012, more than half a million people worldwide were diagnosed with liver cancer. The incidence is rising globally at an alarming rate, more than 80% of liver cancer cases occur in developing countries, largely owing to the widespread infection of hepatitis C virus (HCV) which is becoming a growing serious health challenge worldwide. Chronic infection with HCV is the main causative for liver disease including cirrhosis and liver cancer (Averhoff *et al*, 2012). It is currently estimated that more than 170 million people worldwide are infected with HCV (Harnois, 2012). One of the potential pharmaceuticals proposed to limit the impact of hepatitis is recombinant human interferon gamma (hIFNγ). Some clinical trials showed that recombinant hIFNγ therapy is beneficial, safe and well-tolerated to chronic hepatitis C-infected patients (Kokordelis *et al*, 2014; Muir *et al*, 2006), but *in vitro* studies showed that responses to treatment in liver cancers were minimal (Li *et al*, 2012). One of the most severe limitations for conducting more clinical trials with hIFNγ is the cost of production, partially linked to feedstock and purification of the product, and quality of the biopharmaceutical (Razaghi *et al*, 2016b) (see sections 1.8.3 & 1.11.1). This research aimed to tackle the cost of production bottleneck by using cheap C1-carbon (methane (CH_4) and methanol) utilising expression yeast systems. In addition, the research aimed to unravel whether expression platform and glycosylation status affected the pharmaceutical potency of recombinant hIFNγ. Ovarian cancer cell lines were chosen for this investigation because they have been well studied for hIFNγ therapeutic potential, which was an important aspect for achieving this objective. The following part of the introduction provides the background knowledge necessary to understand the experimental approach chosen and ends by providing a succinct outline for the specific aims of each chapter.

1.3 Introduction

According to the European Union regulations definition, biopharmaceuticals are proteins or nucleic acid constituents which are formulated using biotechnological approaches for therapeutic *in vivo* use (Borden *et al*, 2007). Many substances including vaccines, enzymes, antibodies, and antibiotics have been commercialised under the biopharmaceutical term, among them, interferons (IFNs) are noticeable due to their therapeutic importance against a wide variety of diseases (Borden *et al*, 2007; Meager, 2006; Samuel, 2001).

Interferons are macromolecules which were discovered separately by two research groups in the 1950s and named after the aptitude of these molecules to interfere with viral replication of the flu virus in infected cells (Fensterl & Sen, 2009). In the following decades, IFNs have been studied in fine detail including the mechanisms of transcriptional induction, their antiviral properties, mode of action, viral countermeasures and therapeutic applications against a range of diseases (Fensterl & Sen, 2009; Marciano *et al*, 2004). Subsequently, efforts for cloning and expression of *IFN* genes were carried out in many different protein production systems *viz*., *Escherichia coli*, mammalian cells, yeasts, protozoan and transgenic plants, but only *E. coli* expression systems were at the centre of attention due to high productivities (Chen *et al*, 2011).

The main *IFN* genes (α, β, and γ) have been predominantly expressed in *E. coli* at industrial scale and approved by the FDA (Food and Drug Administration, USA) and marketed under trade-names of ROFERON-A®, ALFERON-N®, INFERON-A®, and AVENOX® (exceptionally produced in hamster ovary cells) for human IFNα , BETASERON® for human IFNβ and both ACTIMMUNE® and γ-IMMUNEX® for hIFNγ (Jonasch & Haluska, 2001; Panahi *et al*, 2012).

Notwithstanding the importance of hIFNγ and the presence of many articles about this biopharmaceutical, no review has specifically dealt with the expression of hIFNγ in different host cells. Thus, the objective of this review is to synthesize outcomes of previous efforts on the whole process of expression, optimisation and purification of hIFNγ in different host cells, and the effect of expression host on glycosylation patterns, in order to discern which protein production system might be more desirable for future studies and applications *e.g.* cancer immunotherapy.

1.4 Overview on interferons

Interferons are cytokines which are expressed by a diverse group of genes and have been cloned from different vertebrates including mammals, birds, fish and even amphibians (Qi *et al*, 2010). Translated proteins of these genes generally vary in size between 165 and 208 amino acids and the protein moieties are further modified by post-translational glycosylation. IFNs are produced in reaction to viral infections harnessing host cells to non-specifically inhibit viral replication (Samuel, 2001; Takaoka & Yanai, 2006). Mammalian IFNs are broadly classified into three groups, according to amino acid sequence homology and their receptors:

***Type I IFNs**,* also known as viral IFNs, as they are induced by viral infection, contain many subtypes of IFNα (13 in humans originating from leukocytes), one IFNβ (originating from fibroblasts), IFNω (originating from leukocytes), IFNτ (originating from ovine trophoblasts), IFNε, IFNκ, and IFNζ. All type I IFN genes are located in a cluster on human chromosome 9 and all interact with the heterodimeric IFNα/β receptor (IFNAR) (Jonasch & Haluska, 2001; Samuel, 2001).

***Type II IFNs**,* also known as immune IFNs, are represented solely by IFNγ, which is distinctly dissimilar to other IFNs and uses a distinct heterodimeric IFNγ receptor (IFNGR) (Samuel, 2001; Takaoka & Yanai, 2006). This type of IFN is induced by either IFNα and β (in the case of viral infection) or IFNγ (in the case of mitogenic or antigenic stimuli) (Samuel, 2001). IFNγ proteins show similar biological activities inherent also to other IFNs; but has the advantage of being 100-10,000 more active as an immuno-modulator than the other IFNs (Farrar & Schreiber, 1993).

Type III IFNs, have been identified lately, containing IFNλ 1, 2, and 3, previously known as Interleukin 29, 28A, and 28B, respectively (Vilcek, 2003). Their genes are located in a cluster on human chromosome 19 and use the heterodimeric IFNλ receptor IL10R2/IFNLR1 (Fensterl & Sen, 2009). This type of IFN is induced directly by viruses or stimulated with IFNα or λ. Thus, they are identified as IFN-stimulated genes (Ank *et al*, 2006).

1.5 Characteristics of human IFNγ

Native hIFNγ is naturally synthesised by $CD4^+$ T helper cell type 1 (T_h1) lymphocytes, $CD8^+$ cytotoxic lymphocytes and natural killer (NK) cells (Bach *et al*, 1997). It is also secreted by other cells, such as B cells, NKT cells, and professional antigen-presenting cells (APCs) (Frucht *et al*, 2001). Secretion of hIFNγ by NK cells and APCs is important

in early host reactions against infection, while production of hIFNγ by T lymphocytes is important in the adaptive immune response (Frucht *et al*, 2001).

1.6 Genomics & proteomics

hIFNγ is encoded by the *IFNG* gene precursor "NCBI: NM_000610.2" which consists of 1240 bp nucleotides on chromosome 12q24.1 with four exons (Chevillard *et al*, 2002).

The resultant protein "UniProtKB: P01579" is a symmetrical homodimeric glycoprotein with 143 amino acid residues (precursor of native hIFNγ composed of 166 amino acids including 23 residues as the N-terminal secretory signal peptide), two glycosylation sites, a total molecular size of approximately 38.8 kDa in a dimeric structure which is an essential structure for its functional biological active mode and no sulphide bridge (Fig. 1.1) (Borden *et al*, 2007; Crisafulli *et al*, 2008; Younes & Amsden, 2002).

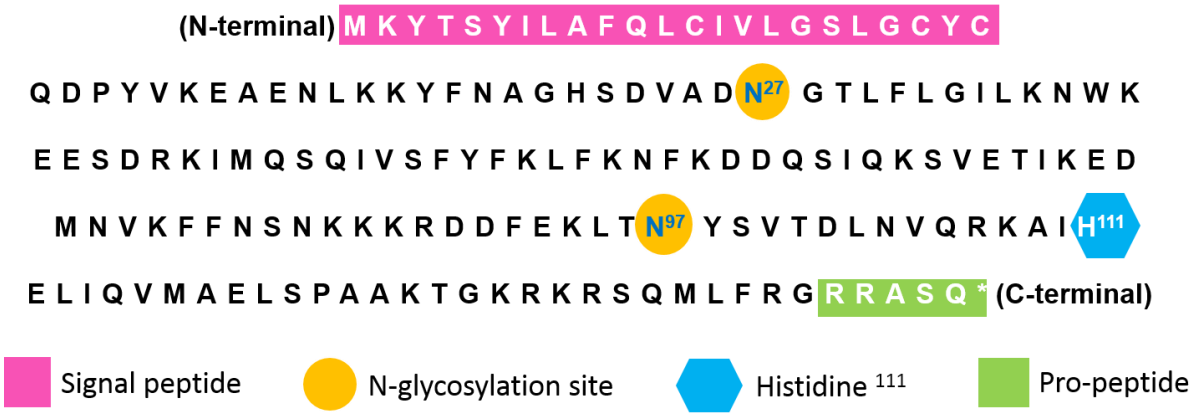

Figure 1.1 Schematic diagram depicting the amino acid sequence, N-glycosylation sites, and signal peptide of the hIFNγ precursor.

The folding pattern of hIFNγ is also unique. Each monomer of recombinant hIFNγ consists of six α helices ranging in length from 9-21 residues. Four helices (A, B, C, and D) from one subunit and two from the other (E' and F') interact to form one of two distinct, symmetrical domains of the protein. The two domains lie at a 55° angle, separated by a V-shaped cleft and a large random coil-structured surface loop (residues 16-27) connects the N-terminal helices A and B (Ealick *et al*, 1991). The functional importance of the N-terminal helix A and the AB-loop has been proven for the unfolding pathway and thermodynamic stability of recombinant hIFNγ (Waschutza *et al*, 1996).

Helix A is also essential for interaction with receptor-ligand and hence biological activity of hIFNγ (Lundell & Narula, 1994). Three regions have been found to be important for receptor binding: a long loop connecting the A and B helices, (histidine) H^{111} (Fig. 1.1) in the F helix and a conserved section of the flexible C-terminal. These three regions may form one continuous binding domain (Lundell & Narula, 1994).

The C-terminal of native hIFNγ is highly variable and extends from (proline) P^{122} to (glutamine) Q^{143}. It has been shown that truncation of the C-terminus decreases yields due to increased solubility of the recombinant protein produced in *E. coli*. Furthermore, truncation of the entire C-terminal domain or deletion of more than 9 amino acids decreased the biological activity of the recombinant protein, yet removal of the last 3, 6, and 9 C-terminal amino acids increased the biological activity of the recombinant protein up to 10-fold (Nacheva *et al*, 2003).

The protein is also heat-sensitive and is irreversibly denatured in solution at a temperature range of 40–65°C (Younes & Amsden, 2002).

1.7 Interactomics

In general terms, hIFNγ has a wide range of antiviral and antitumor activity and is involved in complex interactions of cellular metabolism and differentiation (Jonasch & Haluska, 2001). There are two receptor subunits for hIFNγ, known as IFNGR-α (also known as IFNGR1) which provides binding affinity and IFNGR-β (also known as IFNGR2) which is involved in signal transduction. It has been proposed that the receptor has a tetrameric structure composed of two IFNGR-α and IFNGR-β molecules each (Crisafulli *et al*, 2008). Both subunits bind to Janus Kinase 1 and 2 binding domains (JAK1 and JAK2, respectively). Oligomerisation occurs after ligand-receptor binding, concomitant with trans-phosphorylation of JAKs which is followed by phosphorylation of the cytoplasmic tails of the receptor molecules. This prepares a docking site for the signal transducers and activators of transcription (STATs) which subsequently are phosphorylated by the JAKs; The receptor molecules release the phosphorylated STAT dimers which are translocated to the nucleus to then activate transcription of IFN-stimulated genes (ISGs) (Borden *et al*, 2007; Jonasch & Haluska, 2001; Schroder *et al*, 2004) or IFN-regulated factor 1 (IRF1) (Li *et al*, 2012). The ISG products restrict viral infection and boost host immunity. Once the virus is cleared from the cells; the IFN response will be dampened by an inhibitory feedback loop before it

becomes detrimental to the host. More detailed information about this topic has been published elsewhere (Schroder *et al*, 2004).

Recently, the crystal structure of IFNGR-β also revealed the importance of N-glycosylation for the stability of this protein and approved the structural basis for receptor specificity (Mikulecky *et al*, 2016).

1.8 Production of recombinant hIFNγ

1.8.1 Production in *E. coli*

In the 1980s, hIFNγ was only produced by exposing human T-lymphocytes to mitogenic stimuli or by translating mRNA in oocytes which resulted in low expression and activity of 10^2-10^4 IU mL^{-1}. In addition, there were also some problems with purification due to the formation of cytoplasmic aggresomes and costly denaturation processes (Arbabi *et al*, 2003). However; with the development of recombinant DNA technology, *hIFNγ* cDNA was successfully cloned and expressed in *E. coli* in 1982 (Gray *et al*, 1982). *Escherichia coli* is one of the most frequently used expression systems for the production of heterologous proteins owing to its simple nutrient requirement, high growth rate, and its well-understood physiology and molecular genetics (Babaeipour *et al*, 2010). Attempts for the production of recombinant hIFNγ in *E. coli* were followed by many studies to improve yields (Khalilzadeh *et al*, 2004; Perez *et al*, 1990; Rojas Contreras *et al*, 2010). The expression of recombinant hIFNγ in *E. coli*, like other heterologous expression systems, is strongly affected by many factors and their interactions. These factors include the composition of media, temperature, inducer concentration and induction time (Balderas Hernández *et al*, 2008). Thus, determination of optimal culture conditions is necessary to attain higher expression levels (Perez *et al*, 1990)**.** The objective of optimising the production of recombinant proteins is to produce the highest amount of functional product per unit volume per unit time (Choi *et al*, 2006). Thus far, four strategies have been applied to optimise the production of recombinant proteins in *E. coli*, including, choice of culture media, mode of cultivation, strain development, and expression system control (Babaeipour *et al*, 2010). To date, the production of recombinant hIFNγ in *E. coli* grown on glucose as a carbon substrate is the prime method for providing this recombinant protein on a large scale (Gray *et al*, 1982; Hu & Ivashkiv, 2009). Furthermore, production of recombinant hIFNγ in *E. coli* optimised by response surface methodology and a Box-Behnken

design - compared to un-optimised conditions improved yields up to 13 times (Balderas Hernández *et al*, 2008).

Large-scale production platforms of recombinant hIFNγ in *E. coli* included batch, fed-batch and continuous cultivation modes (Babaeipour *et al*, 2010; Babaeipour *et al*, 2007; Khalilzadeh *et al*, 2003; Vaiphei *et al*, 2009). Among them, fed-batch cultivation is the most productive in terms of biomass and protein production (Table1.1) (Babaeipour *et al*, 2007). Fed-batch cultivation using high cell density cultivation (HCDC) is most often used to obtain high specific productivity of *E. coli* (mg protein per g dry cell weight (DCW)) (Table 1.1) (Babaeipour *et al*, 2007; Khalilzadeh *et al*, 2003). Feeding strategies are critical for achieving HCDC, because of effects on maximum attainable cell concentration and formation of by-products (Babaeipour *et al*, 2007).

Table 1.1 Impact of cultivation mode for *E. coli* on yields of recombinant hIFNγ

Cultivation	Overall productivity mg L^{-1} h^{-1}	Yield mg g^{-1} DCW	Biomass g L^{-1} [DCW]	Reference
Batch	420	300	14	(Babaeipour *et al*, 2010)
	200	330	7	(Varedi *et al*, 2006)
Fed-batch (HCDC)	2570	370	115	(Babaeipour *et al*, 2007)
	900	350	100	(Khalilzadeh *et al*, 2004)
	2500	330	127	(Varedi *et al*, 2006)
	3000	400	127	(Babaeipour *et al*, 2013)
Continuous	75	182	4.8	(Vaiphei *et al*, 2009)

1.8.2 Purification of *E. coli* recombinant hIFNγ

Although the hIFNγ gene is expressed very effectively in *E. coli*, the product is accumulated in the form of dense particles, refractile inclusion bodies (denatured proteins usually aggregate in prokaryotic cytoplasm upon targeted gene overexpression), within the cell's cytoplasm which requires complicated extraction and costly denaturation and refolding processes (Lee *et al*, 2005; Petrov *et al*, 2010).
A standard procedure for extraction and purification of biologically active proteins, like recombinant hIFNγ, from inclusion bodies, consists of the following steps: (1) the inclusion bodies are solubilised in high concentrations of guanidinium hydrochloride (GnHCl) or urea; (2) the denatured proteins are purified (3) proteins are re-folded and (4) the re-folded proteins are purified. During this procedure, the re-folding is the most critical step for the final yield, stability and biological activity of the protein. A few

external factors govern the successful protein re-folding process, including chaotropic agent concentration, salts concentration (0.75 M urea, 20 mM Tris-HCl), and pH (8.2 for hINFγ). (Petrov *et al*, 2010). Recently, a new refolding technique proposed to increase the effectiveness of re-folding process *in vitro* up to 21 times by using a novel type of hairy particles made up of submicron polystyrene cores and brushes of thermo-sensitive poly(*N*-isopropyl acrylamide) grafted onto the cores (Huang *et al*, 2013).
To date, solubilised recombinant hIFNγ has been purified using a range of chromatographic and affinity techniques, including size exclusion gel filtration (Reddy *et al*, 2007; Vandenbroeck *et al*, 1993), immuno-affinity chromatography by monoclonal antibodies (Honda *et al*, 1987), and ion exchange chromatography (Haelewyn & De Ley, 1995; Petrov *et al*, 2010). Approaches for purification of recombinant hIFNγ from inclusion bodies in *E. coli* are summarised in Table 1.2. All approaches used either GnHCl or urea for solubilisation and their purified product yields ranged from 0.3 to 14 mg g^{-1} cell mass with biological activities ranging from10^7–10^8 IU mg^{-1} (Petrov *et al*, 2010; Reddy *et al*, 2007). As yet, the highest biological activity (2 ×10^8 IU mg^{-1}) obtained by addition of a labilizing agent, l-arginine, in the re-folding buffer which improved the refolding and purification of recombinant hIFN*γ* by 10-fold in comparison to other techniques (Table 1.2)(Arora & Khanna, 1996).

Table 1.2 Methods for purification of recombinant hIFNγ from inclusion bodies in *E. coli*

Purification method	Biological activity [IU* mg^{-1}**]	References
Immuno-affinity chromatography	4 ×10^7	(Novick *et al*, 1983)
Ion exchange chromatography		
• Carboxymethyl sepharose	20 × 10^7	(Petrov *et al*, 2010)
• Expanded bed adsorption	0.8 × 10^7	(Jin *et al*, 2006)
• MonoBeads	1–2 × 10^7	(Perez *et al*, 1990)
Gel filtration chromatography		
• Superdex 75	1–4 × 10^7	(Guan *et al*, 2005; Reddy *et al*, 2007)
• Sephadex G-75	1–5 × 10^7	(Arakawa *et al*, 1985)
• Sepharose	20× 10^7	(Arora & Khanna, 1996)
Hydrophobic interaction chromatography	8.7 × 10^7	(Geng *et al*, 2004)

*International unit, **mg recombinant protein

Since unglycosylated recombinant hIFNγ monomers contain hydrophobic domains and possess no disulfide bonds, they have a tendency to aggregate in the solution phase, hence it is important to avoid the formation of aggregation in the isolation and purification process in order to re-fold and dimerise the monomers correctly to attain an active structure of the protein, (Jin *et al*, 2006; Vandenbroeck *et al*, 1993; Yphantis & Arakawa, 1987). For this reason, some later attempts have used hydrophobic chromatographic column matrices for the re-folding process with the intention of avoiding inactive aggregate formation (Geng *et al*, 2004; Reddy *et al*, 2007).

1.8.3 Limitations of the hIFNγ *E. coli* expression system

In general, for glycoproteins, but specifically for hIFNγ, bacterial production platforms face technical problems for industrial production such as:

1) Recombinant hIFNγ forms insoluble intracellular inclusion bodies in *E. coli* where the protein is denatured partially or entirely; the latter complicates its purification because a denaturation/renaturation step is required (Petrov *et al*, 2010).
2) Bacterial expression systems are not capable of assembling glycan branches, resulting in unglycosylated recombinant hIFNγ which has a shorter half-life in the bloodstream circulation in comparison to native hIFNγ (Bocci *et al*, 1985; Sareneva *et al*, 1993).
3) Following the release of protein from *E. coli,* the subsequent solution contains impurities like endotoxins and nucleic acids contaminating the product, which is another disadvantage of this expression system (Mohammadian-Mosaabadi *et al*, 2007; Rojas Contreras *et al*, 2010).
4) Recombinant hIFNγ produced in the bacterial system is glycated (a haphazard non-enzymatic process), which impairs the functionality of proteins (Mironova *et al*, 2003). The formation of advanced glycation end-products (AGEs) causes covalent dimerisation, polymerisation and non-enzymatic proteolysis (degradation of protein due to heat or acidity) which reduces biological activity, shorten the half-life and increases the immunogenicity of recombinant proteins (Mironova *et al*, 2003). Therefore, to solve the half-life deficiency of recombinant proteins; improvement of glycosylation is necessary (especially fucose-containing glycans).

1.8.4 Comparison of recombinant hIFNγ expressed in *E. coli* with native hIFNγ

hIFNγ-1b (Trade-name: ACTIMMUNE®) is the generic name for recombinant hIFNγ industrially produced in *E. coli* (Gray *et al*, 1982; Koh & Limmathurotsakul, 2010). hIFNγ-1b has the same primary structure as native hIFNγ with a few differences as summarised in (Table 1.3) (Rinderknecht *et al*, 1984).

Table 1.3 Comparison between native hIFNγ and hIFNγ-1b

	Native hIFNγ	hIFNγ-1b	References
Source	Blood cells	*E. coli*	(Bach *et al*, 1997; Gray *et al*, 1982)
Modification	Glycosylated	Unglycosylated	(Farrar & Schreiber, 1993; Perez *et al*, 1990; Zhang *et al*, 1992)
Amino acid length	143	143	(Farrar & Schreiber, 1993; Meager, 2006; Miller *et al*, 2009)
Molecular size (kDa) & quaternary structure	Monomeric~25 Dimeric~38.8	Monomeric~17 Dimeric~35	(Crisafulli *et al*, 2008; Farrar & Schreiber, 1993; Malek Sabet *et al*, 2008; Perez *et al*, 1990; Younes & Amsden, 2002; Zhang *et al*, 1992)
Physiological state	Active	Active	(Gray *et al*, 1982)
Biological activity	4-12×10^7 IU mg^{-1}	3×10^6 IU[1] mg^{-1} = 2×10^6 IU mL^{-1}	(Bouros *et al*, 2006; Miyata *et al*, 1986; Nathan, 1983)

[1] IU: International Units

The main difference between native hIFNγ and hIFNγ-1b is attributed to differences in glycosylation. The carbohydrate moiety of native hIFNγ is located at the receptor interaction domain and covers a fairly large surface area of the molecule (Walter *et al*, 1995). Carbohydrate side chains, in general, have been known to play an important role in many biological processes like protein folding, targeting, stability, clearance and cell to cell interactions (Varki, 1993); However, the absence of carbohydrate moieties in the hIFNγ-1b does not deactivate the molecule but affects its physicochemical and pharmaco-kinetic properties (Younes & Amsden, 2002). Generally, it is assumed that glycosylation of native hIFNγ protects the protein from proteolytic degradation, suggesting that glycans have a potential role in therapeutic applications (Bocci *et al*, 1985; Sareneva *et al*, 1996).

1.9 Expression of recombinant hIFNγ in other protein production systems

Due to the unglycosylated form of recombinant hIFNγ from *E. coli* which affects the half-life (Bocci *et al*, 1985), solubility and protease resistance, other expression systems have been used to overcome these problems (Table 1.4) (Leister *et al*, 2014). Most of these studies were performed at laboratory-scale, and result varied widely between each study. Therefore, a more in-depth investigation is required to justify their pros and cons in comparison to *E. coli* platform.

Methylotrophic yeasts have been demonstrated to deliver large amounts of recombinant protein on an industrial scale (Cereghino & Cregg, 2000). Initially, Wang *et al* (2014) claimed overexpression of hIFNγ in the methylotrophic yeast *P. pastoris* which could be promising for industrial production as it lowers the cost of production and the protein would be post-translationally glycosylated. Later, Prabu *et al,* (2016) and Razaghi *et al*, (2016) demonstrated the irreproducibility of the results and actual yields achieved were economically not competitive with *E. coli* (Table 1.4).

Productivity in CHO cells is still lower than *E. coli,* and albeit expression level would be magnified significantly in CHO cells, cultivation still requires bovine serum, which is exorbitantly expensive, and purification of protein from a liquid culture is arduous in the presence of serum (Nakajima *et al*, 1992), however usage of serum-free culture might be an alternative approach to lower the cost of cultivation, but it is still in the challenging stage of development (Rodrigues *et al*, 2013). Recently, in order to enhance the expression of hIFNγ codon optimisation approach was conducted to design synthetic *hIFN*γ coding sequences for heterologous expression in CHO cells based on the fact that recombinant expression of foreign proteins is usually suboptimal due to the usage of non-native codon patterns within the coding sequence (Chung *et al*, 2013). For codon optimisation, two selected design parameters, codon context (CC), and individual codon usage (ICU) optimisations were used by Chung *et al* (2013) , they showed that the CC optimised genes exhibited at least a 13-fold increases in expression level compared to the native hIFNγ sequence while approximately a 10-fold increases were observed for the ICU optimised genes. This shows that CC optimisation is comparatively more effective for improving recombinant hIFNγ expression in CHO cells (Chung *et al*, 2013).

Expression of hIFNγ in the baculovirus-infected insect cells (BIIC) and *Saccharomyces cerevisiae* was not satisfactory due to poor secretion into the culture media, hyper-glycosylation, and improper folding. Similarly, in spite of various attempts for

improvement of production, the yield of expression is still unsuitable for industrial production in comparison to expression in *E. coli* (Davoudi *et al*, 2011).

Table 1.4 Effect of expression systems on yield and activity of recombinant hIFNγ

Expression system	Yield [mg L^{-1}]	Activity[1]	Molecular size [kDa]	Reference
(*Mus* spp.) Mouse mammary gland	23 × 10^{-6}	1 × 10^{7} IU mg^{-1}	20–25	(Bagis *et al*, 2011)
	350-570	1 × 10^{7}- 5 × 10^{7} IU mL^{-1}	*	(Lagutin *et al*, 1999)
(*Rattus* spp.) Rat cells	*	4 × 10^{5} IU mL^{-1}	22-25	(Nakajima *et al*, 1992)
(*Cricetulus* sp.) Chinese hamster ovary cells	*	2.0 × 10^{4}-1.0 ×10^{5} IU mL^{-1}	22-23	(Haynes & Weissman, 1983)
	*	5.5 × 10^{4} IU mL^{-1}	21-25	(Scahill *et al*, 1983)
	*	1-2 × 10^{8} IU mg^{-1}	20-26	(Mory *et al*, 1986)
	15	*	*	(McClain, 2010)
Spodoptera spp. (BIIC)	2	Active*	18-23	(Chen *et al*, 2011)
Solanum lycopersicum (Tomato)	*	Active*	*	(Ebrahimi *et al*, 2012)
Oryzea sativa (Rice)	17 × 10^{-3}	Active*	24-27	(Chen *et al*, 2004)
Bacillus sp. (Bacteria)	2-20	Active*	17	(Rojas Contreras *et al*, 2010)
Leishmania sp. (Protozoa)	9.5	Active*	17	(Davoudi *et al*, 2011)
Saccharomyces cerevisiae (Baker's yeast)	*	2.5 × 10^{4} IU mL^{-1}	Detected E*	(Derynck *et al*, 1983)
Pichia pastoris (Methylotrophic yeast)	1-16 × 10^{-3}	Active*	*	(Razaghi *et al*, 2015; Razaghi *et al*, 2017)[2]
	2.5	Active*	17	(Prabhu *et al*, 2016)[2]
	300	1-1.4 × 10^{7} IU mg^{-1}	15	(Wang *et al*, 2014)[2]
Monkey cells	*	6.2 × 10^{-2} IU mL^{-1}	*	(Gray *et al*, 1982)
Homo sapiens (Human tissue culture)	6	1.93 ×10^{7} IU mg^{-1}	*	(Leister *et al*, 2014)
E. coli	1700	9 × 10^{7} IU L^{-1}	17	(Huang *et al*, 2013)

*** No data, [1]The antiviral assay for quantifying biological activity of human IFNs is based on the induction of a cellular reaction in the transformed human cell line (WISH); the effectiveness of interferon is assessed by comparing its protective effect against a viral cytopathic effect (usually vesicular stomatitis virus) against a calibrated reference in international unit (IU) (Petrov *et al*, 2010).**
[2]These papers were published during the course of my PhD research and are integrated here for completeness.

Despite the fact that expression of recombinant hIFNγ in transgenic mice (TM) was rather comparable to *E. coli*, expression occurred in live transgenic mice, which is impractical for commercial production (Table 1.4).

Comparison of yields in different expression systems reveals that the best results were achieved in prokaryotes followed by mammalian expression system *e.g.* TM (Table 1.4).

One drawback, of studies seeking for an alternative expression system else than *E. coli* (Table 1.4), is that production parameter (yield, biological activity and molecular size of the recombinant protein) were mostly not considered; for example, neither yields were measured in tomato, *Saccharomyces cerevisiae*, rat, hamster, and monkey cells nor was the biological activity quantified in *Bacillus* sp., *Leishmania* sp, tomato, rice and insect cells. Others studies in tomato, mouse, monkey and human cells did also not determine the molecular size of the recombinant protein.

Note: Prior to the start of this thesis in 2012, expression of recombinant hIFNγ in *Pichia pastoris* was patented by Thill and Davis (1989) with reported yields of 1-10 mg L^{-1}, which surprisingly was not followed up with commercial production. The two following studies were published during the course of my PhD and are being discussed in the relevant data chapters, but the detail is provided here in the introduction for completeness of information. However, later a research article by Wang *et al* (2014) reported the expression yields of recombinant hIFNγ of 300 mg L^{-1} in *Pichia pastoris,* and subsequently, another study by Prabhu *et al* (2016) resulted in 2.5 mg L^{-1}. None of these studies has resulted in large-scale/industrial scale production yet (see chapter 3).

1.10 Glycosylation

Many of the approved biotherapeutics are glycoproteins (Zhong & Somers, 2012). Glycosylation of glycoproteins can increase therapeutic efficacy through improving protein pharmaco-dynamics and pharmaco-kinetics. Glycosylation is one of the most multifaceted post-translational modifications, found in many eukaryotic proteins which plays an important role in blood transfusion reactions, selectin-mediated leukocyte-endothelial adhesion, host-microbe interactions, and numerous ontogenic events, including signalling events by the Notch receptor family (Zhong & Somers, 2012). The nature and content of oligosaccharides affect protein folding, stability, trafficking, immunogenicity, half-life and primary activities of the protein *i.e.* a lot of sialic acids increases plasma half-life, whilst in contrast, terminal residues of galactose and

mannose shorten the half-life (Zhong & Somers, 2012). Glycoproteins are generally classified into four groups: N-linked, O-linked, glycosaminoglycan, and glycosylphosphatidylinositol-anchored proteins. N-linked glycosylation is the main form of glycosylation and takes place in both the endoplasmic reticulum and Golgi, through the side chain amide nitrogen of a specific asparagine residue which plays a critical role in protein folding and conformation stabilisation and intracellular trafficking (Zhong & Somers, 2012)

Native hIFNγ has two N-glycosylated sites at asparagine N^{25} (fucosylated complex-type oligosaccharides) and N^{97} (with hybrid and high-mannose structures) (Fig. 1.1) (Farrar & Schreiber, 1993; Kelker *et al*, 1983; Sareneva *et al*, 1996; Yip *et al*, 1982; Younes & Amsden, 2002). It has been shown that native hIFNγ derived from T lymphocytes is heterogeneously glycosylated and doubly, singly, and unglycosylated forms exist resulting in hIFNγ molecules of different molecular masses (16.7-37 kDa) and considerable variation in the carbohydrate structures (>30 different forms) (Sareneva *et al*, 1996). The glycans at (asparagine) N^{25} consisted of fucosylated, mainly complex-type oligosaccharides, with the highest relative frequency 41% for sugar composition of (*N*-acetylneuraminic acid, galactose, mannose, *N*-acetylglucosamine, fucose) which are known to be essential for protease resistance to cathepsin G, granulocyte proteases, plasmin, and purified elastase (Mironova *et al*, 2003; Sareneva *et al*, 1996). In contrast, the glycans at N^{97} were more heterogeneous, with hybrid and high-mannose structures with highest relative frequency at 34% for sugar composition of (*N*-acetylneuraminic acid, galactose, mannose, *N*-acetylglucosamine) (Fig. 1.2) (Sareneva *et al*, 1996).

The glycosylation pattern of recombinant hIFNγ was also confirmed in three expression systems (CHO, BIIC, and TM) for both N^{25} and N^{97} sites. The N^{97} glycans always showed a non-fucosylated pattern which varied between two types; complex and oligomannose (James *et al*, 1995). There are, however, minute differences between the N-glycan structure of native and recombinant forms of hIFNγ such as lack of N-acetylneuraminic acid and insertion of N-acetylglucosamine between galactose and mannose in all recombinant forms (Fig 1.2). In conclusion, comparison of glycosylation similarity revealed that glycosylation patterns achieved in the mammalian CHO expression system were most similar to those in human cells (Fig. 1.2).

The main obstacle for clinical application of unglycosylated recombinant hIFNγ is primarily due to the short *in vivo* half-life of the protein. An investigation in the half-life of proteins showed that unglycosylated hIFNγ has a shorter half-life than glycosylated

forms in human lymphocytes or CHO cells (Bocci *et al*, 1985; Sareneva *et al*, 1993). In addition to glycosylation *per se*, the type of glycan also affects the half-life of proteins, for instance, a mannose-type oligosaccharide of recombinant hIFNγ expressed in insect cells, was eliminated more rapidly in the bloodstream circulation compared to native hIFNγ (Hooker & James, 1998; Sareneva *et al*, 1993; Younes & Amsden, 2002). It has also been stated that hIFNγ-1b disappears from the systemic circulation of human about 4.5 h, as a result, due to the shorter half-life patients are subjected to frequent “subcutaneous injections” which aggravates side-effects *per se* (Miyakawa *et al*, 2011).

1.11 Medical applications

1.11.1 Market prospect

Biopharmaceutical products are the fastest growing and the most technically complex sector within the pharmaceutical industry, the annual revenue for all biopharmaceuticals was reported to exceed US$165 billion in 2012 (Rader, 2013). The predicted market increase for IFNs is the result of the global increase of hepatitis C cases as the main reason for the expanding market (Gohil, 2014). The global consumption market of recombinant IFNs is estimated to be ~4 billion dollars annually at the end of the 20th century (Beilharz, 2000; Ebrahimi *et al*, 2012).This market is covered by a few companies including Biogen™ Idec Inc, Merck Serono ™S.A. and the Roche™ Group, a situation responsible for the high price of this lucrative biopharmaceutical. Recombinant hIFNγ (hIFNγ-1b), as a biopharmaceutical, is commercially available for clinical application under tradenames: “ACTIMMUNE®” (Horizon Pharma Ltd, Ireland) which costs more than US$300/dose, and “γ-IMMUNEX®” (ExirPharma Co, Iran)(Koh & Limmathurotsakul, 2010; Panahi *et al*, 2012).

1.11.2 Therapeutics & side-effects

Therapeutic applications of hIFNγ are being conducted using ACTIMMUNE® has been approved by FDA for clinical application against chronic granulomatous disease to decrease the severity and number of infections in patients and against malignant osteopetrosis to postpone the progression of the disease. It has also been shown that ACTIMMUNE® is effective against a wide variety of diseases, including cancer,

tuberculosis, (*Mycobacterium avium* complex infections), idiopathic pulmonary fibrosis, cystic fibrosis, scleroderma, invasive fungal infections especially in immuno-suppressed patients, such as leukaemia, HIV and transplant patients (Armstrong-James *et al*, 2010; Miller *et al*, 2009). γ-IMMUNEX® also showed the significant result in a clinical trial against atopic dermatitis (Panahi *et al*, 2012).

The therapeutic dosage of the treatment is disease-dependent. As an example, idiopathic pulmonary fibrosis patients received 200 µg of ACTIMMUNE® thrice a week (Raghu *et al*, 2004). Sometimes, treatment with ACTIMMUNE® might be associated with four major side effects which are grouped as constitutional, neuropsychiatric, haematological and hepatic disorders. These side-effects vary in persistence and severity and correlate with high dosage application and duration of interferon therapy (Jonasch & Haluska, 2001; Zaidi & Merlino, 2011). In severe cases, such disorders and symptoms might impair quality of life in patients leading to discontinuation of treatment, but most of the adverse effects are manageable (Vial & Descotes, 1994).

Recombinant hIFNγ is also broadly used for *in-vitro* cellular and molecular, immunological studies in basic research laboratories, *inter alia*, for signal regulation in hematopoietic stem cells or cytotoxicity (Baldridge *et al*, 2011; Noone *et al*, 2013). More detailed information about hIFNγ therapy and toxicity can be found in the following review articles (Jonasch & Haluska, 2001; Miller *et al*, 2009).

1.11.3 Gene therapy

As already stated; the clinical application of recombinant hIFNγ is limited by its short half-life and side effects (Miyakawa *et al*, 2011). Therefore, one possible option to solve these issues is to deliver hIFNγ via a virus, which could achieve efficient and constant expression of the target gene. Thereafter, adenovirus encoded *hIFNγ* (*Ad-IFNγ*), which expresses *IFNγ* cDNA (TG-1041, TG-1042) by adenoviral vectors, showed potential effectiveness both in preclinical (*in vivo*) and clinical trials such as cutaneous lymphoma (Dummer *et al*, 2004; Miller *et al*, 2009). A number of *in vitro* experiments had also proven an inhibitory role of *Ad-IFNγ* on cell growth of prostate cancer (Zhao *et al*, 2007), nasopharyngeal carcinoma (Zuo *et al*, 2011) and pancreatic cancer (Xie *et al*, 2013).

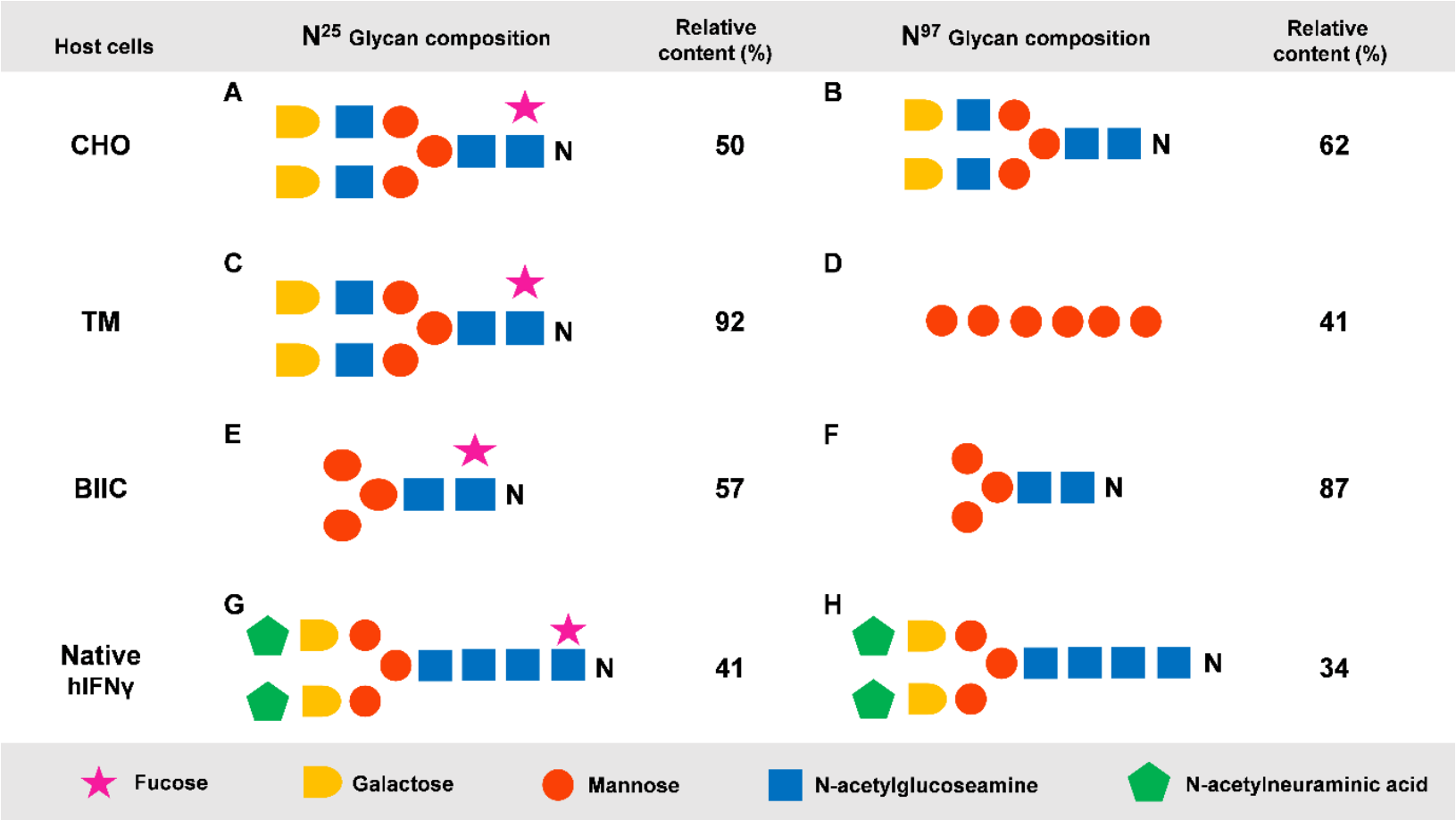

Figure 1.2 N-glycan structures associated with N^{25} and N^{97} glycosylation sites of recombinant hIFNγ expressed in different host systems (James *et al*, 1995; Sareneva *et al*, 1996). **A:** Core fucosylated plus a varied degree of sialyation, **B:** Non-fucosylated complex high mannose oligosaccharide chain, **C:** Core fucosylated plus tri-mannosyl, **D:** Oligomannose (Man 5), **E:** Core fucosylated. **F:** Oligomannose (varied), **G:** Core fucosylated, **H:** Core fucosylated.

1.11.4 Prospect for cancer immunotherapy

The stimulation of the immune system to treat cancer is called immunotherapy which was at the frontline research to win the “War on Cancer” in the past decade (Topalian *et al*, 2015). Interferons, as one class of cytokines, regulate the behaviour of the immune system and are able to enhance anti-tumour activity, thus are a pivotal part of cancer immunotherapy. Type I IFNs, hIFNα and hIFNβ have been used extensively for the treatment of different cancers clinically, *e.g.* hIFNα is approved by the FDA for the treatment of hairy-cell leukaemia, follicular lymphoma, AIDS-related sarcoma and chronic malignant melanoma (Dunn *et al*, 2006).

Unlike type I IFNs, and in spite of the proven crucial role of IFNγ in animal models of anti-tumour immunity, hIFNγ is not approved yet by the FDA for the treatment of any cancer. To date, clinical studies showed no benefit for patients with colon cancer, metastatic renal carcinoma, and small-cell lung cancer (Table 1.5). However, improved survival was observed when hIFNγ was administrated intravesically to patients with bladder carcinoma and some non-melanoma cancers (Dunn *et al*, 2006). The most promising result was achieved in patients with stage -Ic-IIc of ovarian cancer (Table 1.5)(Dunn *et al*, 2006). Clinical trials of hIFNγ are still ongoing.

The *in vitro* study of hIFNγ in cancer cells is more extensive, and results indicate anti-proliferative activity of hIFNγ leading to the growth inhibition or cell death, generally induced by apoptosis but sometimes by autophagy. Some effects of hIFNγ on different types of cancers have been summarised (Table 1.5).

Another possible immunotherapeutic application of hIFNγ against hepatitis C virus (HCV) infection and HCV-associated liver cancer is on the horizon. It has been reported that globally, more than 170 million people are living with HCV infection including its chronic form, which is becoming a growing serious health challenge worldwide. Chronic infection with HCV is the main causative for liver disease including cirrhosis and hepatocellular carcinoma (Averhoff *et al*, 2012). Some clinical trials showed that hIFNγ-1b treatment is beneficial to some chronic hepatitis C infected patients (Muir *et al*, 2006). Additionally, HCV-infected patients who received PEGylated hIFNα in combination with ribavirin showed a sustained virological response (SVR), as a sign of cure, in clinical trials (Dalgard *et al*, 2004; Maylin *et al*, 2009). Therefore the application of PEGylated hIFNγ against HCV might be of interest in future research directions.

1.11.5 Diagnostics

Other than therapeutic usages, recombinant hIFNγ is used to produce lapine or murine anti-interferon gamma antibody, respectively by injection to rabbits (Alfa *et al*, 1987) or mice (Novick *et al*, 1983). This antibody is used in enzyme-linked immuno-sorbent assay (ELISA) or interferon gamma release assays (IGRAs) (Tsiouris *et al*, 2006), which are clinical whole-blood assays for diagnosing *Mycobacterium tuberculosis* infections including either latent tuberculosis (LTB) infection or tuberculosis diseases (TB) (Vesenbeckh *et al*, 2012; Zwerling *et al*, 2012). Use of these assays is currently increasing due to the globally growing population infected with TB. The World Health Organisation (WHO) estimates that one-third of the world's population is infected by LTB which potentially might develop into active disease. To date, two IGRAs are commercially available; the QuantiFERON®-TB Gold In-Tube assay (licensed by Cellestis Ltd, Carnegie, Victoria, Australia), an ELISA-based whole blood test and the T-SPOT®.TB assay (licensed by Oxford Immunotec™, Abingdon, UK) an enzyme-linked immunospot (ELISPOT™) implemented on peripheral blood mononuclear cells (PBMCs) (Santín Cerezales & Benítez, 2011; Zwerling *et al*, 2012). Both kinds of IGRAs principally measure the T-cell release of hIFNγ the following stimulation by antigens unique to *M. tuberculosis* (Santín Cerezales & Benítez, 2011). More detailed information about hIFNγ assays can be found in the following review article (Pai *et al*, 2004).

Table 1.5 Effects of recombinant hIFNγ on different cancers			
Cancer type	**Trial type**	**Results**	**Ref.**
Bladder	Preclinical (*in-vitro*)	Cell growth inhibition; high-grade tumour cells less susceptible.	(Hawkyard *et al*, 1991)
	Clinical	Effective against stage Ta, T_1, grade 2 tumours' recurrence. The proposed mechanism of action: recruitment and activation of intramural leukocytes.	(Giannopoulos *et al*, 2003)
Colon	Clinical	No benefit for patients with high-risk colon cancer, as surgical adjuvant treatment	(Wiesenfeld *et al*, 1995)
	Preclinical (*in-vitro* & *in-vivo*)	Primary cells, label-retaining cancer cells sensitive (*in vitro* & *in vivo*). The proposed mechanism of action: apoptosis. Synergistic effects in combination with oxaliplatin.	(Ni *et al*, 2013)
Liver	Preclinical trial (*in-vitro*)	Cell growth inhibition and cell death. The proposed mechanism of action: autophagy through interferon regulatory factor 1 (IRF-1) signalling.	(Li *et al*, 2012)
	Preclinical (*in-vitro* & *in-vivo*)	Pre-treatment with hIFNγ as chemosensitiser, before the administration of PEGylated liposomal Dox maybe effective on hepatocellular carcinoma.	(Wang *et al*, 2009)
	Preclinical trial (*in-vitro*)	Hep3B and Chang liver cell lines: apoptosis and cell death, Huh7 cell line, insensitive to apoptosis, but autophagy proposed for cell death. HepG2 cell line, insensitive.	(Li *et al*, 2012; Vadrot *et al*, 2006)
Lung	Preclinical trial (in-vitro)	Anti-proliferative effect on nine mesothelioma cell lines. Proposed mechanism of action: cell cycle arrest in the G2 phase, depending on cyclin regulation through $p21^{WAF1/\ CIP1}$- and $p27^{Kip1}$-independent mechanisms.	(Vivo *et al*, 2001)
Melanoma	Preclinical (*in-vitro*)	Cell growth inhibition for A375, WM239, WM9 cell lines at doses (>1000 U per mL). Order of sensitivity (A375 > WM239 > WM9).	(Kortylewski *et al*, 2004)
Ovarian	Preclinical (*in-vitro* & *in-vivo*)	Apoptotic and anti-proliferative activity in OAW42, OVCAR3, OVCAR4, OVCAR5, PEO1, PEO14, PEO16, SW626 cell lines, and 11 of 14 primary cultures. The proposed mechanism of action: Inhibition of the poly (ADP-ribose) polymerase (PARP), involved in DNA repair from damage, causes apoptosis. SKOV3 cell line, insensitive.	(Guan *et al*, 2012; Wall *et al*, 2003)
	Preclinical (*in-vitro*)	OVCAR3 cell line, combinational treatment of co-immobilised group hIFNγ and TNFα enhanced expression of activated p53, Bax, and caspase3, suggesting the mitochondrial pathway of apoptosis.	(Guan *et al*, 2012)
	Preclinical (*in-vitro*)	Stable expression of plasmid-mediated hIFNγ inhibits the proliferation of cells.	(Lv *et al*, 2011)
	Clinical (Phase I & II)	Combinational treatment with carboplatin and paclitaxel is a safe first-line treatment for patients with advanced ovarian cancer.	(Marth *et al*, 2006)
	Clinical (Phase II)	Apparent antitumor activity.	(Welander *et al*, 1988)
	Clinical (Phase III)	Beneficial in the first-line chemotherapy of patients, acceptable toxicity.	(Windbichler *et al*, 2000)
	Clinical (Phase III)	Combinational treatment with carboplatin and paclitaxel has no benefit in the first-line treatment.	(Alberts *et al*, 2008)
Pancreatic	Preclinical (*in-vitro*)	Cell growth inhibition in AsPc-1, Capan-1, Capan-2, Dan-G cell lines. The proposed mechanism of action: apoptosis through expression of functional hIFNγ receptors and the putative tumour suppressor and IRF-1.	(Detjen *et al*, 2001)
Kidney	Clinical	No significant effect in patients with metastatic renal-cell carcinoma.	(Gleave *et al*, 1998)
Soft tissue sarcoma	Clinical	Limb salvage achieved through biochemotherapy of Isolated Limb Profusion with TNFα, hIFNγ, and melphalan.	(Eggermont *et al*, 1996; Lienard *et al*, 1998)

1.12 Thesis objective and structure

As outlined in the general introduction, the demand for application of recombinant hIFNγ is rising due to the increase of infectious diseases like hepatitis and non-infectious diseases like cancer. However, currently there are two main bottlenecks for commercial production of recombinant hIFNγ: 1) a costly production process of recombinant hIFNγ in *E. coli* such as using glucose as a carbon source for growth and tedious process of extraction and purification of recombinant proteins from the prokaryotic expression system. 2) lower quality of recombinant hIFNγ expressed in prokaryotic systems *e.g.* lack of glycosylation and dissimilarity in protein folding with human cells. According to these obstacles, three knowledge gaps/ research questions can be identified: 1) Can production costs be lowered by using cheaper carbon sources (*e.g.* methane or methanol) as a substrate for growth? 2) Can the quality of recombinant hIFNγ be improved by exploiting eukaryotic expression systems (*e.g.* yeast or mammalian systems)? and 3) Do expression platforms influence the therapeutic efficacy of recombinant hIFNγ *e.g.* against cancer cells. Thus the main objectives of this thesis were:

- To examine the applicability of using cheap and abundant C1 carbon sources as a substrate for growth of yeast for production of recombinant hIFNγ.
- To explore the productivity of a C1-carbon utilising yeast as a eukaryotic expression system.
- To understand how expression systems, influence the quality of recombinant hIFNγ *e.g.* whether mammalian expression system can be used as an alternative production platform to improve the therapeutic efficacy of recombinant hIFNγ.

Driven by these objectives, the aims were:

Aim 1) To evaluate the growth of the methanotrophic yeast *Rhodotorula glutinis* on waste methane for the potential use to produce recombinant eukaryotic hIFNγ (chapter 2). In contrast to previous publications, my study showed that *R glutinis* does not utilise either methane or intermediates resulting from methane oxidation (*i.e*. methanol, formaldehyde or formate), changing the experimental approach to utilise *Pichia pastoris*, a commonly used methylotrophic yeast for heterologous protein expression, to preserve the cheap C1 carbon cultivation approach of this research (chapter 3).

Aim 2) To examine the impact of strains, sequence codon optimisation and vectors on hIFNγ expression in the methylotrophic yeast *Pichia pastoris*. As achieved yields remained low, the next chapter investigated the applicability of the adjacent gene – selective pressure hypothesis for increased expression of hIFNγ in *Pichia pastoris*.

Aim 3) To increase expression of recombinant hIFNγ in *P. pastoris* by a novel technique; using amino acid selective pressure on the adjacent *HIS4*$^{+}$ gene in order to enhance the transcription/expression of hIFNγ (chapter 4). Although this technique increased expression by ~55%, achieved yields were still substantially below those required for commercial production.

Aim 4) To explore the effects of expression system (eukaryotic vs. prokaryotic) and glycosylation on the therapeutic efficacy of recombinant hIFNγ against ovarian cancer cell lines, SKOV3 & PEO1 (chapter 5).

Finally, Chapter 6 presents a synopsis of key results described in each of the previous chapters, outlines how the research presented in this thesis, as a whole, contributes to the evaluation of expression systems (yeast) of recombinant hIFNγ and showing the superiority of mammalian expression system for therapeutic efficacy. It concludes with an outlook for further research.

Chapter 2. Methane oxidation by the oleaginous yeast *Rhodotorula glutinis* – fact or fiction?

The following chapter is a collaborative effort of which each author's contribution is outlined at the start of the thesis.

2.1 Abstract

Rhodotorula glutinis, an oleaginous carotenoid synthesising yeast with the rapid rate of growth, has been reported as a methane-oxidizing yeast. Methane, a potent greenhouse gas, could lend this species to be employed in point source methane utilisation with a great potential for valuable co-product production, *e.g.* lipids, carotenes and recombinant proteins. This study investigated the potential of *R. glutinis* for growth on cheap C1 carbon sources (methane and methanol) to evaluate the species potential for lowering production costs of recombinant immuno-therapeutics. Here we report that, even under near-identical experimental conditions to those reported, *R. glutinis* did not utilise any C1 carbon source, nor did it grow in the absence of C2 or more complex carbon sources. It is therefore concluded that *R. glutinis* is neither a methanotrophic nor methylotrophic yeast and not suitable as a cheap carbon-sustained expression system.

2.2 Introduction

Rhodotorula glutinis is a unicellular red yeast belonging to basidiomycetes forming rapidly growing mucoid colonies found in air, soil, and water (De Hoog *et al*, 2000). *Rhodotorula glutinis* has a wide range of potential applications and is especially known as a carotenoid-producing yeast which synthesises different carotenoids like torulene, torularhodin, and β-carotene (Aksu & Eren, 2007; Bhosale & Gadre, 2001a; Bhosale & Gadre, 2001b; Perrier *et al*, 1995). Typical carotenoids concentrations ranging from 50 to 350 µg g^{-1} dry weight have been reported (Bhosale & Gadre, 2001b; Perrier *et al*, 1995; Schneider *et al*, 2013a). Other potential applications for *R. glutinis* are the production of L-phenylalanine, an essential amino acid for human nutrition (El-Batal, 2002), and invertase, an important enzyme in food industries (Rubio *et al*, 2002). It is also an oleaginous yeast which accumulates large amounts of lipids primarily as triacylglycerol (TAG) containing long-chain fatty acids (Li *et al*, 2007; Rubio *et al*, 2002). For this reason, it has been considered as a potential option for biodiesel generation from microbial lipids (Li *et al*, 2007; Saenge *et al*, 2011; Schneider *et al*, 2013b; Xue *et al*, 2008).

Despite many promises of microbial industrial bio-product applications, provision of carbon source has been identified as the main cost factor (Schneider *et al*, 2013b). To date, a broad range of carbon substrates have been investigated for *R. glutinis* for microbial lipid production such as glucose (Li *et al*, 2007), glycerol (Saenge *et al*, 2011), xylose (Dai *et al*, 2007), molasses (Buzzini, 2001; Buzzini & Martini, 2000), soluble starches (Schneider *et al*, 2013b), and distillery (Gonzalez-Garcia *et al*, 2013), brewery (Schneider *et al*, 2013a) and glutamate wastewater (Xue *et al*, 2008) in order to find a cheap feedstock which can considerably enhance economic profitability.

Another cheap carbon source is methane (CH_4) which is a potent greenhouse gas (GHG) with global warming potential of 25 times that of CO_2; contributing to 18 % (*i.e.* 0.509 $W.m^{-2}$) of the total climate forcing. Methane has an extended lifespan of 7 to 12 years in the atmosphere. Anthropogenic CH_4-emissions are derived from agricultural and anthropogenic activities with landfills, oil, and gas, and enteric fermentation being the main pollution sources and projected to reach 7,904 MMT-CO_2eq by 2020 (Karthikeyan *et al*, 2017). For example, it is reported that approximately 15% of Australia's GHG emissions originate from agriculture, including methane from ruminant animals like sheep and cattle. It is, therefore, necessary to mitigate methane emissions to reduce the impact of global climate change. Mitigation could potentially be coupled with co-product production using methanotrophs, which would provide an economic

incentive. Methanotrophs can fix CH_4, a biologically inert compound, producing methanol in the first step, which is further metabolised to formaldehyde and ultimately formate, the latter being used for growth, *i.e*. converted to biomass carbon (Higgins *et al*, 1981; Van Dijken & Harder, 1975). Only methanotrophs provide a biological carbon sink by converting CH_4 to biomass. (Karthikeyan *et al*, 2017).

Four basidiomycetes *(Rhodotorula glutinis*, *Rhodotorula rubra*, *Sporobolomyces roseus,* and *Sporobolomyces gracilis*) have been reported to utilise CH_4 as a sole carbon source (Wolf & Hanson, 1980; Wolf *et al*, 1980; Wolf & Hanson, 1979). Yeast cultivation is well known and used to produce bio-products (El-Batal, 2002; Saenge *et al*, 2011; Satyanarayana & Kunze, 2009), but utilisation of CH_4 as a free carbon source from landfills and agricultural activities *e.g.* intensive dairy, piggeries, *etc.* (Jiang *et al*, 2010) offers the potential to couple the bio-product potential of these species to CH_4-emission abatement. In the case of *R. glutinis*, its biomass produced on methane could be used for the production of value-adding renewable products (*e.g.* pigments, amino acids, enzymes, and lipids). Therefore, this study investigated the CH_4-utilisation potential of *R. glutinis* to evaluate the potential for genetically modified C1- carbon reared *R. glutinis* for the production of recombinant human interferon gamma – an important cytokine with anti-viral/-microbial and anti-cancer potential -, whilst simultaneously producing other co-products (*e.g.* carotenes and lipids). Our results query prior publications on the CH_4 and methanol utilisation capacity of *R. glutinis* (Wolf & Hanson, 1979) and provide evidence that this yeast is neither a methanotroph nor a methylotrophic yeast.

2.3 Material and methods

2.3.1 Cultivation

A pure culture of red yeast *Rhodotorula glutinis*, strain FRR-4522, was purchased from the Commonwealth Scientific and Industrial Research Organisation (CSIRO) Culture Collection, Australia. A sub-culture of *R. glutinis* was maintained on 2% agar plates prepared with Yeast Malt (YM) medium (3 g L^{-1} yeast extract; 3 g L^{-1} malt extract; 5 g L^{-1} casein peptone; 10 g L^{-1} glucose). Seeding cultures were prepared from exponentially growing cultures in Yeast Malt Broth (YMB), pH: 5.5, containing the above components without agar. Biomass was harvested by centrifugation (3,995 g for 10 min; 5810 R Eppendorf AG, Germany).

2.3.2 Growth on different carbon substrates

Rhodotorula glutinis was cultured for 19 days in 200 mL basal medium (BM) containing KH_2P0_4, 0.85 g; K_2HP0_4, 0.15 g; $MgS0_4$, 0.5 g; NaCl, 0.1 g; $CaCl_2$, 0.1 g; H_3B0_4, 500 pg; $CaSO_4$, 40 pg; KI, 100 pg; $FeCl_2$, 200 pg; $MnSO_4$, 400 pg; Na_2MoO_4, 200 pg; $ZnSO_4$,400 pg. KNO_3, 2 g. pH-5.5 per litre distilled water, supplemented with 1% (v/v) (methanol (C1) acetate (C2), ethanol (C2), or glycerol (C3)) and methane (C1) (v/v). For CH_4 utilisation studies, the headspace was purged with a CH_4: air mixture of 20–25% CH_4, using calibrated thermal mass flow controllers (Red-y, Vogtlin, WI, USA). Headspace CH_4 was replenished every 24 h over 19 days. The inlet and outlet of the gas vents were connected with flexible Tygon tubing and sealed after every purging cycle. Sterile air-filters (0.2 µM, PTFE, Acro®50; VWR International, Murarrie, QLD-4172, Australia) were fitted in the gas vents to avoid contaminations while purging. Cultures were incubated at 25 °C with continuous agitation at 200 rpm. Biomass growth was measured daily spectrophotometrically at 540 nm (EnSpire® Multimode Plate Reader, PerkinElmer, Glen Waverly, VIC, Australia).

2.3.3 Methane fixation assessment

Cultivation of *Rhodothorula glutinis* followed the procedure published by Wolf and Hanson (1980), except that the gas mix did not contain additional CO_2. Twenty-one mg dry weight of *R. glutinis* was incubated in 10 mL BM (pH-5.5) in air-tight serum vials (50 mL). The headspace of the vials was firstly vacuumed then filled with 70%: 30%

methane: air (v/v) (see above for the method for purging methane) and batch cultures were maintained at 20 °C without shaking for 48 h. BM supplemented with CH_4 without *R. glutinis* served as a non-biological CH_4 dissolution control.

Methane samples were collected from the vial headspace every 24 h using an air-tight syringe (Hamilton; 100 lL, Model 1710 RN, Grace Davison Discovery Science, Vic., Australia) for analysis by gas chromatography equipped with thermal conductivity and flame ionisation detectors (GC-TCD-FID; Varian-CP 3800, VIC., Australia) (Chidambarampadmavathy *et al*, 2016).

2.3.4 Analytical procedures and reagents

Methane was measured using a GC-TCD-FID fitted with a fused silica column (BR-Q PLOT; 30 m × 0.53 mm × 20 µm supplied by Bruker Pty., Ltd., Australia), containing CP-SIL 8CB, *i.e.* 5 % phenyl; 95 % dimethylpolysiloxane, D.F-0.12 as coating materials. The carrier and makeup gas were high purity helium regulated at the flow rate of 1 mL min^{-1}. The GC was calibrated using standard CH_4 gas (10–50 %), and regression factors were calculated. A gas volume of 1000 µL was used for the analysis of gas samples, which was injected by auto-sampler (Bruker, Australia), as described in (Chidambarampadmavathy *et al*, 2016).

All chemicals and reagents were purchased from Sigma-Aldrich (Castle Hill, NSW, Australia) and gases (CH_4, helium, and compressed air) were ISO certified and supplied by BOC, a member of the Linde Group, Townsville, Australia. Calibration gases (99.9 % pure CH4, 10–50 % CH_4 with air, CO2 1–30 %) and compressed air (N2 78.08 %; O2 20.94 %) were also supplied by BOC, Townsville, Australia.

2.4 Results and Discussion

Repetition of the experimental condition of Wolf and Hanson (1979) omitting CO_2 showed that *R. glutinis* did not fix CH_4. Instead, the observed decline of CH_4 concentrations was due to the dissolution of CH_4 into the medium (non-organism control, Fig. 2.1). Wolf and Hanson (1979) used radio-isotopic labelling for determination and measurement of conversion of $^{14}CH_4$ to $^{14}CO_2$ and incorporation of radiolabelled carbon into centrifuged biomass, with no centrifugation conditions specified. The rate of CH_4, oxidation was also determined using a Rank oxygen electrode. *Rhodothorula glutinis* was obtained during an enrichment for facultative CH_4-oxidizing bacteria from soil samples, although a mixture of antibiotics was used during the isolation of yeast species, no antibiotics were applied during methane oxidation experiments. Therefore it is possible that methanotrophic bacteria were not eliminated during the isolation/purification process, as most methanotrophic bacteria are capable of forming cysts/resting spores (Hanson & Hanson, 1996), which can re-emerge in later stages of cultivation Thus, as no tests of culture axenicity were carried out, the reported methane fixation by *R. glutinis* is likely a misinterpretation due to possible cross-contamination with methanotrophic bacteria.

In addition, Wolf and Hanson (1979), conducted the methane oxidation experiment under (70% CH_4, 20% air and 10% CO_2), which results in microaerobic conditions. Although there are no reports on whether or not *R. glutinis* can grow in microaerobic conditions, type -I methanotrophic bacteria can oxidise CH_4 under these conditions without showing active growth (Chidambarampadmavathy *et al*, 2016).

Nineteen-day growth investigations of *R. glutinis* on five different carbon substrates showed that the highest growth was achieved on BM supplemented with glycerol (C3 carbon source) (Fig. 2.2), while no growth was observed with C1 carbon sources *i.e.* CH_4 (20-25%) or methanol. The growth on C2 carbon sources *i.e.* acetate and ethanol were more and less comparable (Fig. 2.3). *Rhodotorula glutinis* has been shown to grow on complex carbon substrates like glucose (Li *et al*, 2007; Schneider *et al*, 2013b; Xue *et al*, 2008), diesel (Bento & Gaylarde, 2001) and even food-wastes (Razaghi *et al*, 2016a). Thus, this indicates that *R. glutinis* can be grown on C2, C3, and more complex carbon sources, but not C1 carbon sources. In this context it is noteworthy that *R. glutinis* failed to grow on methanol, formaldehyde and formate (Wolf & Hanson, 1980; Wolf *et al*, 1980; Wolf & Hanson, 1979), which are intermediate products of bacterial CH_4 oxidation and typically readily accepted as substrates for growth by methanotrophic bacteria (Hanson & Hanson, 1996). Furthermore, due to the stability of

the CH_4 molecule, all known methanotrophic bacteria use an enzyme known as methane monooxygenases (MMO) which is essential for catalysing the oxidation of methane to methanol, *i.e.* methanol is a key intermediary molecule in the methane oxidation pathway (Hanson & Hanson, 1996). Similarly, in methylotrophic yeasts like *Pichia pastoris* which are able to assimilate/ utilise methanol directly as a sole carbon source (Yurimoto *et al*, 2011) and possess the enzyme alcohol oxidase (AOX), which is necessary for oxidation of methanol (Couderc & Baratti, 2014), but neither the presence of the MMO nor AOX enzymes has been reported for *R. glutinis*. Wolf *et al* (1980), proposed that increased number of micro-bodies in cells of *R. glutinis* grown in CH_4 may be related to the presence of alcohol oxidase but the presence of alcohol oxidase was not confirmed, and the chemical pathway of either methane and methanol utilisation was not investigated in their study. Additionally, Wolf et al 1980 localised catalase activity to micro-bodies and suggested a role for it in eukaryotic methane oxidation. Catalases are a very diverse group of enzymes present in any living cell and serve the purpose to detoxify highly reactive oxygen species (ROS, *i.e.* H_2O_2); based on this it seems unlikely that the presence of catalases would be a suitable marker for methane oxidation/metabolism in cells (Chelikani *et al*, 2004).

In this regard, future research must ascertain whether or not *R. glutinis* has the biochemical capacity to oxidise methane in the first place, using methanotrophic bacterial MMO sequences in search for their potential yeast counterparts, granting, that methane is a biologically resilient molecule with a tetrahedral arrangement. Therefore it is expected that the catalytic centres of the MMOs should be highly conserved (high sequence homology) among different species.

2.5 Conclusion

Our results show that the C1 carbon sources, CH_4 and methanol do not support the growth of *R. glutinis* which suggests that earlier reports by Wolf and Hanson (1979), Wolf and Hanson (1980), Wolf *et al* (1980) on methano-/methylotrophy in *R. glutinis* could represent substrate dissolution misinterpreted as biological conversion. Lack of CH_4 and methanol utilisation by the yeast forestalls the objective to use CH_4 as a cheap, abundant carbon source for the cultivation of *R. glutinis* for co-production of cheaper immunotherapeutics, such as human interferon gamma and co-products (*e.g.* carotenes, lipids, etc.).

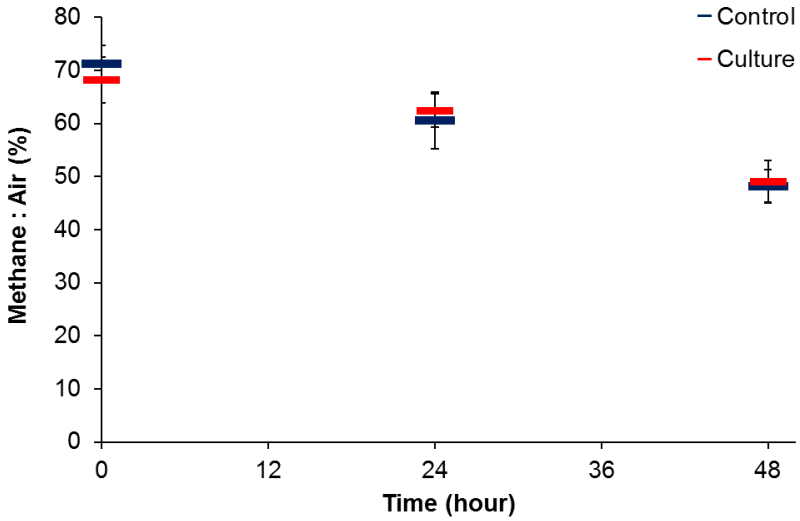

Figure 2.1 Methane fixation assessment of *Rhodotorula glutinis.* Headspace CH_4 concentrations were analysed by gas chromatography–mass spectrometry (GC-MS) as an indication of methane consumption. BM without an inoculum was used as a CH_4 dissolution control (Mean ± SD. n = 5).

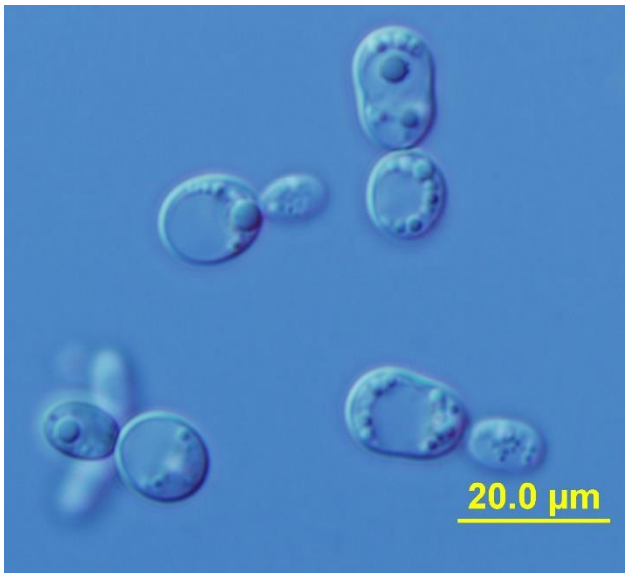

Figure 2.2 Differential interference micrograph of budding *Rhodotorula glutinis* cells (1,000x magnification, on an Olympus CX21LED, Philippines)

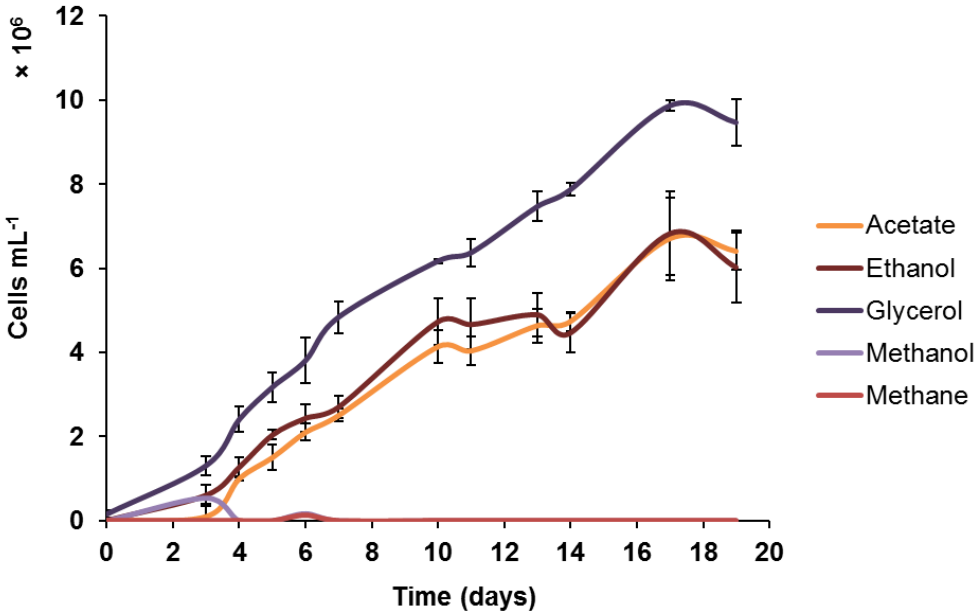

Figure 2.3 Nineteen-day growth trial of *Rhodotorula glutinis* on five carbon substrates (acetate, ethanol, glycerol, methanol and methane). Growth is presented as a number of cells per millilitre of medium (Mean ± SD. n = 3).

Chapter 3. Is *Pichia pastoris* a realistic platform for industrial production of recombinant human interferon gamma?

The following chapter is a collaborative effort of which each author's contribution is presented at the start of the thesis.

Published: Razaghi Ali, *et al*. "Is *Pichia pastoris* a realistic platform for industrial production of recombinant human interferon gamma?" *Biologicals* 45 (2017): 52-60.

3.1 Abstract

Human interferon gamma (hIFNγ) is an important cytokine in the innate and adaptive immune system and is currently produced commercially in the prokaryote *Escherichia coli.* It has also been shown to be effective against of wider range of diseases like cancer and hepatitis. Prokaryotic expression results in a short half-life, formation of hIFNγ inclusion bodies in the bacterium and potential for endotoxin contamination of the product, which do not exist in eukaryotic systems. Efficient expression of hIFNγ has been reported once for *Pichia pastoris* - a proven heterologous expression system. Based on this, we expanded the study of hIFNγ expression in *P. pastoris* using four different strains (X33: wild type; GS115: HIS-Mut^{+}; KM71H: Arg^{+}, Mut^{-} and CBS7435: Mut^{S}) and three different vectors (pPICZαA, pPIC9, and pPpT4αS). In addition, transformations included using the natural sequence (NS) and two codon-optimised sequences (COS1 and COS2) for *P. pastoris*. Following methanol induction, no expression/ secretion of hIFNγ was detected in X33 with highest levels recorded for CBS7435: Mut^{S} (~16 µg L^{-1}). RT-qPCR for GS115-pPIC9-COS1 proved low abundance of mRNA, based on mRNA copy number calculations. In contrast to the previous report, we conclude that this platform system is not an economically viable platform for commercial production of low-cost, high-quality eukaryotic recombinant hIFNγ. It is therefore recommended that commercial production focuses on other eukaryotic expression systems such as Chinese hamster ovary cells (CHO) and that research is designed to unravel the cause of low expression in the yeast to overcome that hurdle for economic viability.

3.2 Introduction

Natural human interferon gamma (hIFNγ) is a glycoprotein comprised of 166 amino acids including a secretory signal sequence of 23 amino acids, encoded by a single gene on chromosome 12 (Marciano *et al*, 2004; Schroder *et al*, 2004). hIFNγ is classed a cytokine with miscellaneous functions in the regulation of innate and adaptive immune system responses. It has been reported to be an immuno-modulatory clinically effective drug due to its pleiotropic effects against a wide range of diseases like cancers, hepatitis, and tuberculosis (Chung *et al*, 2013).

To date, commercial production of recombinant hIFNγ is limited to expression in *Escherichia coli*, which is branded as Actimmune® and approved by the US-Food & Drug Administration, (FDA) for the treatment of chronic granulomatous disease and severe malignant osteopetrosis (Marciano *et al*, 2004; Schroder *et al*, 2004). This recombinant form of hIFNγ is an unglycosylated monomer composed of 143 amino acids, rendering it less protease-resistant, resulting in a shorter half-life in the bloodstream compared to the glycosylated form (Chung *et al*, 2013; Marciano *et al*, 2004; Schroder *et al*, 2004). Other drawbacks associated with *E. coli* expression systems include the potential for endotoxin contamination and the formation of intracellular protein aggregates, termed inclusion bodies, requiring a complex purification and protein refolding process. This increases the final cost of the product (Chung *et al*, 2013).

To overcome these limitations, expression of recombinant hIFNγ was attempted in various hosts like *Saccharomyces cerevisiae* 20B-12 (Derynck *et al*, 1983), insect cells lines *Spodoptera frugiperda*, *S. exigua,* and *S. litura*. (Chen *et al*, 2011), Chinese hamster ovary (CHO) (Chung *et al*, 2013; Fox *et al*, 2004), wild-type mice strain C57BL/6 (Bagis *et al*, 2011), rat cell line 3Y1-B (Nakajima *et al*, 1992), monkey and human cells (Gray *et al*, 1982); however; high costs of cultivation and purification, contamination, low yields, low biological activity and short half-life of the product also adversely impacted by the use of these expression systems(Moharir *et al*, 2013; Wang *et al*, 2014).

Another yeast-based expression system for recombinant hIFNγ is the methylotrophic yeast, *Pichia pastoris* (synonym. *Komagataella pastoris*), a proven successful heterologous expression system for the production of hundreds of recombinant proteins (Ahmad *et al*, 2014). The *Pichia pastoris* expression systems offer distinct advantages such as easy manipulation, high cell densities, cultivation in low acidity reducing the chance of contamination, low cost of production, eukaryotic post-

translational modification and secretion, including protein folding and glycosylation (Ahmad *et al*, 2014).

Commercially available *P. pastoris* strains are the auxotrophic strains GS115 (the *HIS4* mutant), KM71H (the *AOX1* and *ARG4* mutant), the reconstituted prototrophic strain X-33 and protease-deficient strains such as SMD1168. However, use of these strains for commercial applications is restricted by intellectual property (Ahmad *et al*, 2014). In contrast, some strains of *P. pastoris* like CBS7435, are not protected by patent and, thus represent an alternative for production purposes (Ahmad *et al*, 2014).

The most commonly used promoter capable of driving recombinant protein expression in *P. pastoris* is the strong alcohol oxidase (*AOX*) promoter which is only inducible with methanol (Pla *et al*, 2006). Two *AOX* operons can be found in the *P. pastoris* chromosome: *AOX1* is responsible for the major *AOX* activity, and *AOX2*, which plays a minor role (Pla *et al*, 2006). Recombinant gene techniques for transformation of *P. pastoris* can leave either, or both *AOX* gene sets functional, only the *AOX2*, or neither. Thus, the resulting phenotypes are referred to as Mut^{+} (methanol utilisation plus), Mut^{S} (methanol utilisation slow), or Mut^{-} (methanol utilisation minus), respectively. Expression efficiency for a recombinant protein in a particular recombinant is not predictable, and available information is at odds in this respect (Pla *et al*, 2006).

This study was based on the study by Wang *et al* (2014) using native and *P. pastoris* codon-optimised sequences of hIFNγ and expanded the study using eight combinations of *P. pastoris* strains, vectors and sequences. Surprisingly, expression were orders of magnitudes lower than previously reported (Wang *et al*, 2014).

3.3 Material and Methods

3.3.1 Strains, sequences, vectors and cloning

Strains

Four strains of *P. pastoris* with different characteristics were used; **X33:** wild-type strain containing two active *AOX* genes resulting in Mut^+ phenotype, **GS115:** A His^- mutant (mutation of *HIS4*), with the His^- Mut^+ phenotypes, **KM71H:** A mutant strain with *ARG4* (arginosuccinate lyase) and disruption of *AOX1*, creating a Mut^S Arg^+ phenotype, **CBS7435, Mut^S:** a knockout of the *AOX1* gene derived from the wild-type CBS7435 strain.

Sequences

In this study, two distinct codon-optimised sequences of *hIFNγ* were synthesised based on the codon preference of *P. pastoris* by Invitrogen™, GeneArt™ Strings, and one copy of the native sequence of *hIFNγ* "NCBI: NM_000610.2; UniProtKB: P01579" was used as a positive control (Fig. 3.1).

Vectors

The vectors used in this study for the transformation of *P. pastoris* are shown in (Fig. 3.2). **pPIC9:** was provided by Invitrogen™ (catalogue no. K1710-01). This plasmid contains a methanol-inducible *AOX1* promoter, the α-mating secretion signal at the 5' end of the gene of interest (GOI) and the *HIS4* gene for selection enabling the GS115 strain to biosynthesise histidine. The sequence of the GOI was inserted at *NotI* and *EcoRI* restriction sites. Then, the construct was linearized using *SalI* restriction endonuclease prior to transformation. **pPICZαA:** was provided by Invitrogen™ (catalogue no. K1710-01). This plasmid contains a methanol-inducible *AOX1* promoter, the α-mating secretion signal, and a polyhistidine tag (HIS-tag) at 5.' and 3' ends of the GOI, respectively. The Zeocin™ resistance gene (*Sh ble*) is placed in the plasmid which allows selection of successful transformants on Zeocin™ containing medium plates. The sequence of the GOI was inserted at *EcoRI* and *NotI* restriction sites. Then, 5 µg of the construct was linearized using *SacI* restriction endonuclease prior to transformation. **pPpT4αS:** was provided by Protein Expression Facility at The University of Queensland (Brisbane, Australia).

```
NS      ATGAAATATACAAGTTATATCTTGGCTTTTCAGCTCTGCATCGTTTTGGGTTCTCTTGGC
COS1    ATGAAGTACACATCCTACATCTTGGCTTTCCAGTTGTGTATCGTTTTGGGTTCCTTGGGT
COS2    ATGAAATACACCTCTTATATACTTGCCTTCCAGTTATGCATTGTCTTGGGTAGTCTGGGG
        ***** ** **    ** **  * ** ** *** * ** ** ** ******    * **

NS      TGTTACTGCCAGGACCCATATGTAAAAGAAGCAGAAAACCTTAAGAAATATTTTAATGCA
COS1    TGTTACTGTCAGGACCCATACGTTAAGGAAGCTGAGAACTTGAAGAAGTACTTCAACGCT
COS2    TGTTATTGCCAAGATCCATATGTGAAAGAAGCCGAAAACCTGAAAAAGTACTTCAACGCC
        ***** ** ** ** ***** ** ** ***** ** *** * ** ** ** ** ** **

NS      GGTCATTCAGATGTAGCGGATAATGGAACTCTTTTCTTAGGCATTTTGAAGAATTGGAAA
COS1    GGTCACTCCGACGTTGCTGATAACGGTACTTTGTTCTTGGGTATCTTGAAGAACTGGAAA
COS2    GGACATAGTGATGTTGCAGACAACGGCACACTATTTCTTGGTATTCTAAAGAACTGGAAG
        ** **    ** ** ** ** ** ** **  * **  * ** **  * ***** *****

NS      GAGGAGAGTGACAGAAAAATAATGCAGAGCCAAATTGTCTCCTTTTACTTCAAACTTTTT
COS1    GAAGAGTCCGACAGAAAGATCATGCAGTCCCAGATCGTTTCATTCTACTTCAAGTTGTTC
COS2    GAGGAGTCTGACCGTAAAATTATGCAATCACAAATCGTTTCTTTTTACTTTAAACTATTC
        ** ***   *** * ** ** *****    ** ** ** ** ** ***** **  * **

NS      AAAAACTTTAAAGATGACCAGAGCATCCAAAAGAGTGTGGAGACCATCAAGGAAGACATG
COS1    AAGAACTTCAAGGACGACCAGTCCATCCAGAAGTCCGTTGAGACTATCAAAGAAGATATG
COS2    AAAAATTTTAAAGATGACCAATCAATTCAAAAGTCCGTTGAGACGATTAAAGAAGATATG
        ** ** ** ** ** *****    ** ** ***   ** ***** ** ** ***** ***

NS      AATGTCAAGTTTTTCAATAGCAACAAAAAGAAACGAGATGACTTCGAAAAGCTGACTAAT
COS1    AACGTTAAGTTCTTCAACTCCAACAAGAAAAAGAGAGATGACTTCGAGAAGTTGACTAAC
COS2    AATGTCAAGTTTTTCAACTCAAACAAAAAGAAGAGGGACGACTTTGAAAAGTTAACTAAT
        ** ** ***** *****    ***** ** **  * ** ***** ** *** * *****

NS      TATTCGGTAACTGACTTGAATGTCCAACGCAAAGCAATACATGAACTCATCCAAGTGATG
COS1    TACTCCGTTACTGACTTGAACGTTCAGAGAAAGGCTATCCACGAGTTGATCCAGGTTATG
COS2    TATTCCGTAACCGATTTGAACGTTCAGAGGAAGGCAATCCATGAGTTGATACAGGTTATG
        ** ** ** ** ** ***** ** **  * ** ** ** ** **  * ** ** ** ***

NS      GCTGAACTGTCGCCAGCAGCTAAAACAGGGAAGCGAAAAAGGAGTCAGATGCTGTTTCGA
COS1    GCTGAATTGTCTCCAGCTGCTAAGACTGGTAAGAGAAAAAGATCCCAGATGTTGTTCAGA
COS2    GCAGAACTGTCCCCCGCTGCCAAAACAGGAAAGAGAAAAAGATCACAAATGCTTTTCAGG
        ** *** **** ** ** ** ** ** ** *** *******    ** *** * **  *

NS      GGTCGAAGAGCATCCCAGTAA
COS1    GGTAGAAGAGCTTCCCAGTAA
COS2    GGTAGACGTGCTTCTCAATAA
        *** ** * ** ** ** ***

POI     MQDPYVKEAENLKKYFNAGHSDVADNGTLFLGILKNWKEESDRKIMQSQIVSFYFKLFKN
        FKDDQSIQKSVETIKEDMNVKFFNSNKKKRDDFEKLTNYSVTDLNVQRKAIHELIQVMAE
        LSPAAKTGKRKRSQMLFRGRRASQ
```

Figure 3.1 DNA sequences of *hIFNγ*; **NS:** Native sequence, **COS1:** Codon-optimised sequence 1, **COS2**[1]**:** Codon-optimised sequence 2. **POI:** Protein of interest *i.e. an* amino acid sequence of hIFNγ. **(*):** Presence of this symbol shows the similarity in the bases. The first 23 amino acid sequence (eq. 69 bp nucleotides) is the native secretion signal at the N-terminal of the amino acid sequence.

[1] **Footnote;** In this study, several codon-optimised sequences were designed for *P. pastoris* based on codon preference. COS1 was selected according to similarity of GC% and T_m to the NS. Upon review, RNA truncation due polyadenylation (poly A) signals appeared possible. COS2 was designed by replacing putative poly A signals (bases 292-297, 331-338 and 457-466) and lowering the predicted minimum free energy (MFE) of the mRNA compared to COS1 (section Chapter 0).

This plasmid contains the methanol-inducible *AOX1* promoter and the α-mating secretion signal at the 5' end of the GOI. The Zeocin™ resistance gene (*Sh ble*) was placed in the plasmid which allows selection of successful transformants on Zeocin™ containing medium plates (Näätsaari *et al*, 2012) The native secretion signal was omitted from the sequence of the GOI followed by insertion at *SnaBI* and *NotI* restriction sites. Then, 5 µg of the construct was linearized using *SwaI* restriction endonuclease prior to transformation.

Gene sequences in vectors (pPICZαA and pPpT4αS) were verified by using ABI BigDye Terminator v3.1 sequencing, conducted by the Australian Genome Research Facility (AGRF). Data analysis was performed using the software Sequencer™ 4.7 (Gene Codes Corporation).

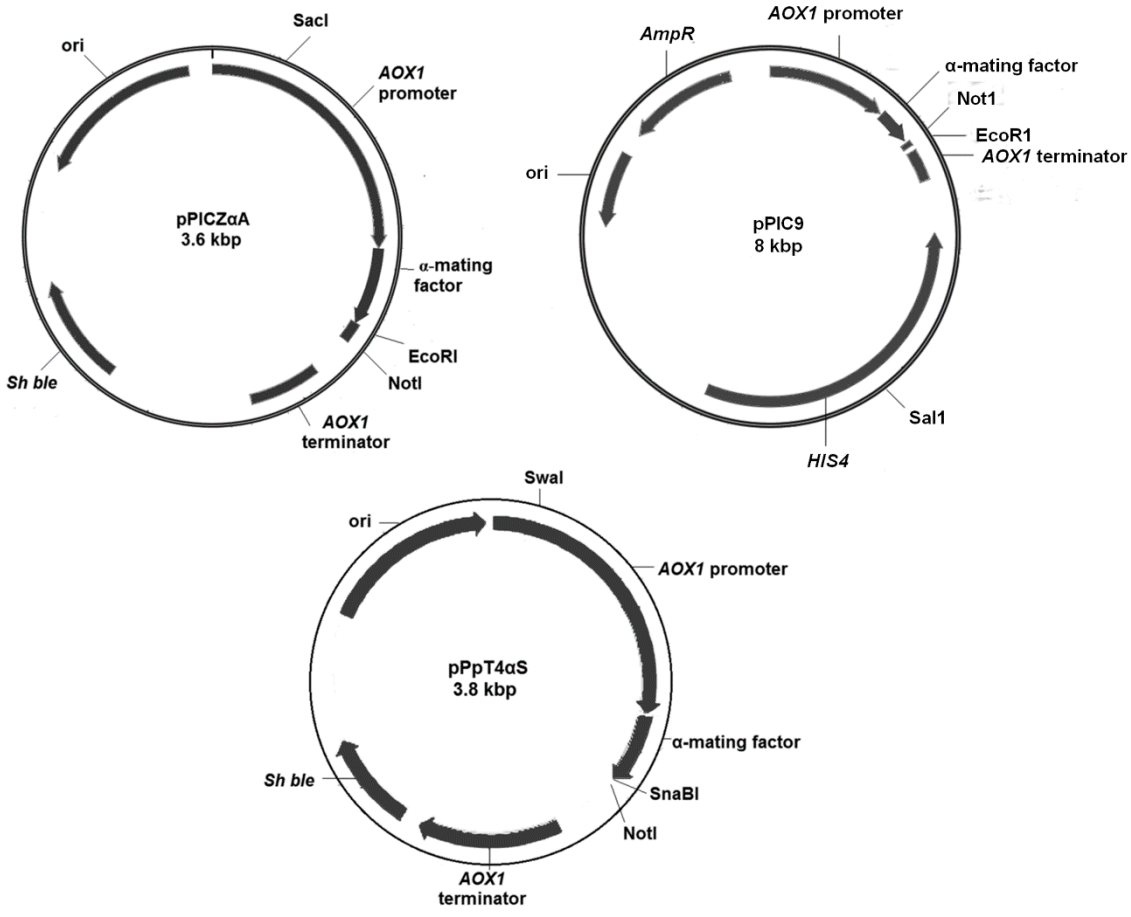

Figure 3.2 Generic plasmid vector maps of pPIC9, pPICZαA, pPpT4αS. **Ori:** the origin of replication, for more information consult the text. **6His-tag:** polyhistidine tag. ***Sh ble***: The Zeocin™ resistance gene ***AOX***: alcohol oxidase gene.

3.3.2 Transformation into *Pichia pastoris*

Order of transformation

In order to generate the construct; each sequence was flanked with suitable restriction enzymes listed in (Fig. 3.2) and inserted into the vectors between the same restriction sites. Prior to transformation, each construct was linearized using suitable restriction enzymes for the vector (Fig. 3.2). The combinational order for generating each transformant is listed in (Table 3.1).

Table 3.1 Combinational order of expression systems, strains, vectors and sequences which have been used for cloning and transformation.

Expression system	Strain	Vector	Sequence of GOI	Transformant	Phenotype
Pichia pastoris	GS115	pPIC9	COS1	GS115- pPIC9-COS1	His^+Mut^+
			COS2	GS115- pPIC9-COS2	
	X33	pPICZαA	NS	X33- pPICZαA-NS	Mut^+
			COS2	X33- pPICZαA-COS2	
		pPpT4αS	COS2	X33- pPpT4As-COS2	Mut^+
	KM71H	pPICZαA	NS	KM71H- pPICZαA-NS	Mut^S
			COS2	KM71H- pPICZαA-COS2	
	CBS7435	pPpT4αS	COS2	CBS7435-pPpT4As-COS2	Mut^S

NS: Natural sequence, **COS1:** Codon-optimised sequence 1, **COS2:** Codon-optimised sequence 2.

Electroporation of Pichia pastoris

Each plasmid pPIC9-COS1 & pPIC9-COS2 were linearized with suitable corresponding restriction enzymes (Fig. 3.2) and then transformed into the *P. pastoris* GS115 strain by electroporation (Electroporator 2510™, Eppendorf) following the protocols for electro-competent cell production and electroporation (Invitrogen™).
Each plasmid pPICZα-NS, pPICZα-COS2, pPpT4αS-NS & pPpT4αS-COS2, were linearized with suitable corresponding restriction enzymes (Fig. 3.2) and then transformed into either X33, KM71H or CBS7435 strains of *P. pastoris* by electroporation (Electroporator Thermo Hybaid CelljecT Pro®, ADP-400) following the protocols for electro-competent cell production and electroporation (Lin-Cereghino *et al*, 2005).

Screening for transformants

pPIC9-COS1 & pPIC9-COS2-transformed GS115 (Table 3.1) were screened for HIS^+ phenotype on Minimal Dextrose (MD) (1.34% Yeast Nitrogen Base (YNB), 2% dextrose) agar plates in 30°C, as successful transformants should have regained histidine auxotrophy. With the intention of determining the methanol utilisation (Mut) phenotype of the strain, colonies with HIS^+ phenotype were re-plated on Minimal Methanol (MM) (1.34% YNB, 0.5% methanol) as the sole carbon source, the methanol utilisation plus (Mut^+) phenotype was chosen by the ability to grow on both media agar plates after 24 h while methanol utilisation slow (Mut^S) cells grow normally on MD, but their growth on MM was negligible.
The remainder of the transformants which were obtained from other strains of *P. pastoris i.e.* X33, KM71H and CBS7435 (Table 3.1) were selected by plating onto selective medium (1% Yeast 2% Peptone 1% Dextrose plus Zeocin™ 100 µg mL^{-1}) after 5 days' incubation at 30°C.

Confirmation of integration into gDNA by PCR

To determine, whether *hIFNγ* was integrated into the *P. pastoris* genome, colony PCR was conducted for X33, KM71H and CBS7435 transformants, while genomic DNA was extracted from GS115 transformants using the Wizard® Genomic DNA Purification Kit, (Promega) for PCR. The integration of *hIFNγ* into the genome of *P. pastoris* was confirmed by PCR using primers listed in Table 3.2. Genomic DNA of untransformed *P. pastoris* strains was used as a negative control. PCR amplification was run according to the standard protocol for *P. pastoris* (Invitrogen™).
Successful integration of *hIFNγ* into *P. pastoris* genome was demonstrated by detecting the expected ~500-800 bp fragment size using agarose (1.5%) gel electrophoresis.

Table 3.2 Primer sequences for each vector and their hybridising points on the target DNA.			
Transformant	**Primer sequence**		**Hybridising point**
GS115-pPIC9-COS1/ COS2	Forward	5´TACTATTGCCAGCATTGCTGC3´	5' end of the α-factor region
	Reverse	5´GCAAATGGCATTCTGACATCC3´	3´ end of the *AOX1* TT
X33-pPICZαA-NS	Forward	5'GAGAAAAGAGAGGCTGAAGCTCAGGACCCATATGTAAAAGAAGC3'	5' end of the GOI
	Reverse	5'GTTCTAGAAAGCTGGCGGCCTTAATGATGATGGTGGTGATGCTGGGATGCTCTTCGACCT3'	3' end of the GOI
X33-pPICZαA-COS2	Forward	5'GAGAAAAGAGAGGCTGAAGCTCAAGATCCATATGTCAAAGAAGC3'	5' end of the GOI
	Reverse	5'TTCTAGAAAGCTGGCGGCCTTAATGATGATGGTGGTGATGCTGAGAAGCTCTTCTACCTC3'	3' end of the GOI
X33-pPpT4αS-COS2	Forward	5'GACTGGTTCCAATTGACAAGC3'	3' end of the *AOX* promoter
	Reverse	5'GGCATTCTGACATCCTCTTGATTACTGAGAAGCTCTTCTACCTC3'	3' end of the GOI
KM71H-pPICZαA-NS	Forward	5'GACTGGTTCCAATTGACAAGC3'	3' end of the *AOX* promoter
	Reverse	5'GTTCTAGAAAGCTGGCGGCCTTAATGATGATGGTGGTGATGCTGGGATGCTCTTCGACCT3'	3' end of the GOI
KM71H-pPICZαA-COS2	Forward	5'GAGAAAAGAGAGGCTGAAGCTCAAGATCCATATGTCAAAGAAGC3'	5' end of the GOI
	Reverse	5'TTCTAGAAAGCTGGCGGCCTTAATGATGATGGTGGTGATGCTGAGAAGCTCTTCTACCTC3'	3' end of the GOI
CB7435-pPpT4αS-COS2	Forward	5'GAAGAGAGAGGCCGAAGCTCATCACCACCATCATCATCAAGATCCATATGTCAAAGAAGC3'	5' end of the GOI
	Reverse	5'CCCAAACCCCTACCACAA3'	3' *AOX1* TT
GOI: gene of interest (*i.e. hIFNγ*), ***AOX1* TT*:*** *AOX* transcription terminator.			

3.3.3 Expression of hIFNγ

Standard expression in P. pastoris in buffered medium

Transformant cells (GS115-pPIC9-COS1 and GS115-pPIC9-COS2) were cultivated in 25 mL buffered Minimal Glycerol (BMGY) medium (1.34% YNB, 1% glycerol,100 mM potassium phosphate, pH 6.0) in a 250 mL baffled flask and incubated for 48 h at 28°C on a shaking plate at 200 rpm until reaching an $OD_{600} \geq 2$ (log-phase growth) (EnSpire® Multimode Plate Reader, PerkinElmer). Next, the cells were harvested by centrifugation for 5 min at 3,000 *g* at room temperature. Then, cell pellets were resuspended in 50 mL PBS buffer (0.1 M Phosphate Buffer Saline, pH 7.4) to wash off residual glycerol. Finally, cell pellets were resuspended in 50 mL buffered methanol-complex (BMMY) medium (2% peptone, 1% yeast extract, 1.34% YNB, 1% methanol, 100 mM potassium phosphate, pH 6.0) to a starting OD_{600} =1 in a 250 mL baffled flask. Methanol was added to a final concentration of 1% (v/v) every 24 h to induce expression of hIFNγ. The culture supernatant was obtained after 72 h of cultivation by

centrifugation at 1,500 *g* for 5 min to analyse the expression of hIFNγ*,* untransformed *P. pastoris* GS115 cell culture was used as negative control (Razaghi *et al*, 2015).

High throughput expression in P. pastoris in buffered medium

Small-scale expression screens were performed in 24 deep-well plates for the transformant strains of X33, KM71H, and CBS7435. It was shown that oxygenation for the deep well plates used was comparable to levels achieved in baffled flasks (Nielsen, 2003). Following inoculation of 5 mL BMGY media with a single colony, cultures were grown at 30°C with shaking at 250 rpm for 48 h. Then, the BMGY media was removed by centrifugation at 1,000 *g* for 10 min, and each cell pellet was washed with 4 mL of PBS twice. After the second wash, the cell pellets were resuspended in 5 mL of BMMY medium to induce expression. Methanol was added to 1% (v/v) every 24 h until harvest. Samples were harvested 96-hour post-induction (hpi) for analysis. Untransformed strains of X33 (Mut^+), CBS7435 (Mut^S) and KM71H (Mut^S) were used as negative controls, and a positive control (P-Protein) was cultured along with the test clones.

Expression in P. pastoris in unbuffered medium

There are some recombinant proteins susceptible to proteases after secretion into the culture medium. In this case, it is usually possible to use unbuffered media such as Minimal Glycerol Medium (MGY) (1.34% YNB and 1% glycerol) and Minimal Methanol (MM) (1.34% YNB and 1% methanol) to inactivate secreted proteases, as the pH drops to 3 or below during cultivation, inactivating many proteases, while *P. pastoris* is tolerant to the acidic condition (Valencia Jiménez *et al*, 2014). Expression was performed in unbuffered MGY/MM instead of BMGY/BMMY following the same protocol as detailed in Chapter 4.

3.3.4 Cell lysis for protein extraction

A modified version of the standard cell lysis technique for *P. pastoris* was used (Invitrogen™) following this procedure; 1 mL of culture (as detailed in Chapter 4) was centrifuged for 5 min at 3,000 *g* to remove the supernatant then washed once in Breaking Buffer (50 mM sodium phosphate, pH 7.4, 1 mM EDTA, 5% glycerol plus 1 dissolved tablet of Sigma FAST™ Protease Inhibitor Cocktail Tablet #S8830 in 100 mL

of distilled water) by resuspension and centrifugation at 3,000 *g* at 4°C for 5 min. Cells were resuspended in 1 mL of Breaking Buffer, and an equal volume of acid-washed glass beads was added, the mixture was vortexed for 30 s, then incubated on ice for 30 s, which was repeated 7 times. The sample was centrifuged at 4°C for 5 min at 12,000 *g,* and hIFNγ was quantified by ELISA of the cleared supernatants. Cell lysates of untransformed *P. pastoris* GS115 were used as negative controls.

3.3.5 SDS-PAGE and western blotting

Sample supernatants were loaded on 4-12% Bis-Tris SDS-PAGE under denatured and reduced conditions (using NuPAGE® LDS sample buffer, catalogue no. NP0007). Novex® Sharp Pre-Stained Protein Standard (Catalogue no: LC5800, ThermoFishers™) was used as molecular weight ladder ranging 3.5-260 kDa. Gels were blotted to PVDF membrane and probed with the polyhistidine-HRP conjugated antibody (Miltenyi Biotec, catalogue no. 130-092-785, Lot# 5141126111) at a dilution of 1: 6,000. The analysis was performed using a Bio-Rad Chemi-Doc™ XRS+ imaging system, and the molecular weight was calculated using ProtParam.

3.3.6 ELISA

Recombinant hIFNγ protein levels were quantified by indirect ELISA. A standard curve 0, 1.25, 2.5, 5, 10, 20 µg L^{-1} (R^2=0.9904 and $y = 13.981x - 1.7371$) was prepared by serial dilution of the recombinant hIFNγ (Abcam catalogue no. ab51240) (Razaghi *et al*, 2015).

3.3.7 Detection and determination of mRNA copy number by RT-qPCR

PureLink® RNA Mini Kit (Life Technologies™ catalogue no. 12183018A) was used for extraction of total RNA equivalent to ~16.66 × 10^3 amount of yeast cells (GS115-pPIC9-COS1), followed by reverse transcription to cDNA using the Tetro cDNA Synthesis Kit (BIOLINE catalogue no. BIO-65050). This kit applies both Oligo dT (18) primers for priming cDNA synthesis; using the poly-A tail found at the 3' end of the eukaryotic mRNAs that ensures the 3' end of mRNAs is represented, and random hexamer primers which randomly cover all regions of the RNA to create a cDNA pool. The synthesised cDNA was divided into equal triplicates for treatment with the QuantiTect SYBR® Green PCR Kit (Qiagen catalogue no. 204141) for the two-step reverse transcription-PCR (RT-qPCR; determining copy number of mRNA transcript)

using primers forward 5´ACTTCAACGCTGGTCACTC 3´ and reverse 5´ CGGACTTCTGGATGGACTG 3´ to amplify 168 bp amplicon close to the 5´ end of the COS1 *hIFNγ* sequence (Razaghi *et al*, 2015).

Standard curves for qPCR were prepared with purified DNA amplicons of 699 bp of which 501 bp belong to the hIFNγ gene (section Chapter 4). Dilution series of DNA amplicons according to copy number (n/per total volume of reaction) were used to prepare standard curve with 0, 1.33×10^2, 1.33×10^3, 1.33×10^4 and 1.33×10^5 copy number ($R^2 = 0.998$, Overall efficiency=101% and $y = 10^9 . e^{-0.699x}$)

Each 50 µL reactions contained 25 µL (2x) QuantiTec SYBR® GreenPCR Master Mix, 10 µM forward and reverse primers with final concentrations of 0.3 µM (5 µL each), 6 µL sample (~2 µg cDNA quantified by NanoDrop®, ND-1000 Spectrophotometer) and 9 µL RNase-free water. qPCR reactions were run on a Peltier Thermal Cycler-200 (BioRad) (Razaghi *et al*, 2015). Total RNA of untransformed *P. pastoris* GS115 was used as a negative control.

Approximate copy number of hIFNγ mRNA transcripts per cell were calculated as per equation 1 (eq. 1);

$$Approx.\, hIFN\gamma\ mRNA\ transcript \left(\frac{Copy\ number}{Cell\ number\ per\ batch\ of\ reaction}\right) \approx {}^{Determined\ copy\ number\ of\ transcripts\ \ per\ volume\ of\ reaction}/_{16.66 \times 10^3}$$

(eq. 1)

3.3.8 Prediction of mRNA secondary structure

RNA secondary structure regulates expression of many gene transcripts, and plays a substantial role in regulating transcription, splicing RNA, editing, and transcript degradation and translation. RNA secondary structure is formed through hydrogen-bonding between pairs of complementary nucleotides in a transcript. In order to study the functional role of a transcript, it suffices to know its RNA secondary structure (Proctor & Meyer, 2013). All RNA folding tools calculate the minimum free energy (MFE) by adding up individual energy contributions from base pair stacking, bulges, hairpins, internal loops and multi-branch loops. The RNAfold server was selected for analysis, because it uses both the Wuchty algorithm and the McCaskill algorithm, which offers a wide variety of functions, having the benefit of computing all possible secondary structures within a narrow free-energy range (Gruber *et al*, 2008; Schroeder,

2009). This approach leads to the creation of one most likely structure. In contrast, some software servers predict secondary structures by calculating thermodynamics, *e.g.* UNAfold and RNA Structure use the Zuker algorithms to calculate the MFE and systematically sample structures within a percentage range of free-energy to create a set of diverse sub-optimal structures without providing a preference for the most likely outcome. Thus in this study, in order to predict the secondary structure of each hIFNγ mRNAs, minimum free energy (MFE) structures and base pair probabilities from single RNA sequences, RNAfold WebServer (Vienna RNA Websuite) was used (Gruber *et al*, 2008).

3.4 Results

3.4.1 Confirmation of integration into *P. pastoris*

PCR products were amplified at the expected size for ~ 50 clones for all constructs using gene-specific forward and reverse primers. Amplification resulted in bands of the correct sizes of 0.5-1 kbp which was confirmed by sequence analysis at the AGRF demonstrating successful integration of the *hIFNγ* gene into the yeast genome.

3.4.2 SDS-PAGE & Western blotting

Secretion of hIFNγ in *P. pastoris* cultures was not detected using SDS-PAGE and anti-His Western blotting analysis. In contrast, expression of secreted positive control (P-Protein) was observed.

3.4.3 ELISA

Low expression of secreted hIFNγ was detected in some transformant cells of *P. pastoris* (Table 3.3), with highest levels found in CB7435- pPpT4αS-COS2 and lowest in GS115-pPIC9-COS1, indicating that codon-optimisation of the sequence had no impact on expression yields. This was confirmed by non-detectable yields in the X33 strains transformed with the NS and COS2 sequences of hIFNγ, respectively. As the latter results were also independent of vector used, this also indicates that expression of hIFNγ was strain-dependent and affected by their resulting phenotype rather than the choice of vector and gene codon optimisation.

ELISA analysis of cell lysates of *P. pastoris* GS115-pPIC9-COS2 transformants demonstrated that hIFNγ was successfully secreted to medium (Table 3.3). GS115-pPIC9-COS2 transformant cells cultivated in unbuffered media yielded similar amounts of secreted hIFNγ to that using buffered medium (Table 3.3) suggesting that extracellular proteolytic degradation of the product not be the cause of low yields. Despite the low expression, expression was enhanced 10-fold in using the codon-optimised sequence COS2 which had a lower MFE (GS115-pPIC9-COS2 in comparison to GS115-pPIC9-COS1 (Table 3.3)) (Section Chapter 4).

Table 3.3 Maximal yield of secreted hIFNγ expressed in *P. pastoris* after 72 hpi (Mean ± SD, n = 3)

Transformant (Strain-vector-sequence)		Phenotype	Material Analysed	Max. Yield (μg L^{-1})
Pichia pastoris	GS115-pPIC9-COS1	His^+Mut^+	Supernatant/buffered	0.17 ± 0.02
	GS115-pPIC9-COS2	His^+Mut^+	Supernatant/buffered	1.8 ± 0.06
			Cell lysate/buffered	0.4 ± 0.2
			Supernatant/unbuffered	1 ± 0.2
	X33- pPICZαA-NS	Mut^+	Supernatant/buffered	n.d.
	X33- pPICZαA-COS2	Mut^+	Supernatant/buffered	n.d.
	X33- pPpT4αS-COS2	Mut^+	Supernatant/buffered	n.d
	KM71H- pPICZαA-NS	Mut^S	Supernatant/buffered	12 ± 0.02
	KM71H- pPICZαA-COS2	Mut^S	Supernatant/buffered	9 ± 0.5
	CB7435- pPpT4αS-COS2	Mut^S	Supernatant/buffered	16 ± 3

n.d.: not detected

3.4.4 RNA analysis

mRNA secondary structure

Although the secondary structures of mRNAs appeared to be different in bi-dimensional models, both codon-optimised sequences possessed similar predicted levels of the MFE compared to the natural sequence of *hIFNγ*. Thus, a similar level of RNA stability would be expected (Fig. 3.3).

Detection of hIFNγ mRNA

Analysis of RT-qPCR result showed that approximately 2-3 copy number of hIFNγ mRNA were found per cell (Table 3.4), which is considered as low abundance RNA.

Table 3.4 *hIFNγ* cDNA (= mRNA) copy number of GS115-pPIC9-COS1 *P. pastoris* transformants (Mean ± SD, n = 3)

C(t)	14.4 ± 0.3
Initial copy number of *hIFNγ* cDNA per volume reaction	$43 \times 10^3 \pm 7 \times 10^3$
Approx. hIFNγ mRNA copy number per cell	2.6 ± 0.4

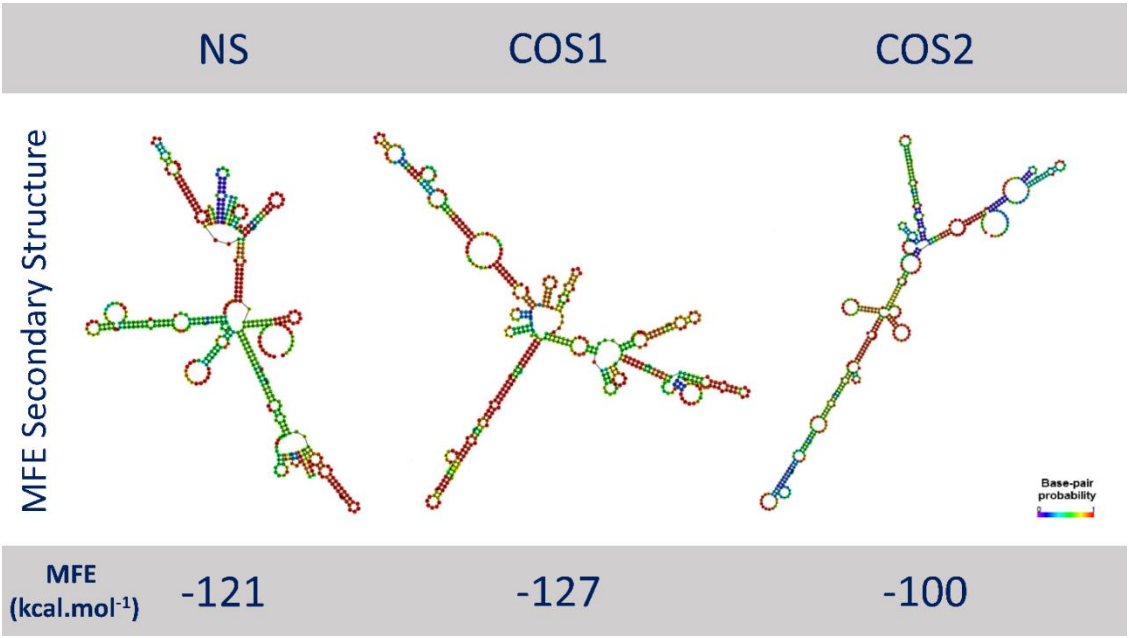

Figure 3.3 Bi-dimensional modelling of mRNA secondary structure predicted based on the MFE. **NS:** Native sequence, **COS1:** Codon-optimised sequence 1, **COS2:** Codon-optimised sequence 2

3.5 Discussion

Codon preference between the recombinant gene and expression host has been established to be one bottleneck for protein translation in heterologous expression systems, hindering the translation of the recombinant gene transcript (Gustafsson *et al*, 2004). To overcome this potential problem, codon optimisation was used to adapt the foreign recombinant gene for successful and efficient heterologous expression in yeast systems (Welch *et al*, 2009). Studies investigating the correlation between codon usage patterns and expression level for *hIFNγ* proved that codon bias exists in CHO cells (Chung *et al*, 2013; Gustafsson *et al*, 2004). In contrast, our results did not show a significant impact on the expression of codon-optimised (COS1 & COS2) and non-codon-optimised, native (NS) sequences (Table 3.3). The potential for premature RNA truncation due to the poly A signals in COS1 was refuted by proving that the poly A tail was in the correct location of the hIFNγ mRNA using reverse transcription with the Oligo dT (18) primer and a primer pair binding close to the 5´ end. This would suggest that RNA instability was not the cause of low expression. Moreover, analysis of the predicted secondary structures of mRNAs revealed more similar MFE levels of two sequences (NS, COS1) and slightly lower MFE level for the COS2 (Fig. 3.3).which could be the reason for enhancing the expression of the COS2 by 10 folds, this result is in conformity with previous reports indicating that manipulation of secondary structure

of mRNA can effectively improve translation and heterologous expression of recombinant proteins in yeast (Gaspar *et al*, 2013).

All transformants showed low to no expression of hIFNγ. However, an improvement of 100-fold was, achieved with transformants of the Mut^S phenotype (Table 3.3). Several hypotheses can be formulated to explain this outcome.

1. The large difference in yields between Mut^S and Mut^+ phenotypes could indicate that lack of the *AOX2* gene in the Mut^S phenotype would result in higher yields. This raises the question whether the activity of *AOX2* interferes with transcription of *hIFNγ*. This hypothesis can be tested by using constitutive promoters in *P. pastoris e.g.* GAP promoter.

2. Undesired proteolysis of heterologous proteins expressed in *P. pastoris* and/or inefficient secretion could have caused lower product yields of the recombinant protein (Ahmad *et al*, 2014). Proteolysis may occur in two ways; firstly, intracellularly, during vesicular transport of recombinant protein by secretory pathway-resident proteases and secondly extracellularly, by proteases being secreted or released into the culture medium (Ahmad *et al*, 2014). For example, the yield of ovine interferon τ decreased due to proteolysis and eventual degradation of the recombinant protein (Sinha *et al*, 2005). In contrast, our results render the low expression of hIFNγ due to extracellular proteolytic activity and/or incomplete secretion unlikely. Furthermore, as the α-mating factor secretion signal was incorporated into the design, neither addition nor deletion of the native secretion signal altered expression levels, as expected, and presence or absence of the His tag also had no impact.

3. A distinct possibility for the observed low expression in our study could be the low abundance of mRNA (estimated 2-3 copy numbers of hIFNγ mRNA transcripts). To explain this, it needs to be noticed that a typical average cell contains ~10-30 pg total RNA composed of ~360,000 mRNA molecules. Low abundance mRNA species may have a copy number as low as 5-15 molecules per cell (Alberts *et al*, 2014) This could be explained by assuming that either the *AOX* promoter was not activated to initiate transcription of hIFNγ mRNA or induction of *AOX2* adversely impacted on transcription of hIFNγ mRNA.

4. Intracellular degradation of the recombinant protein may be an additional cause for the low yields, which is supported by the apparent mismatch between anti-His Western blot detection and ELISA results which could have resulted in the removal of the His-

tag prior to secretion. To examine this hypothesis, the use of protease-deficient strains of *P. pastoris* in future studies could be useful.

5. Protein misfolding in the endoplasmic reticulum (ER) has been reported as one of the possible reasons for low production rates of proteins in yeast (Prabhu *et al*, 2016).

The *P. pastoris* expression system has only recently been investigated for the commercial production of hIFNγ, reporting secretion of around 300 mg L^{-1} with a specific activity of 1×10^7-1.4×10^7 IU mg^{-1}, using the pPICZα vector and the alcohol oxidase (*AOX1)* promoter (Wang *et al*, 2014). Our yields of hIFNγ were much lower, and these outcomes were not improved using additional strains, vectors, codon-optimised sequences. In contrast to Wang *et al* (2014), protein quantification was carried out in this study via ELISA instead of using the Bradford assay and purity-determination by HPLC. As we did not use the same restriction sites, it could be possible that KEX2 and/or STE13 cleavage was not efficient, leading to ineffective secretion because the processing of the signal sequence of human interferon gamma occurs in two steps, firstly cleavage by KEX2 then STE13. Whilst we cannot exclude incomplete processing and secretion, our antibody detects the secreted protein, which would indicate that the antibody does not target the secretion signal sequence. In addition, we checked the cell lysate of GS115-pPIC9-COS2 and found that the protein was efficiently secreted with little remaining. We would, therefore, expect the same outcome for pPICZ, as we used the same cloning sites EcoRI/NotI. This, to our point of view, would suggest that the observed low yields are the result of more than just inefficient secretion, *i.e.* low mRNA copy numbers remain a highly likely reason.

Furthermore, the molecular weight of the unglycosylated recombinant hIFNγ expressed in *E. coli* is 17.6 kDa; however, generally, the molecular weight of proteins increases due to glycosylation (Moharir *et al*, 2013) Therefore, the expected molecular weight of hIFNγ expressed in *P. pastoris* would be higher. The Western blot result, however, shown in Wang *et al* (2014) identified a 15 kDa band as hIFNγ which is theoretically impossible unless the target protein was truncated and unglycosylated, which highlights the possibility of misidentification in the small-scale experiments. In contrast, the authors verified the nature of the secreted protein by N-terminal sequencing following HPLC purification, suggesting that obtained yields might be achievable

Comparison of the translated amino acid sequence shown in Wang *et al* (2014) (derived from the published optimised DNA sequence) to the native amino acid sequence of hIFNγ revealed defects in three positions, *i.e.* there is a deletion of serine ^{43} and an addition of serine ^{51} and replacement of leucine ^{50} by phenylalanine ^{50} in the

native polypeptide in the recombinant protein. While these differences may not impact on the determination of yields, it could alter the three-dimensional structure of the protein with potential impacts on biological activity.

Taken together, irrespective of sequence, vector and expression strain used, this study showed that the yield of hIFNγ expressed in *P. pastoris* is too low for industrial-scale production. Similarly, a very recent study by Prabhu et al (2016) also did not achieve high expression yields of hIFNγ (< 2.5 mg. L^{-1}), using a *P. pastoris* codon-optimised hIFNγ sequence, the same strain of *P. pastoris* (GS115) and vector (pPICZα) under the control of *AOX1* promoter, or a multiple copy number integration approach (pPIC9K, a multiple copy integrating vector) and process fermenter parameter optimisation, *viz*. agitation rate, inoculum size, methanol concentration, pH and temperature (Prabhu *et al*, 2016).
Although glycosylation of the protein by *P. pastoris* should lead to a longer half-life of the recombinant protein and higher biological activity, it needs to be considered that recombinant proteins can on occasions become over-glycosylated and content of high mannose glycans could cause immunogenicity in patients, which are two disadvantages of this expression system. Therefore, we recommend future studies to focus on improvement of expression of hIFNγ in mammalian systems, as glycosylation patterns should be more similar to those found in human cells (Chung *et al*, 2013). Among mammalian expression systems; CHO was the focal point of studies from the 1990s onward, achieving laboratory-scale secretion of 15 mg L^{-1} of hIFNγ (McClain, 2010) and studies included overexpression, optimisation of cultivation, scale-up production and purification (Chung *et al*, 2013; Fox *et al*, 2004; Mols *et al*, 2005; Pm *et al*, 1995). An order of magnitude greater expression yields of hIFNγ (570 mg mL^{-1}) was achieved in mammary glands of transgenic mice *in vivo*, which is comparable to productivity in *E. coli* (Bagis *et al*, 2011; Lagutin *et al*, 1999). Studies in mammalian expression systems are ongoing to improve productivities further and to lower the cost of production, which is essential to make mammalian expression systems at the industrial scale competitive with the currently used *E. coli* expression system.

3.6 Conclusions

Around 50 transformant colonies of *P. pastoris* were screened for expression of hIFNγ with yields ranging from not detectable to low. This was most likely the result of the low abundance of mRNA transcript and/or inefficient secretion. We, therefore, conclude that industrial production of hIFNγ in *P. pastoris* is economically unrealistic, unless

transcription/translation can be significantly increased. It is therefore recommended that commercial production focuses on other eukaryotic expression systems *e.g.* CHO, mammary gland expression in transgenic mice or even human embryonic kidney 293 (HEK293) cells. In addition, research has to focus on unravelling the cause of low expression of hIFNγ in *P. pastoris* to overcome low yield hurdles to make the system competitive economically.

Chapter 4. Increased expression and secretion of recombinant *hIFNγ* through amino acid starvation-induced selective pressure on the adjacent *HIS4* gene in *Pichia pastoris*

The following chapter is a collaborative effort of which each author's contribution is provided at the start of the thesis.

Published: Razaghi, Ali *et al*. "Increased expression and secretion of recombinant hIFNγ through amino acid starvation-induced selective pressure on the adjacent *HIS4* gene in *Pichia pastoris*." *Acta Facultatis Pharmaceuticae Universitatis Comenianae* 62.2 (2015): 43-50.

Note*:* data chapters 3 and 4 were conducted simultaneously, and the transgenic *P. pastoris* strain used in chapter 4 belonged to the early stage of chapter 3. However later using other vectors and codon-optimised sequences enhanced the production 10-100 folds which were higher than yields achieved in data chapter 4.

4.1 Abstract

Transcriptional co-regulation of adjacent genes has been observed in prokaryotic and eukaryotic organisms, alike. High levels of gene adjacency were also found in a wide variety of yeast species with a high frequency of co-regulated gene sets. The aim of this research was to study how selective pressure on the Histidinol dehydrogenase gene (*HIS4*), using amino acid starvation, affects the level of expression and secretion of the adjacent human interferon gamma gene (*hIFNγ*) in the recombinant *Pichia pastoris* GS115 strain, a histidine-deficient mutant. *hIFNγ* was cloned into the pPIC9 vector adjacent to the *HIS4* gene, a gene essential for histidine biosynthesis, which was then transformed into *P. pastoris*. The transformed *P. pastoris* was cultured under continuous amino acid starvation in the amino acid-free minimal medium for ten days, with five inoculations into unspent medium every second day. Under these conditions, only successfully transformed cells (*hIFNγ –HIS4*$^{+}$) are able to synthesise histidine and therefore thrive. As shown by ELISA, amino acid starvation-induced selective pressure on *HIS4* improved expression and secretion of the adjacent hIFNγ by 55% compared to unchallenged cells. RT-qPCR showed that there was also a positive correlation between duration of amino acid starvation and increased levels of the hIFNγ RNA transcripts. According to these results, it is suggested that these adjacent genes (*hIFNγ* and *HIS4*) in the transformed *P. pastoris* are transcriptionally co-regulated and their expression is synchronised. To the best of the knowledge of the authors; this is the first study demonstrating that amino acid starvation-induced selective pressure on *HIS4* can alter the regulation pattern of adjacent genes in *P. pastoris*.

4.2 Introduction

There is increasing evidence that eukaryotic genes are co-regulated based on their location within the genome. Adjacent genes are subjected to tighter transcriptional co-regulation compared to distantly placed genes. This type of co-regulation appears to be an evolutionary conserved and a vital regulatory mechanism in eukaryotes including yeasts and has a functional significance for maintaining coordinated levels of gene expression (Arnone *et al*, 2012). For example, adjacent genes in *Saccharomyces cerevisiae* display similar patterns of expression (Kruglyak & Tang, 2000), which is substantiated by genome-wide expression studies in a number of organisms, such as *Drosophila* (Boutanaev *et al*, 2002), nematodes (Lercher *et al*, 2003), mice (Purmann *et al*, 2007), humans (Purmann *et al*, 2007), and *Arabidopsis* (Arnone *et al*, 2012; Williams & Bowles, 2004).

Another remarkable example is the genes encoding ribosomal proteins and the rRNA biosynthesis pathway exhibiting a high percentage of adjacent gene pairs (Wade *et al*, 2006). This phenomenon is wide-spread in a variety of yeast species with approximately 24% of the ribosome and rRNA biosynthesis genes being positioned as adjacent gene pairs in *Candida albicans* (Arnone & McAlear, 2011). These genes remain tightly co-regulated even under changing cellular growth status (Arnone *et al*, 2012; Dai & Lu, 2008; Grewal *et al*, 2005). In addition, elevated levels of gene expression, and silencing/repression of expression have also reported for adjacent genes (Grunstein, 1997). This correlation between the expression levels of genes and their relative location to each other can be explained by multiple biochemical, evolutionary, genetic, and technological factors (Bozinovic *et al*, 2013; Fraser, 2013; Gilad *et al*, 2006; Hurst *et al*, 2004; Michalak, 2008; Sproul *et al*, 2005). For example, it has been theorised that co-expression of adjacent genes can be defined by chromatin domains (Hurst *et al*, 2004), *i.e.* unzipping chromatin during gene expression can concurrently facilitate expression of genes from neighbouring opened region (Sproul *et al*, 2005).

Despite the potential importance of variation of gene regulation, so far little is known about the effects of selective pressures acting on regulatory patterns. Correlation between gene expression and selective pressure has been observed in model organisms and primates (Gilad *et al*, 2006). These findings suggest that statistically significant changes in gene expression contribute to phenotypic changes and large morphological differences (Bozinovic *et al*, 2013). For example in humans, the selective pressure in the form of solar radiation is a probable explanation for observed

changes in expression levels of genes involved in the UV radiation response, diabetes-related pathways and immune cell proliferation (Fraser, 2013).

The *HIS4* (histidinol dehydrogenase) gene is essential for histidine biosynthesis, and its transcriptional regulation has been studied extensively in *S. cerevisiae*. Transcriptional control of *HIS4* is carried out by either of two mechanisms: “basal control” is driven by transcriptional factors *Bas1* and *Bas2* binding independently to the *HIS4* promoter under amino acid-rich condition while “general control” is driven by the transcriptional factor Gcn4p, which is activated under starvation of even a single amino acid and leads to an induction of 40 genes in 12 pathways required for the biosynthesis of amino acids (Lamas-Maceiras *et al*, 1999; Zaman *et al*, 1999) Gcn4p binds as a homodimer protein to the consensus sequence rrTGASTCA(T)n and activates the transcription of genes in either direction at a distance of approximately 600 bp. Five such binding sites have been identified in the *HIS4* promoter *of S. cerevisiae* (Lamas-Maceiras *et al*, 1999). The *Gcn4p* gene itself is regulated by the fluctuation of the amino acid availability (Zaman *et al*, 1999). It has also been shown that amino acid starvation can increase *HIS4* expression three to four-fold above unstressed levels (Hinnebusch, 2005).

The aim of this study was to assess the effect of amino acid starvation-induced selective pressure on *HIS4* on the level of expression of adjacent genes in the recombinant *Pichia pastoris*. For this purpose; the human interferon gamma (*hIFNγ*) gene, which has a therapeutic value against a wide variety of diseases like cancer, hepatitis, and tuberculosis (Miller *et al*, 2009), was cloned into the *pPIC9* vector adjacent to the *HIS4* gene. Then it was transformed into the *Pichia pastoris* GS115 strain, a histidine-deficient mutant. The transformant, containing the *HIS4* gene, was cultured under continuous amino acid starvation in modified Yeast Nitrogen Based medium (YNB) void of amino acids, leading to an expression of the *HIS4* gene. Finally, the expression levels of *hIFNγ* were measured to evaluate the possibility of co-regulation of these adjacent genes.

4.3 Material and methods

4.3.1 Cloning and transformation

Cloning: To generate *pPIC9-hIFNγ*, the coding sequence of *hIFNγ*, flanked with *EcoRI* and *NotI*, was synthesised by Life Technologies, GeneArt Strings, and modified based on the codon preference in *P. pastoris*. Subsequently, the fragment was inserted into the *pPIC9* vector between the same restriction sites; adjacent to the *HIS4* gene, which is essential for the biosynthesis of histidine. The optimised sequence encoding *hIFNγ* and its resultant amino acid sequences are shown in (Fig.1-A).
Transformation & Integration in P. pastoris: The non-linearized plasmid *pPIC9-hIFNγ* was transformed into the GS115 strain of *P. pastoris* by electroporation (Electroporator 2510, Eppendorf) following the protocols for electro-competent cell production and electroporation (Life Technologies). Gene integration occurs at the *AOX* (GS115) locus by a single crossover between the *AOX* locus and any of the three *AOX* regions on the vector: the 5' *AOX* promoter, the *AOX* transcription termination region (TT) or the 3´ *AOX*. This results in the integration of one or more copies of the vector into the genome with the resultant phenotype of *His*$^+$ Mut$^+$ for the transformed *P. pastoris* (GS115) (Fig.4.1-B).
Screening for Mut$^+$ *transformants:* Transformant colonies with *HIS4*$^+$ phenotype were selected on Minimal Dextrose (MD) (1.34% YNB, 2% dextrose) agar plates based on complementation of histidine auxotrophy. To confirm the methanol utilisation (Mut) phenotype of the strain, colonies with *HIS4*$^+$ phenotype were transferred to plates with either MD or Minimal Methanol (MM) (1.34% YNB, 0.5% methanol) as the carbon source. This allows differentiating between Mut^s (slow methanol utilisation) and Mut$^+$ (can utilise methanol effectively as a carbon source) phenotypes, with the latter growing well on MM agar plates, while the former shows insignificant growth. As expected, only the Mut$^+$ phenotype was detected based on growth on both agar media after 24 h.

4.3.2 Confirmation of integration to genomic DNA by PCR

To determine whether *hIFNγ* was integrated into the *P. pastoris* genome, genomic DNA from colonies with *HIS4*$^+$Mut$^+$ phenotype were isolated (Wizard® Genomic DNA Purification Kit, Promega). The integration of *hIFNγ* into the genome of *P. pastoris* was confirmed by PCR using the α-Factor sequencing primer as a forward primer 5´-TACTATTGCCAGCATTGCTGC-3´ which hybridizes within the 5' end of the α-factor

region paired with the 3´ *AOX1* sequencing primer as a reverse primer 5´-GCAAATGGCATTCTGACATCC-3´ which hybridizes with 3´ end of the *AOX1* transcription terminator (TT) region (Fig.4.1).

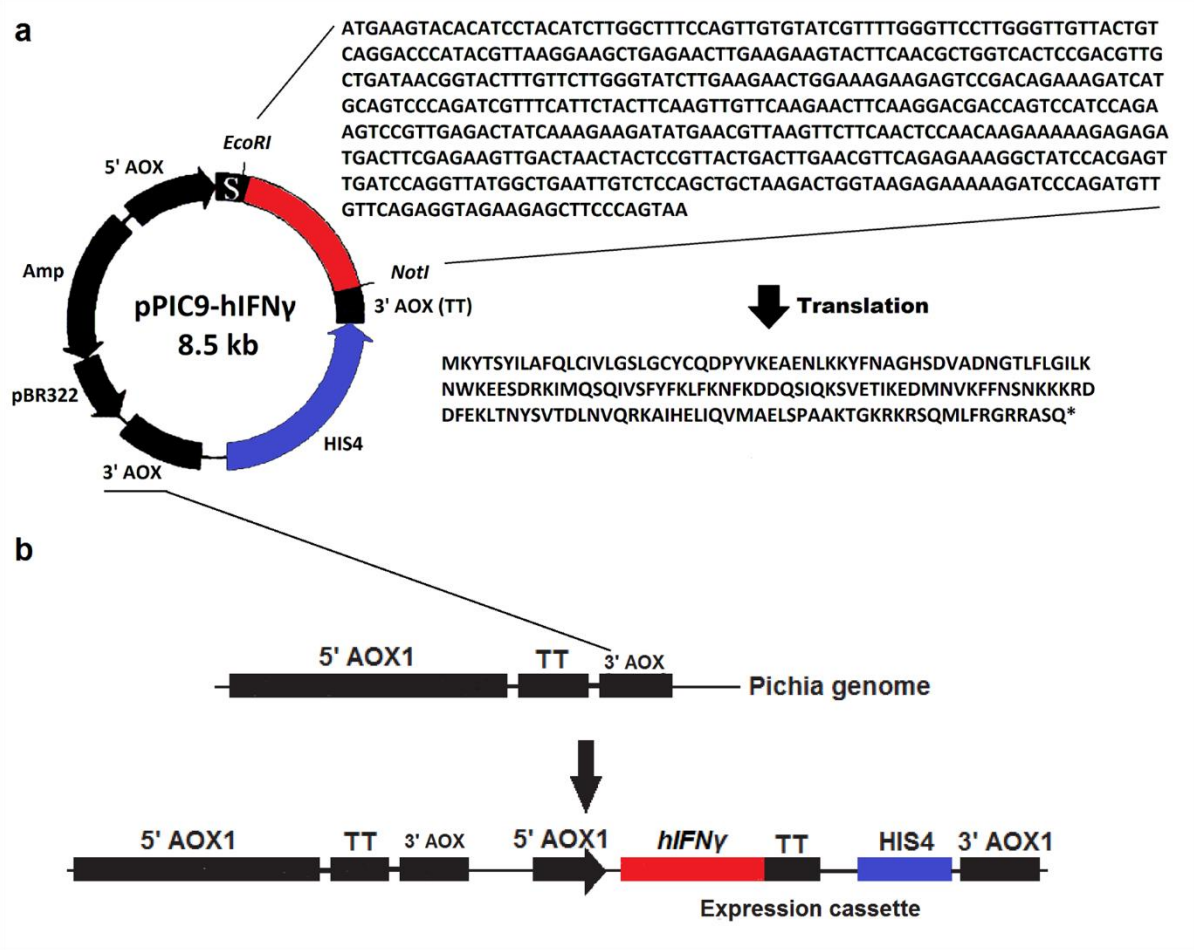

Figure 4.1. Placement of the two adjacent genes, *hIFNγ* and *HIS4,* as part of the *pPIC9-hIFNγ* vector (a) and result of the integration of the vector between the 3´AOX into the intact *AOX1* locus (Mut$^+$) and the gain of promoter 5' *AOX1*, *hIFNγ gene*, and *HIS4* (expression cassette) (b). *5'AOX1*: 5' Alcohol oxidase promotor gene which requires methanol for induction, S: α-factor secretion signal, *hIFNγ*: optimised human interferon gamma gene for *P. pastoris*, *3'AOX (TT)*: Alcohol oxidase transcription terminator, *HIS4*: Histidinol dehydrogenase gene which is essential for histidine biosynthesis, *pBR322*: origins from *E. coli*, Amp: Ampicillin resistance gene.

Genomic DNA of untransformed *P. pastoris* GS115 was used as a negative control. Thirty amplification cycles were performed at 94˚C for 30 s, 55˚C for 30 s, and a final extension for 5 min at 72˚C.

Successful integration of the *hIFNγ* into the *P. pastoris* genome was demonstrated by the expected ~700bp fragment size using agarose (1.5%) gel electrophoresis which

was verified by DNA sequencing at the Australian Genome Research Facility Ltd. (AGRF).

4.3.3 Protein expression under amino acid starvation-induced selective pressure on *HIS4*

Successfully transformed *P. pastoris* cells were kept under amino acid starvation by cultivation in buffered Minimal Glycerol (BMG) medium (1.34% YNB without amino acids, 100 mM potassium phosphate, pH 6.0, and 1% glycerol). Under these conditions, only successfully transformed cells can synthesise histidine and therefore thrive. Explicitly, continuous amino acid starvation was maintained for 10 days; re-inoculating into fresh BMG medium every 2 days (Fig. 4.2A). An *HIS4*$^{+}$ colony was inoculated into 25 mL of BMG in a 250 mL baffled flask and incubated at 28˚C for 48 h with a shaking speed of 200 rpm until reaching an OD_{600}≥2 (log-phase growth) (EnSpire® Multimode Plate Reader, PerkinElmer). Subsequently, the cells were harvested by centrifugation at 3000 *g* for 5 min at room temperature. Cell pellets were resuspended in 50 mL PBS buffer (0.1M Phosphate Buffer Saline, pH 7.4) to remove residual glycerol. Finally cell pellets were resuspended in 50 mL buffered methanol-complex (BMMY) medium (1% yeast extract, 2% peptone, 1.34% YNB, 100 mM potassium phosphate, pH 6.0, 0.5% methanol) to a starting OD_{600}=1 in a 250 mL baffled flask (Fig.4.2-B). To induce expression of *hIFNγ*, pure methanol was added to a final concentration of 1% (v/v) every 24 h. The culture supernatant was obtained by centrifugation at 1500 *g* after 72 h of cultivation to analyse the expression of *hIFNγ*; cell pellets were used for genomic DNA extraction for qPCR and total RNA extraction for RT-qPCR.

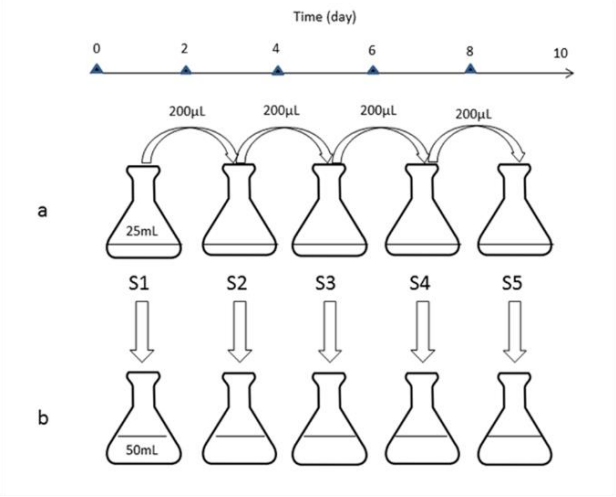

Figure 4.2. Diagram showing continuous amino acid starvation over 10 days in buffered Minimal Glycerol (BMG) medium (a) and protein expression in buffered methanol-complex (BMMY) medium (b). S: Serial passage.

4.3.4 ELISA

Recombinant *hIFNγ* protein levels in supernatants were quantified using a modified indirect ELISA protocol (Abcam). Replicated sample aliquots (50 µL) were added to each well of a polyvinyl chloride micro-titre plate and incubated overnight at 4 °C. Wells were washed three times with 200 µL Tris-buffered saline (Tris-HCl 20 mM, NaCl 150 mM, pH 7.5). Protein-binding sites were blocked by adding 200 µL blocking buffer (5% Bovine Serum Albumin (BSA) in TBS) per well, followed by incubation for 1 h at 37ºC in a shaking incubator chamber (HO35™ Hybridisation Oven, Ratek), followed by washing twice with TBS. 100 µL of diluted (0.5 $\mu g \cdot mL^{-1}$) primary antibody (polyclonal rabbit-anti-*hIFNγ*, Abcam cat no. ab9657) was added to each well and incubated for 1 h at 37ºC in a shaking incubator chamber. Plates were washed four times with TBS. 100 µL of conjugated secondary antibody (polyclonal goat anti-rabbit, Abcam cat no. ab98505) diluted 1/1000 in blocking buffer was added to each well and incubated for 1 h at 37ºC in a shaking incubator chamber. After washing four times with TBS, 50 µL of Alkaline Phosphatase Yellow (pNPP) Liquid Substrate (P7998 SIGMA) was added per well. Absorbance at 405 nm was recorded after 30 min on a spectrophotometer (EnSpire® Multimode Plate Reader, PerkinElmer). The supernatant of cell culture of untransformed *P. pastoris* GS115 was used as negative control.
A standard curve 0.0, 1.25, 2.5, 5, 10 µg L^{-1} ($R^2 = 0.993$ and y = 12.169*x*-1.1321) was prepared by serial dilution of the recombinant *hIFNγ* (Abcam cat no. ab51240).

4.3.5 Immuno-blotting

Immunoblotting (dot blot) was performed to qualitatively detect the presence of *hIFNγ* in the medium supernatant, following standard procedures described by Abcam. In brief, a nitrocellulose membrane (pore size 0.2 µm N7892 SIGMA**)** was gridded, and 2 µl of samples were spotted onto the nitrocellulose membrane at the centre of each grid square. The membrane was left to dry for 30 min. Unspecific binding sites were blocked with 1% BSA in TBS-T (Tris-buffered saline-TWEEN 20 0.05%) for 30 min at room temperature on a rocking shaker (VSR-50® Laboratory Platform Rocker). The membrane was then incubated with the primary antibody (polyclonal rabbit anti-*hIFNγ*, Abcam cat no. ab9657) (0.1 $\mu g \cdot mL^{-1}$) dissolved in TBS-T over night at room temperature. The membrane was washed for 5 min three times with TBS-T. Thereafter, the membrane was incubated for 2 h at room temperature with the secondary antibody (polyclonal goat-anti-rabbit, Abcam cat no. ab98505), conjugated to alkaline phosphatase. Finally, the membrane was washed twice for 5 min with TBS-T and

incubated with SIGMA *FAST*™ BCIP/NBT (5-bromo-4-chloro-3-indolyl phosphate/nitro blue tetrazolium) dissolved in 10 mL deionised water, and left until colour developed (Fig. 4.3). The supernatant of cell culture of untransformed *P. pastoris* GS115 was used as negative control.

4.3.6 qPCR, RNA extraction & RT-qPCR

QuantiTect SYBR® Green PCR Kit (Qiagen cat no. 204141) was used for both real-time PCR (qPCR; assessing gene copy number) and two-step reverse transcription-PCR (RT-qPCR; assessing transcription level of the RNA) using primers as per Table 4.1. A set of primers was designed to amplify 168 bp of the *hIFNγ* sequence.

Genomic DNA of each serial passage was extracted at the end of the experiment, and 50 ng of DNA (NanoDrop®, ND-1000 Spectrophotometer) for each serial passage was used in qPCR. Total RNA was extracted using the PureLink® RNA Mini Kit (Life Technologies cat no. 12183018A), followed by DNase treatment and reverse transcription to cDNA using the QuantiTect Reverse Transcription Kit (Qiagen cat no. 205310). For each serial passage, 500 ng of cDNA was quantified by NanoDrop based on the optical absorbance at OD_{260}. Two replicated RT-qPCRs were performed using the same primer set as for qPCR (Table 4.1). Genomic DNA and total RNA of untransformed *P. pastoris* GS115 were used as negative control for qPCR and RT-qPCR, respectively.

Standard curves for qPCR were prepared with purified DNA amplicons (section 2.2) [699 bp amplicon containing 501bp *hIFNγ* plus secretion signal and parts of the *AOX* gene promoter and transcription terminator]. Dilution series of DNA amplicons according to mass concentration (ng/per total volume of reaction) were used to make standard curves with, 10^{-3}, 10^{-4}, 10^{-5} and 10^{-6}, 0 ng DNA ($R^2 = 0.998$, *Overall efficiency*=101.1% and $y = 11.149e^{-0.699x}$).

For calculation of approximate gene copy number, the following equation was used, based on the fact that 699bp dsDNA amplicon weighs ~75.33×10^{-10} ng.

Gene copy number = Initial concentration of detected DNA amplicon (ng) / 75.33×10^{-10} ng

Each 50 µL reaction contained 25 µL (2x) QuantiTec SYBR GreenPCR Master Mix, 10 µM forward and reverse primers with a final concentration of 0.3 µM (5 µL each), 10 µL sample (genomic DNA or cDNA) and 5 µL RNase-free water. qPCR reactions were run

on a Peltier Thermal Cycler-200 (BioRad) under the following conditions: PCR initial activation step 95˚C for 15 min, followed by 45 cycles of denaturation at 94 ˚C for 15 s and annealing at 57 ˚C for 30 s, and extension at 72 °C for 30 s.

4.3.7 Statistical analysis

Data on *hIFNγ* protein secretion levels and C(t) of RT-qPCR were statistically analysed via one-way ANOVA using Microsoft Office Excel, Data Analysis. Homogeneity of variances was confirmed using Levene's Test. The critical value was set to ($\alpha = 0.05$), and results were deemed statistically significant at $p \leq 0.05$. If statistical significance was detected, Tukey-Kramer HSD post-hoc tests were performed to identify samples significantly different to each other.

Table 4.1. Primer design for qPCR /RT-qPCR.

Orientation	Sequence	Length [bp]	T_m	GC%
Forward primer	5' ACTTCAACGCTGGTCACTC 3'	19	57.71	52.63
Reverse primer	5' CGGACTTCTGGATGGACTG 3'	19	57.25	57.89

4.4 Results

4.4.1 Transformation and confirmation of integration

Six clones were retained, and their phenotypic *HIS4*$^+$ status was confirmed on Minimal Dextrose and Mut$^+$ status on Minimal Methanol agar plates. The successful integration of the *hIFNγ* was confirmed by PCR using 5′ and 3′ primers of the *AOX1* and α-factor partial sequence, respectively. Agarose gel electrophoresis of *HIS4*$^+$ Mut$^+$ transformants confirmed PCR products between 500-1000 bp according to a DNA ladder (EasyLadder I, Bioline), while negative controls (untransformed *P. pastoris*) showed no band. Results of DNA sequencing at the Australian Genome Research Facility Ltd. (AGRF) confirmed that amplicons sequences match the optimised *hIFNγ*.

4.4.2 Protein expression under amino acid starvation-induced selective pressure on *HIS4*

The strain (C 6) yielded the strongest agarose gel signal and was used for protein expression and secretion studies. The amount of secreted *hIFNγ* was assessed 72 h after induction in BMMY medium by immunoblots (Fig. 4.3) and ELISA, with the latter detecting, secreted yields of 0.18 to 0.28 µg L^{-1} of *hIFNγ* (Fig. 4.4). Culture supernatants of the untransformed *P. pastoris* were used as negative controls. Immunodot blots using culture supernatant of the untransformed *P. pastoris* yielded no positive signal (Fig. 4.3), further demonstrating that the construct, ***pPIC9-hIFNγ*****,** was successfully expressed in *P. pastoris*.

Levene's test for determining the homogeneity of variances validated the assumption of equal variances ($p=4.95 \times 10^{-75}$). A one-way ANOVA showed that there was a significant difference in levels of *hIFNγ* secretion between one or more pairs of serial passages (Table 4.2). A significant difference between serial passages 1 and 5 was detected (Tukey-Kramer HSD test: $p = 0.029$), while serial passages 2-4 were not significantly different to either serial passage 1 or serial passage 5 ($p>0.05$).

Figure 4.3. Dot blot is showing *hIFNγ* positive cultivation media of two cultures exposed to amino acid starvation (a) and supernatant of cell culture of untransformed *P. pastoris* GS115 (negative control) (b).

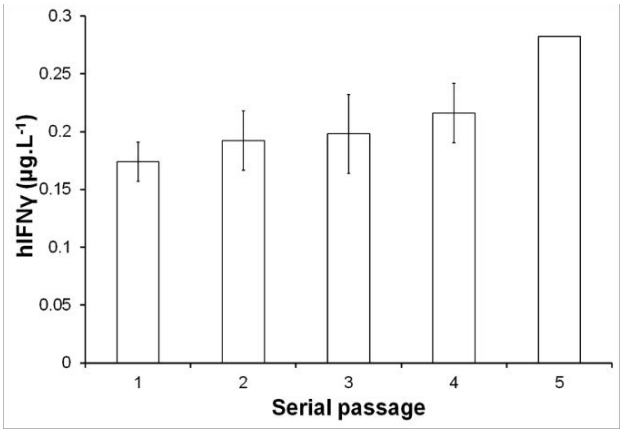

Figure 4.4. Amino acid starvation-induced levels of secreted hIFNγ over 5 serial passages of *P. pastoris* GS115 transformed with *hIFNγ* and *HIS4* (Mean ± SD, n = 2)

Table 4.2. Summary of one-way ANOVA results for 5 serial passages of transformed *P. pastoris* producing *hIFNγ*.						
Source of Variation	***SS***	***df***	***MS***	***F***	***F crit***	***P-value***
Between Groups	0.015841	4	0.00396	6.961538	5.192168	0.028203
Within Groups	0.002844	5	0.000569			
Total	0.018685	9				

4.4.3 Gene quantification and gene copy number analysis

The results of the qPCR for determining the concentration of target gene showed consistent and similar amounts of amplified the 168 bp amplicon, suggesting equal *hIFNγ* gene numbers across serial passages (Table 4.3 and 4.4).

Table 4.3. Approximate *hIFNγ* gene copy number and *hIFNγ* DNA amplicon concentration [ng] of serial passages 1, 3 and 5 of *hIFNγ –HIS4*$^{+}$ *Mut*$^{+}$ *P. pastoris* transformants under amino acid starvation.			
Content	**C(t)**	**Initial Concentration of *hIFNγ* DNA amplicons (ng)**	**Approx. gene copy number**
Serial passage 1	13.93	65.84×10^{-5}	$\sim 87.34 \times 10^{3}$
Serial passage 3	13.79	72.61×10^{-5}	$\sim 96.37 \times 10^{3}$
Serial passage 5	13.97	64.02×10^{-5}	$\sim 85.96 \times 10^{3}$

Table 4.4. C(t) values of RT-qPCR for quantification of *hIFNγ* RNA and calculated initial concentration of the cDNA amplicons (Mean ± SD, n = 2).		
Content	**C(t)**	**Initial Concentration of cDNA amplicons (ng)**
Serial passage 1	24.79 ± 0.035	$3.34 \times 10^{-07} \pm 0.08 \times 10^{-07}$
Serial passage 3	25.02 ± 0.162	$2.89 \times 10^{-07} \pm 0.33 \times 10^{-07}$
Serial passage 5	23.28 ± 0.028	$9.55 \times 10^{-07} \pm 0.19 \times 10^{-07}$

4.4.4 Transcriptional analysis of *hIFNγ* RNA

Levene's test for determining the homogeneity of variances validated the assumption of equal variances ($p=1.3\times10^{-41}$). A one-way ANOVA on C(t) values showed that there was a significant difference between one or more pairs of serial passages ($p = 0.0007$). A Tukey-Kramer HSD test revealed no significant differences between serial passages 1 and 3 ($p > 0.01$), but a significant difference between serial passages 1 and 5 ($p < 0.01$) and serial passages 3 and 5 ($p < 0.001$). These results conformed to the protein expression/secretion results obtained by ELISA (section 3.2).

4.5 Discussion

Studies in model organisms propose that the expression levels of most genes change and evolve under stabilising selective pressure which has been proposed to be the dominant mode of evolutionary changes in gene expression (Gilad *et al*, 2006). Gene expression in yeast has also been shown to change in response to environmental stress; for example, the expression of a significant number of genes (1372) was altered distinctively when *S. cerevisiae* was cultivated for either five or twenty-five generations under microgravity, compared controls cultured under identical conditions in normal gravity (Sheehan *et al*, 2007). Therefore, as a driving force of evolution, the outcomes of selective pressures are generally well documented, while the linkage to direct genetic effects is less understood.

Much of the work on regulatory networks has focused on the yeast *S. cerevisiae*, for which data are most copious (Babu *et al*, 2004). To the best of our knowledge, the effects of amino acid starvation-induced selective pressure on *HIS4,* and the transcriptional co-regulation of adjacent recombinant genes in *P. pastoris* has not been documented to date. As predicted in our study, amino acid starvation-induced selective pressure on *HIS4* increased expression of the adjacent *hIFNγ* gene by ~55%., suggesting co-regulation, as increased secretion levels were positively correlated with RNA transcription levels. Investigation of gene copy number of *hIFNγ* in every other serial passage showed no variation (Table 4.3), suggesting that increased level of protein expression and RNA transcription not be due to “gene duplication” making transcriptional co-regulation between *hIFNγ* and the adjacent *HIS4* gene highly likely.

At least three mechanisms have been proposed to explain adjacent gene co-regulation:

1) *Localised chromatin modification;* where there is a correlation between histone *H4* acetylation domains and genome-wide histone *H3K14* acetylation which correlate with transcriptionally co-expressed genes in budding yeast (Deng *et al*, 2010). When a gene is being transcribed, the localised chromatin is forming a more open permissive transcriptional state (Sproul *et al*, 2005), which can affect the transcription of genes in adjacency (Ebisuya *et al*, 2008).

2) *Local DNA sequence looping;* which has been observed between genes on the same and different chromosomes in yeast (Duan *et al*, 2010), where adjacent genes can be silenced via a localised loop of DNA sequences when the promoter of the adjacent gene is in physical contact with silencing factors (Valenzuela *et al*, 2008).

3) *Adjacent gene co-regulation through sub-nuclear compartmentalisation;* where transcriptionally active sets of genes are lodged at the nucleolar periphery upon activation (Berger *et al*, 2008). Active genes have been seen to associate with

‘transcription factories,' which are the spot of nascent RNA production and associated transcription factors (Osborne *et al*, 2004). As a result, if one gene gains entry to an active sub-nuclear compartment, the adjacent gene could hypothetically follow the same regulatory process (Arnone *et al*, 2012).

In the study here, while gene co-regulation through DNA looping are possible scenarios for other non-investigated genes, expression of *HIS4* would have been activated by amino acid starvation (as shown by (Hinnebusch, 2005)), and, since increased transcription (mRNA) and expression/secretion was also improved, co-regulation of these two genes would need to be achieved through either mechanism 1 or 3. It is much harder to differentiate between the potential roles of localised chromatin modifications and sub-nuclear compartmentalisation in the co-regulation of *HIS4* and *hIFNγ* because these two mechanisms are not mutually exclusive in operation. There is some evidence supporting “localised chromatin modifications” playing a greater role in gene co-regulation in eukaryotes *e.g.* yeast (Babu *et al*, 2004). Latest evidence also suggests that the environment can stably affect the establishment of the epigenome which is referred to as “transgenerational epigenetic inheritance” (Daxinger & Whitelaw, 2010). The role of localised chromatin modifications as an epigenomic co-regulatory mechanism would require investigating the stable inheritance of *HIS4* and *hIFNγ* expression when the selective pressure of amino acid starvation is removed. This should be ideally conducted simultaneously with experiments aiming to identify the transcriptional localisation of *HIS4* and *hIFNγ* within the nucleus to examine the potential for a contribution of nucleolar transcriptional factories.

It could be equally argued that gene co-expression might be regulated by simple regulatory networks, which do not necessarily require any of the above regulatory mechanisms. For example, it was shown that external conditions *e.g.* stress induced topologically simple regulatory networks, characterised by involving a limited number of steps and transcription factors in yeast (Babu *et al*, 2004). In relevance to the study here, amino acid starvation activated the transcription factor Gcn4p, resulting in transcriptional induction of almost all genes involved in amino acid biosynthesis (Hinnebusch, 2005), including *HIS4*. Additionally, a wide array of genes unrelated to amino acid biosynthesis, *i.e.* close to one tenth of the yeast genome was activated (Natarajan *et al*, 2001), which designates a role for Gcn4p as a “master regulator” of gene expression (Hinnebusch & Natarajan, 2002). Thus the involvement of Gcn4p in the regulation of both *HIS4* and *hIFNγ* can be hypothesised as a probable scenario explaining the increased level of *hIFNγ* under amino acid starvation.

4.6 Conclusion

This study showed that the adjacent localisation of *hIFNγ* and *HIS4* genes result in co-regulation of *hIFNγ* expression and secretion, the first step for potential improvement of *hIFNγ* yields using this expression system. Additionally, the recombinant system developed should lend itself for detailed studies regarding the underpinning nature of the regulatory mechanism.

Chapter 5. Therapeutic efficacy of recombinant human interferon-γ is improved by mammalian expression system in the drug-resistant ovarian cancer cell line SKOV3

The following chapter is a collaborative effort of which each author's contribution is outlined below.

Contribution:

Ali Razaghi: Conception and execution of project, writing, and editing chapter.

Kirsten Heimann: Supervision, editing.

Leigh Owens: Supervision

Submitted: Razaghi, Ali, *et al*. " Therapeutic efficacy of recombinant human interferon-γ is improved by mammalian expression system in the drug-resistant ovarian cancer cell line SKOV3" *British Journal of Cancer* (2017).

5.1 Abstract

Background: Human interferon gamma (hIFNγ) affects tumour cells and modulates immune responses, showing promise as an anti-cancer therapeutic. This study investigated the effect of glycosylation and expression system of recombinant hIFNγ in ovarian carcinoma cell lines.

Methods: The efficacy of bacterially- (*E. coli*) and mammalian-expressed hIFNγ (hIFNγ-CHO and -HEK293, glycosylated/de-glycosylated) on cytostasis (Guava cell cycle flow cytometry), cell death (MTT, and TUNEL, Guava via count flow cytometry) and apoptotic signalling (Western blot of Cdk2, histone H3, procaspase-3, FADD, cleaved PARP, and caspase-3) was studied in PEO1 and SKOV3.

Results: PEO1 was more sensitive to hIFNγ (~70% cell death, ~60% cytostasis arrest in G2-phase) than SKOV3 (~30% cell death, ~20-45% cytostasis arrest in S-phase). Responses were dose-dependent (IC50 = 200 ng mL^{-1}) and expression platform/glycosylation status-independent in PEO1, whereas SKOV3 was only affected by mammalian-expressed hIFNγ in a dose-independent manner. Cleaved PARP and caspase-3 were not detected for either cell line, but FADD was expressed in SKOV3 with levels increasing following treatment.

Conclusion: hIFNγ did not induce apoptosis in either cell line. Mammalian- expressed hIFNγ increased cell death and cytostasis in the drug-resistant SKOV3. The presence of FADD in SKOV3, which may inhibit apoptosis through activation of NF-κB, could serve as a novel therapeutic target.

5.2 Introduction

Human interferon-gamma (hIFNγ) is a cytokine with immunomodulatory properties vital for innate and adaptive immunity against viral (through inhibition of viral replication)/microbial infections and cytotoxic/cytostatic activity against cancer cells. Native hIFNγ is naturally synthesised by $CD4^+$ T helper cell type 1 (T_{h1}) lymphocytes, $CD8^+$ cytotoxic lymphocytes and natural killer (NK) cells (Farrar & Schreiber, 1993; Razaghi *et al*, 2016b; Young & Hardy, 1995).

The active form of native hIFNγ is a soluble homodimer, and each monomer is composed of 144 amino acids polypeptide with only two N-glycosylation sites on asparagines (N^{25} & N^{97}) on the surface of the dimmer (Farrar & Schreiber, 1993; Young & Hardy, 1995). The glycans at N^{25} are fucosylated and are mainly complex-type sialylated oligosaccharides with the sugar composition of N-acetylneuraminic acid, galactose, mannose, N-acetylglucosamine, and fucose. In contrast, the glycans at N^{97} are non-fucosylated hybrid high-mannose structures with a sugar composition of N-acetylneuraminic acid, galactose, mannose, and N-acetylglucosamine (Razaghi *et al*, 2016b; Sareneva *et al*, 1995).

Recombinant hIFNγ is commonly expressed in *Escherichia coli* (generic name: human interferon gamma-1b (hIFNγ-1b), tradename: ACTIMMUNE®). Thus far, it has been approved for clinical treatment of chronic granulomatous disease and malignant osteopetrosis, and its application as an immunotherapeutic against hepatitis and cancer is a growing prospect (Razaghi *et al*, 2016b). The use of hIFNγ-1b is, however, limited due to significantly shortened half-life in the bloodstream resulting from lack of glycosylation (Miyakawa *et al*, 2011). Furthermore, production of inclusion bodies and endotoxin contamination make the purification process from prokaryotic expression platforms tedious and costly (Razaghi *et al*, 2016b). To overcome these limitations; expression in eukaryotic production platforms such as yeast, protozoa, and mammalian expression systems (*e.g.* Chinese hamster ovary (CHO), HEK293, mice, rat) has been pursued (Razaghi *et al*, 2015; Razaghi *et al*, 2017). Among them, the best results have been achieved in mammalian expression systems due to higher productivities, the similarity in glycosylation and protein folding with native hIFNγ (Razaghi *et al*, 2016b; Razaghi *et al*, 2017). Despite similarities, some differences exist; for example, the N-glycan structure of hIFNγ expressed in CHO is not sialyated which potentially can affect its stability and cause issues with immunogenicity (Dumont *et al*, 2016; Razaghi *et al*, 2016b).

Apart from the importance of glycan residues in protease resistance (Sareneva *et al*, 1995), the type of glycans also affects the half-life and pharmacokinetics of hIFNγ. For example, a mannose-type oligosaccharide of recombinant hIFNγ expressed in insect cells had a shorter half-life in the bloodstream compared to native hIFNγ (Sareneva *et al*, 1993). However, detailed knowledge of the effects of glycosylation of hIFNγ on its therapeutic efficacy is limited. Therefore one objective of this study was to explore how recombinant hIFNγ from three different production platforms, *E. coli,* CHO and human embryonic kidney 293 (HEK293), affect the ovarian cancer cells, PEO1 and SKOV3, (the latter being used as a negative control, as the cell line is insensitive to treatment with hINFγ (Wall *et al*, 2003)), to evaluate whether or not mammalian expressed recombinant hIFNγ can be a superior substitute for the prokaryotic product. Furthermore, the deglycosylated form of the mentioned mammalian expressed hIFNγ were used to investigate whether deglycosylation of hIFNγ altered its therapeutic efficacy according to the fact that glycosylation has been proven to be essential for the therapeutic efficacy of protein drugs (Sola & Griebenow, 2010).

In women, ovarian cancer is the 5th deadliest cancer (Siegel *et al*, 2015). Treatment of ovarian cancer with hIFNγ-1b underwent phase I, II & III clinical trials with mixed results. Some of the identified obstacles were tumour insensitivity to hIFNγ and inability to deliver hIFNγ locally (Alberts *et al*, 2008; Dunn *et al*, 2006; Marth *et al*, 2006; Windbichler *et al*, 2000). In contrast, preclinical studies (*in vitro* & *in vivo*) using ovarian cancer cell lines were far more successful, as they all showed a degree of sensitivity to hIFNγ-1b, except for SKOV3 which was insensitive (Table 5.1).

To date, two principal mechanisms of action have been proposed for hIFNγ in ovarian cancer cells: 1) “cytostasis” (synonyms: antiproliferation or cell growth inhibition) through activation of p53, p21 leading to cell cycle arrest (Fig. 5.1 and 5.2) “cytotoxicity” causing cell death. The latter was subdivided into “pyroptosis” through activation of interferon regulatory factor-1 (IRF-1) and caspase-1, and “apoptosis” through intrinsic signal transduction by activation of the IRF-1, caspase-8, cytochrome-c release from mitochondria, the caspase cascade and finally inhibition of poly-ADP-ribose polymerase (PARP) (Fig. 5.1) (Table 5.1). For example, OVCAR3 has been an extensively studied ovarian cancer cell line, and treatment with recombinant unglycosylated hIFNγ from *E. coli* led to both apoptosis and cytostasis. Prior work on PEO1 also showed the possibility for both cytostasis and apoptosis (Barton *et al*, 2005; Wall *et al*, 2003). Burke et al (1999) investigated the p53 pathway, which leads to cell cycle arrest (Fig. 5.1) and concluded, based on STAT1 activation, that hIFNγ also had induced cytotoxic effects in addition to cytostasis (Burke *et al*, 1999). Therefore, one

objective of this research was to confirm apoptosis by detection of cleaved PARP and caspase-3. Numerous studies proposed that Fas-associated death domain protein (FADD) regulates cell cycle progression, proliferation, tumorigenesis and necroptosis (Alappat *et al*, 2005; Lee *et al*, 2012; Pasparakis & Vandenabeele, 2015; Tang *et al*, 2011). For example, it has been demonstrated that high levels of phosphorylated FADD correlated with increased activation of the anti-apoptotic transcription factor NF-κB (nuclear factor kappa-light-chain-enhancer of activated B cells). NF-κB is a biomarker for aggressive phenotypes in *e.g*. lymphomas, lung and colorectal carcinomas where tumour cells show resistance to chemotherapeutic agents, leading to poor clinical outcomes (Fig. 5.1) (Patel *et al*, 2014; Schinske *et al*, 2011). FADD can also induce extrinsic apoptosis by bridging death receptor signalling to the caspase cascade (Fig. 5.1). hIFNγ has been shown induce the Fas pathway through export of the FasL (Boselli *et al*, 2007), which can activate FADD, potentially leading to either of the above outcomes (Fig. 5.1). Therefore this study also examined whether Fas-Associated Death Domain (FADD) protein plays a role in the hIFNγ-induced signalling pathway leading to necroptosis or extrinsic apoptosis of ovarian cancer cells.

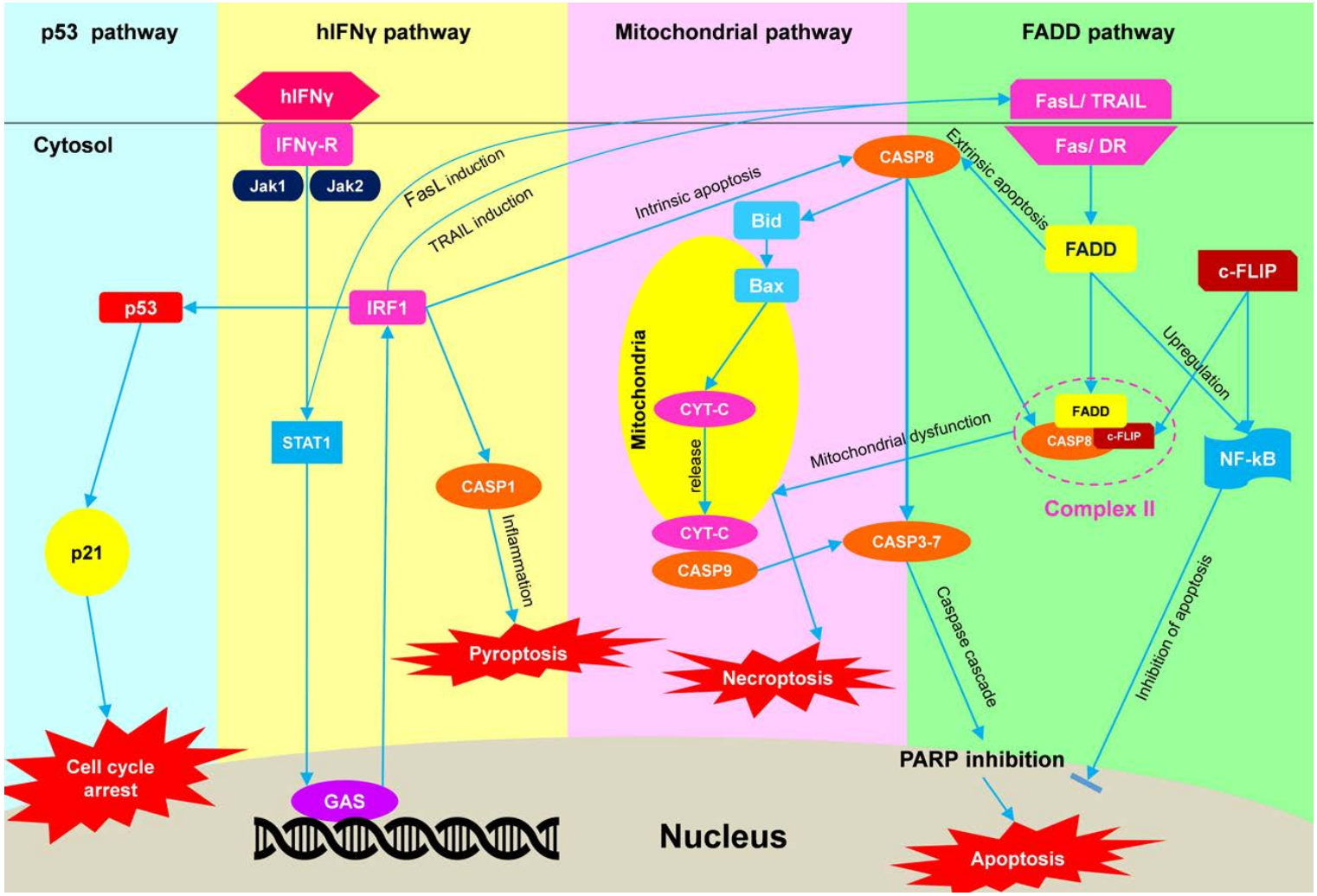

Figure 5.1. hIFnγ-induced signal transduction in ovarian carcinoma cells. Involvement of the FADD pathway is hypothetical. The figure has been composed based on information obtained from (Alappat *et al*, 2005; Barton *et al*, 2005; Bell *et al*, 2008; Boselli *et al*, 2007; Burke *et al*, 1999; Jean *et al*, 1999; Kim *et al*, 2002; Lee *et al*, 2012; Li *et al*, 2011; Park *et al*, 2004; Pasparakis & Vandenabeele, 2015; Patel *et al*, 2014; Pyo *et al*, 2005; Schinske *et al*, 2011; Thapa *et al*, 2011; Wall *et al*, 2003; Xu *et al*, 1998).
Bax, Bcl-2-associated X protein, **Bid,** BH3 interacting domain death agonist**, CASP1, 3, 7, 8, 9,** Caspase1, 3, 7, 8, 9; **CYT-C,** Cytochrome-C; **c-FLIP,** Cellular FLICE (FADD-like IL-1β-converting enzyme)-inhibitory protein; **FADD,** Fas-Associated Death Domain Protein; **Fas,** Cell surface death receptor; **FasL,** Fas Ligand; **GAS,** Gamma interferon-activated sequence; **IRF-1,** Interferon-regulated factor-1; **Jak,** Janus kinase; **NF-κB,** Nuclear factor kappa-light-chain-enhancer of activated B cells; **PARP,** Poly (ADP-ribose) polymerase; **STAT1,** Signal transducer & activator of transcription-1; **TRAIL,** TNF-related apoptosis-inducing ligand; **DR,** Death receptor.

Table 5.1. Summary of preclinical treatments of ovarian cancer cell lines with hIFNγ-1b			
Cell Line	**Mechanism of action**	**Signalling molecules detected**	**Reference**
2774	Apoptosis	Nitric oxide*	(Rieder *et al*, 2001)
	Pyroptosis	Induction of IRF-1 & activation of caspase-1	(Kim *et al*, 2002)
HOC7	Apoptosis	Nitric oxide*	(Rieder *et al*, 2001)
OAW42	Apoptosis	PARP inhibition	(Wall *et al*, 2003)
OVCAR3	Apoptosis	Nitric oxide*	(Rieder *et al*, 2001)
	Less sensitive	Induction of IRF-1	(Kim *et al*, 2002)
	Apoptosis	PARP inhibition	(Wall *et al*, 2003)
	Cytostasis/ Apoptosis	Cell cycle arrest; G_1, G_2, and S phases; Induction of p53, Bax, and caspase-3**	(Guan *et al*, 2012)
	Cytostasis	Increasing p21 mRNA	(Burke *et al*, 1999)
OVCAR4, OVCAR5	Cytostasis/ Apoptosis	PARP inhibition	(Wall *et al*, 2003)
PA1	Pyroptosis	Induction of IRF-1 & activation of caspase-1	(Kim *et al*, 2002)
PEO1	Apoptosis/ Cytostasis	Depolarization of mitochondrial membrane, release of cytochrome C & activation of caspase-9	(Barton *et al*, 2005)
		Induction of caspase-8 & 9	(Wall *et al*, 2003)
	Cytostasis	Increasing STAT1 & p21 mRNA	(Burke *et al*, 1999)
PEO14, PEO16	Cytostasis/ Apoptosis	PARP inhibition	(Burke *et al*, 1999)
SKOV3	Insensitive	Initial expression of p21, IRF-1 mRNA detected. However, later the pattern of expression was reduced to the level of untreated cells.	(Burke *et al*, 1999; Kim *et al*, 2002; Wall *et al*, 2003)
SW626	Cytostasis/ Apoptosis	PARP inhibition	(Wall *et al*, 2003)
Note: * Polytherapy of hIFNγ, interleukin 1 beta (IL1β), and tumour necrosis factor alpha (TNFα), ** Polytherapy of hIFNγ plus TNFα			

5.3 Material & methods

5.3.1 Ovarian carcinoma cell lines & cultivation

Two ovarian carcinoma cell lines, PEO1 (passage No. ≥ 40) (Catalogue No.10032308) and SKOV3 (passage No. ≥ 20) (Catalogue No. 91091004), were purchased from the European Collection of Authenticated Cell Cultures (ECACC), UK. Cell lines were maintained at 37°C in a humidified growth chamber in 5% CO_2 in RPMI-1640 medium supplemented with L-glutamine and sodium bicarbonate (Sigma # R8758, Castle Hill, NSW 1765, Australia) and addition of 10% Fetal Bovine Serum (FBS) (Sigma #F4135; USA origin); penicillins (100 U mL^{-1}) and streptomycin (100 µg mL^{-1}). Cells were sub-cultured when confluent. For the passage, cells were dislodged from the culture-ware surface through the addition of Gibco® Trypsin-EDTA (0.25%) solution (ThermoFisher Scientific, Newstead, QLD 4006, Australia). Subsequently, trypsin was deactivated by addition of complete medium containing the FBS (see above). Sub-cultures were seeded at with 50 $\times 10^3$ cells per T-25 flask (25 cm^2 cap vented, Orange Scientific, Sydney, NSW, Australia). Culture medium was changed every three days.

5.3.2 Recombinant hIFNγ

Products from three different protein expression platforms were purchased; recombinant hIFNγ expressed in *E. coli* (Abbrev. hIFNγ-1b) (Sigma, #SRP3058), recombinant hIFNγ expressed in CHO (Abbrev. hIFNγ-CHO) (SinoBiologicals, #11725-HNAS, Beijing, China) and recombinant hIFNγ expressed in HEK293 (Abbrev. hIFNγ-HEK) (Acrobiosystems, #IFG-H4211, Newark, DE 19711, USA).

5.3.3 Deglycosylation

The removal of glycans is a technique to investigate the function of a glycoprotein, which allows the assignment of specific biological functions to a particular component of the glycoprotein *i.e.* removal of N-linked glycans may alter the half-life of the protein and its therapeutic potency (Varki, 2017).

For enzymatic elimination of all N-linked glycans from hIFNγ-CHO and hIFNγ-HEK, GlycoProfile™ II Enzymatic In-solution N-Deglycosylation Kit (Sigma, # PP0201) was used, following the manufacturer's instructions with the following modifications: β-

mercaptoethanol, a denaturant, was not added due to the potential cytotoxic effects on cancer cells (as both N-linked glycans position are located on the surface of hIFNγ dimmer (see introduction (Sareneva *et al*, 1995) thus denaturation is not required), and heat-inactivation of hIFNγ at 100°C was omitted as per recommendation in the protocol (hIFNγ is deactivated at a temperature range of 40-64°C).

Samples of 45 µL plus 5 µL of 1X Reaction Buffer (final concentration of hIFNγ;1 µg μL^{-1}) was prepared, then 5 µL PNGase F Enzyme Solution (500 U mL^{-1}) was added to the samples and incubated at 37°C overnight. Hence deglycosylated hIFNγ-CHO (Abbrev. deglyco-hIFNγ-CHO) and deglycosylated-hIFNγ-HEK293 (Abbrev. deglyco-hIFNγ-HEK) were produced.

5.3.4 *In-vitro* treatment

50 $\times 10^3$ cells were inoculated per T25-flask (n=3 per treatment) and incubated for 24 h. 5 mL of complete RPMI-1640 medium supplemented with 100 ng mL^{-1} of each six treatment conditions (hIFNγ-1b, hIFNγ-CHO, deglyco-hIFNγ-CHO, hIFNγ-HEK and deglyco-hIFNγ-HEK) was added and incubated for 72 h before dislodgement of cells for cell counts and viability, cytostasis and apoptosis analyses.

5.3.5 Cytotoxic & cytostatic measurements

A Guava® easyCyte 8HT Benchtop Flow Cytometer (Merck, #0500-4008) was used for conducting assays as follows;

i. **Cell counting & viability:** Absolute cell counts, identification of dead cells, and viability data were determined using the Guava® ViaCount® Reagent (Merck, # 4000-0040, USA) on cell suspensions. This assay differentiates between viable and non-viable cells according to the differential permeability of DNA-binding dyes in the reagent. The percentile of the cytostatic effect of each treatment was calculated as per equation 1 (eq. 1):

$$\text{Cytostasis (\%)} = \frac{\text{Control [total cells]} - \text{Treatment [total cells]}}{\text{Control [total cells]}} \times 100 \qquad \text{eq. 1}$$

ii. **TUNEL assay:** DNA fragmentation was analysed using the TUNEL assay (Terminal deoxynucleotidyl transferase (TdT) dUTP Nick-End Labelling). Specifically, to quantify the percentage of cells in late apoptosis (an indirect proxy for the inhibition of PARP) the In Situ Cell Death Detection Kit, Fluorescein

(Roche, #11684795910, Sigma) was used. The TdT labels the 3´ blunt ends of DNA resulting from DNA breakage, which occurs during late apoptosis.

iii. **Cell cycle analysis:** The percentile of cells in G_0/G_1, S, and G_2 phases was determined based on DNA content. Prior to treatment, cells were firstly synchronised in G_0 by culturing for 24 h in RPMI medium without FBS. Following treatment (see above), the Guava® Cell Cycle Reagent (Merck, #4500-0220) was used following the manufacturer's protocol for cell cycle analysis.

5.3.6 Protein extraction & determination

Following detachment at confluency after 72 h treatment, cells were washed with PBS then lysed by adding 0.5 mL ice-cold lysis buffer (10 mM Tris-HCl, 100 mM NaCl, pH 8, 25 mM EDTA, pH 8, 0.5% SDS, 1 Protease inhibitor cocktail tablet (Boehringer, #1697498, Mannheim, Germany) per 10 mL) and vigorous pipetting. Afterwards, lysates were frozen at -20°C overnight, before defrosting and centrifugation at 12,000 *g* for 5 min at 4°C. The total protein content of the cell lysate supernatant was determined spectrophotometrically at 562 nm on an EnSpire® Multimode Plate Reader (PerkinElmer, Glen Waverly, VIC, Australia) using the Pierce™ BCA Protein Assay Kit (ThermoFisher, #23225) using bovine serum albumin (BSA) as a standard.

5.3.7 Denaturing polyacrylamide gel electrophoresis (SDS-PAGE) & Western blot analysis

To denature samples; 20 µg of total protein was added to Laemmli sample buffer (200 mM Tris-Cl, (pH 6.8), 400 mM Dithiothreitol, 8% SDS, 0.4% bromophenol blue, 40% glycerol) followed by heating in 95°C for 5 min. Samples were loaded on 12% Mini-PROTEAN® TGX™ Precast Gels (Biorad, #4561044, Gladesville, NSW 2111, Australia). Electrophoresis was conducted at 200 V for 30 min using 1X running buffer (25 mM Tris, 192 mM glycine, and 0.1% SDS). Precision Plus Protein™ standard (Biorad, #1610373) was used to determine product size. Proteins were transferred to PVDF membranes using Trans-Blot® Turbo™ Mini PVDF Transfer Packs (Biorad, #1704156) and a Trans-Blot® Turbo™ Transfer System (Biorad) using the manufacturer's 3-min protocol. Blots were incubated in blocking buffer (5% BSA in Tris-buffered saline with Tween 20 (TBST) buffer; 20 mM Tris base, pH 7.5, 150 mM NaCl, 0.1% Tween 20) at room temperature with agitation for 1 h. Antibodies (see below) were diluted in blocking buffer. Blot membranes were exposed to the primary antibody

at 4°C overnight and to the secondary antibody with agitation at room temperature for 1 h. Clarity Max™ Western ECL Substrate (Biorad, #1705062) and the Syngene G: Box XRQ chemiluminescent system were used for detection and imaging, respectively.

Western blot results were translated into statistical values with densitometry ImageJ software (version 1.51i, USA), using the Gel Analyser function. The relative intensity of blots was calculated as per equation 2 (eq. 2):

$$\text{Relative intensity} = \frac{Blot\ of\ interest\ [\ arbitrary\ unit]}{Corresponding\ blot\ of\ the\ loading\ control\ (\beta-actin)[arbitrary\ unit]} \quad \text{eq. 2}$$

5.3.8 Antibodies

Apoptosis Western Blot Cocktail kit (pro/p17-caspase 3, cleaved-PARP, β-actin) (Abcam, # ab136812, Melbourne, VIC, Australia) was used with dilution for primary antibody cocktail 1: 250 and 1:100 for goat HRP-conjugated secondary antibody cocktail. Cell Cycle and Apoptosis WB Cocktail kit (Cdk2 pTyr15 (pCdk), Histone H3 pSer10 (pHH3) /β-actin/PARP) (Abcam, #ab139417) was used with dilution for primary antibody cocktail 1: 250 and 1:2500 for secondary antibody cocktail. Anti-FADD antibody (Abcam, #ab24533) were used with dilution for primary antibody 1:1000 and 1:100 for goat HRP-conjugated secondary antibody.

5.3.9 Dose-response assay

Dose-response was evaluated using the CellTiter 96® Non-Radioactive Cell Proliferation (MTT) Assay (Promega, #G4000, Alexandria, NSW 2015, Australia). Approximately 3,000 cells were inoculated per 100 µL volume of complete RPMI-1640 medium per well of a 96-well assay plate in dilution series of hIFNγ-1b and hIFNγ-HEK (0-500 ng mL^{-1}). Following the manufacturer's protocol, absorbance was recorded spectrophotometrically at 570 nm on an EnSpire® Multimode Plate Reader (PerkinElmer, Glen Waverly, VIC, Australia).

5.3.10 Microscopy

Cultured cells were imaged with an inverted microscope (Olympus IX53, Japan) directly in the tissue culture flasks (T25) after 72 h of incubation in hIFNγ treatments or untreated controls using phase contrast at 100X magnification.

5.3.11 Statistics

Data were analysed via one-way ANOVA using S-PLUS® software, version 8.0. The critical value (α) was set to α = 0.01. The homogeneity of variance in data was assessed using the Leven's test. Normality was checked using the Shapiro-Wilks test. If statistical significance was detected, Tukey-Kramer HSD posthoc tests were performed and only results with $p < 0.01$ were considered significant. All the experiments were conducted in triplicate.

5.4 Results

5.4.1 Cytotoxic effect of recombinant hIFNγ on PEO1 and SKOV3

In general, the effect of hIFNγ was much stronger in PEO1 (~70% dead cells) compared to effects on SKOV3 (max. ~30% dead cells) (Fig. 5.2A). In PEO1, treatment with 100 ng mL^{-1} of recombinant hIFNγ from *E. coli*, CHO and HEK293, glycosylated and de-glycosylated for the latter two, induced significant total cell death (Fig. 5.2 A). However, no significant difference was observed among treatments ($p < 0.01$), suggesting that the choice of expression platform and status of glycosylation had no effect on the cytotoxicity of recombinant hIFNγ against this cell line. Determination of TUNEL-positive ($TUNEL^+$) cells showed a significant effect of treatments against the control in PEO1. However, no significant difference was observed among treatments ($p < 0.01$). Additionally, percent of $TUNEL^+$ cells of the total dead cells decreased significantly after treatment with hIFNγ with no difference observed between treatments (Fig. 5.2B). As expected, neither cleaved PARP nor cleaved caspase-3 was detected in western blots, but a slight reduction in relative levels of procaspase-3 (an inactive form of caspase 3) was observed after treatment with all types of hIFNγ (Fig. 5.3D). Expression of FADD also not detected.

In SKOV3, a statistically significant effect of treatment on the number of total dead cells ($p < 0.01$) was identified with cytotoxic efficacy declining in this order (Fig. 5.2A): hIFNγHEK = deglycolhIFNγHEK = hIFNγCHO > deglycolhIFNγCHO ≥ hIFNγ1b ≈ control.

Determination of $TUNEL^+$ cells also showed a significant difference between all treatments, except hIFNγ-1b, against the control. However, no significant difference was observed among mammalian expressed hIFNγ treatments ($p < 0.01$).

Furthermore, close to 50% of total dead cells were TUNEL$^+$ (Fig. 5.2B). Western blot analysis detected procaspase-3 (Fig. 5.3A), with levels not being affected by treatment, but cleaved PARP and caspase-3 were not detected. In contrast to PEO1, in SKOV3 FADD was detected in all treatments and the control (Fig. 5.3B). FADD levels were upregulated particularly after treatment with mammalian expressed hIFNγ, with highest levels observed after treatment with hIFNγ-CHO (Fig. 5.3B).

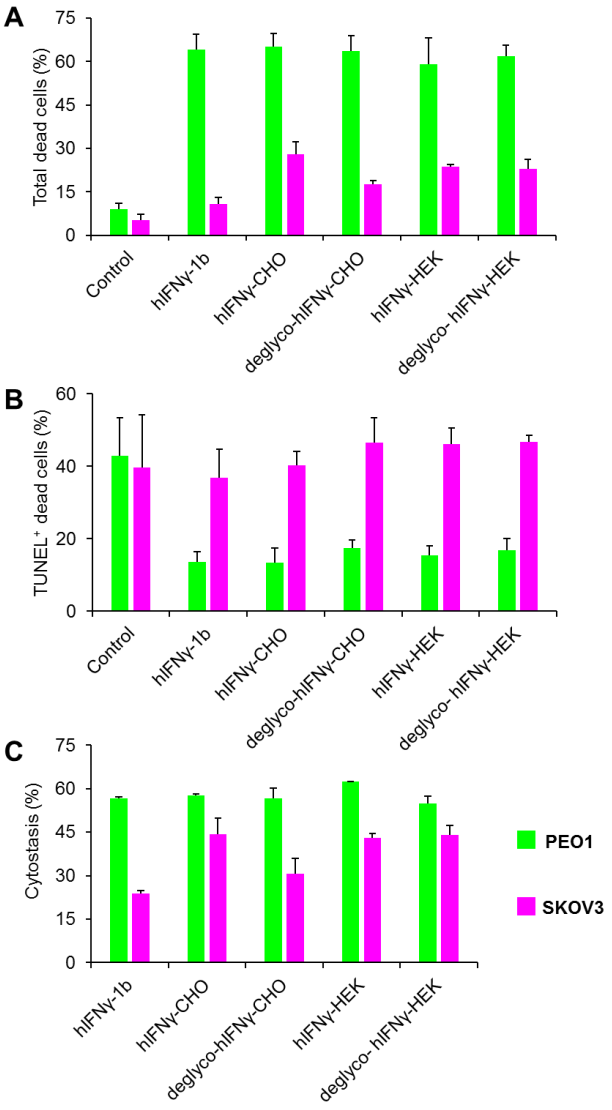

Figure 5.2. Cytotoxic and cytostatic effect of hIFNγ on PEO1 and SKOV3
(A) Percentage of total dead cells, and **(B)** percent TUNEL-positive cells of dead cells, **(C)** and cytostasis after 72 h exposure to recombinant hIFNγ from three different expression systems and their deglycosylated forms (Mean ± SD, n= 3).

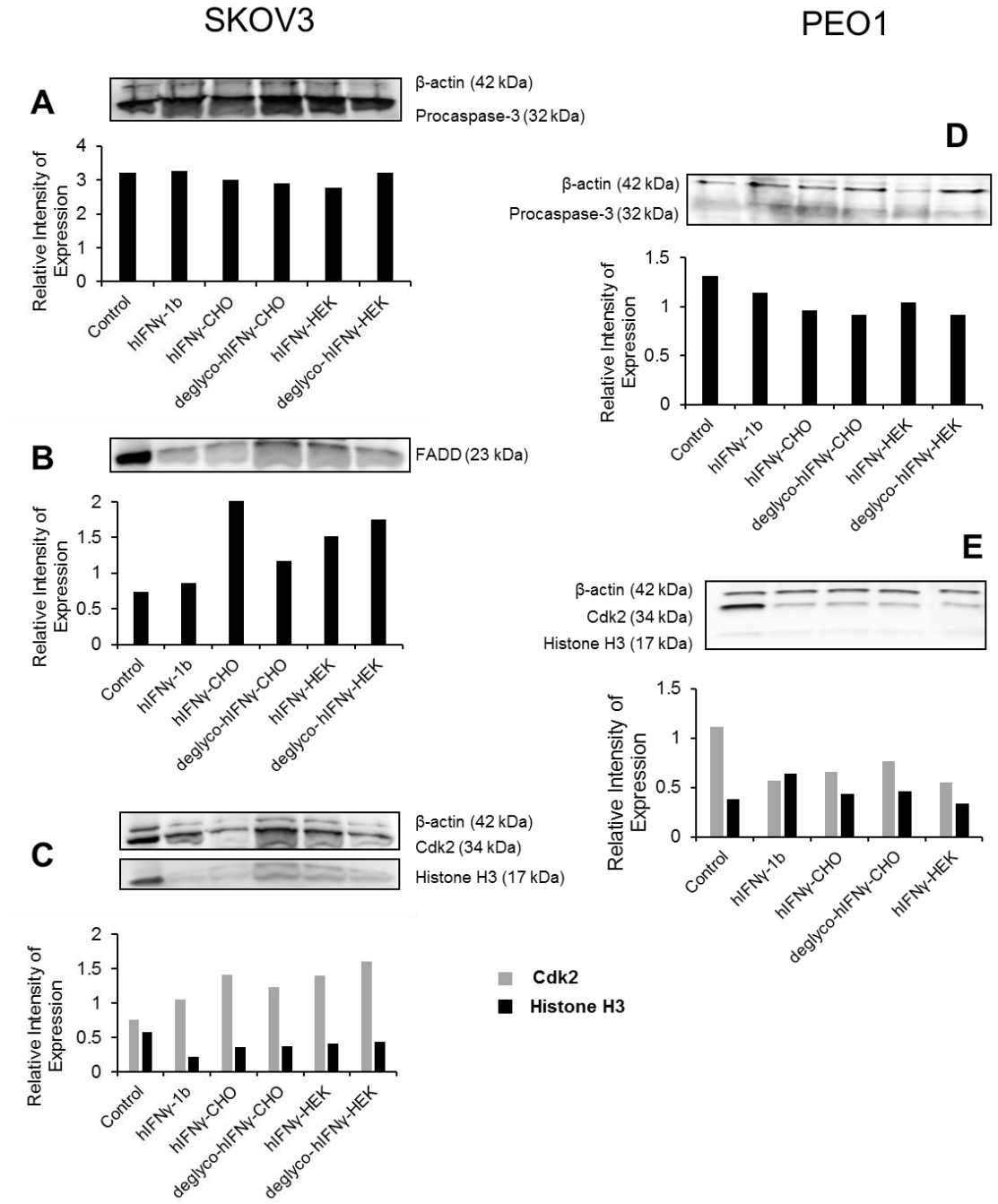

Figure 5.3. Western analysis of recombinant hIFNγ-induced signalling molecules in SKOV3 and PEO1. **(A, D)** procaspase-3 (inactive form of caspase-3), **(B)** FADD, **(C, E)** Cdk2 (as an indication of G_1/S phase), Histone H3 (as a biomarker of M phase), Untreated cells (control) were used to determine un-induced signalling molecule levels and β-actin, a housekeeping protein, was used as a loading control to obtain relative intensity histograms with Image J.

5.4.2 Cytostatic effect of recombinant hIFNγ on PEO1 and SKOV3

In general, comparison of cytostasis following treatment with recombinant hIFNγ showed that PEO1 is 10-30% more sensitive than SKOV3 (Fig. 5.2C). Based on cell number analysis, ~60% of treated PEO1 cells were cytostatic, with the slightly stronger and statistically significant effect ($p < 0.01$) observed in cells treated with recombinant hIFNγ expressed in HEK (Fig. 5.2C).

Flow-cytometric analysis of DNA content showed an effect of recombinant hIFNγ on the cell cycle of PEO1 cells, with fewer treated cells in G_1 and more cells in G_2 compared to controls ($p < 0.01$), but no significant difference was observed between treatments (Fig. 5.4A). Western blot analysis confirmed reduced levels of Cdk2 in treated PEO1 cells compared to controls (Fig. 5.3E). Levels of the M-phase indicator Histone H3 were more and less comparable between controls and treatments (Fig. 5.3E).

In contrast, analysis of SKOV 3 cells showed a significant increase cytostasis following treatment with recombinant hIFNγ with largest effects observed for hIFNγ from HEK (glycosylated and deglycosylated) and CHO (glycosylated) (Fig. 5.2C) ($p < 0.01$). Deglycosylation of hIFNγ from CHO cells decreased the efficacy of the treatment, and the unglycosylated hIFNγ-1b was least effective.

In addition, flow-cytometric analysis of DNA content in SKOV 3 cells showed a significant percent of cells arrested in S-phase with simultaneously reduced numbers observed in G_2 following treatment with recombinant hIFNγ, with no impact of source of hIFNγ or glycosylation status (Fig. 5.4B).

Western blot analysis also confirmed an increase in Cdk2 and reduced levels of Histone H3 in treatments compared to controls which supports the flow cytometric cell cycle analysis based on DNA content (Fig. 5.3C).

SKOV3 cells exposed to hIFNγ-CHO, deglyco-hIFNγ-CHO, hIFNγ-HEK, and deglyco-hIFNγ-HEK showed changes in cell morphology (Fig. 5.5), with cells becoming thin and elongated more frequently, while such alterations were not observed for PEO1.

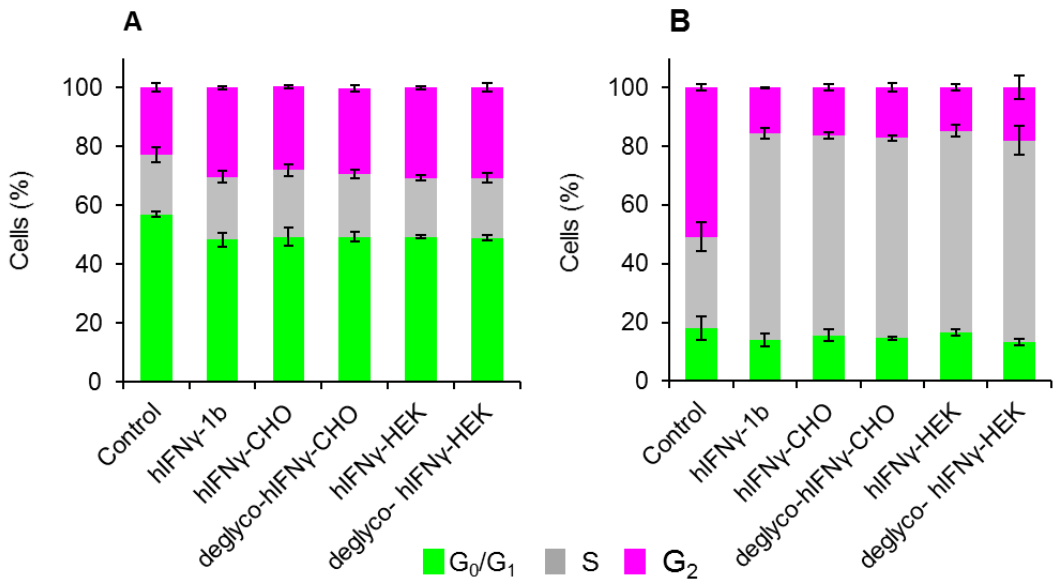

Figure 5.4. Cell cycle analysis of PEO1 (A) and SKOV3 (B) following a 72 h exposure to recombinant hIFNγ from three different expression platforms and their deglycosylated forms. (Mean ± SD, n= 3).

5.4.3 Dose-effect of hIFNγ-1b and hIFNγ-HEK on growth of PEO1 and SKOV3

The growth of PEO1 was inhibited by hIFNγ-1b and hIFNγ-HEK in a "dose-dependent" manner (Fig. 5.6A). However, no significant difference was observed between the two sources of hIFNγ, and the calculated IC_{50} was ~200 ng mL^{-1} for both (Fig. 5.6A).

In contrast, no dose-dependent effect hIFNγ-1b and hIFNγ-HEK on the growth of SKOV3 was observed in a range of 15-500 ng mL^{-1} (Fig. 5.6B). Treatment with 15-500 ng mL^{-1} inhibited growth by approximately 15% and 25% for hIFNγ-1b and hIFNγ-HEK respectively. Since no dose response was observed, an IC_{50} of hIFNγ could not be calculated for this cell line.

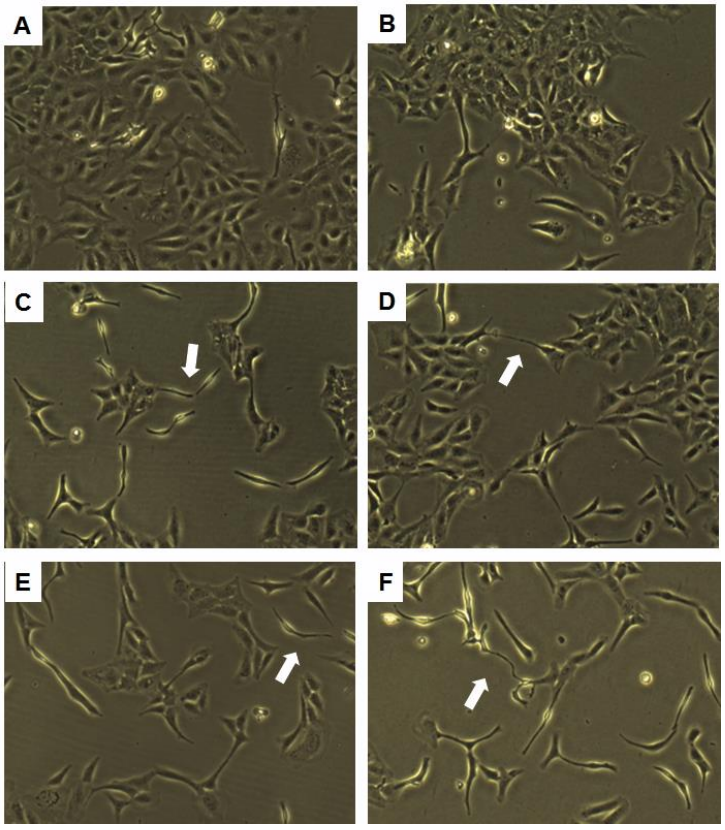

Figure 5.5. Recombinant hIFNγ induces cell elongation in SKOV3 cells. Phase contrast micrographs of SKOV3 cells after 72 h treatment with the elongated thin shape. **A)** Control **B)** hIFNγ-1b **C)** hIFNγ-CHO **D)** deglyco-hIFNγ-CHO **E)** hIFNγ-HEK **F)**. deglyco-hIFNγ-HEK. White arrows point to elongated thin-shaped cells.

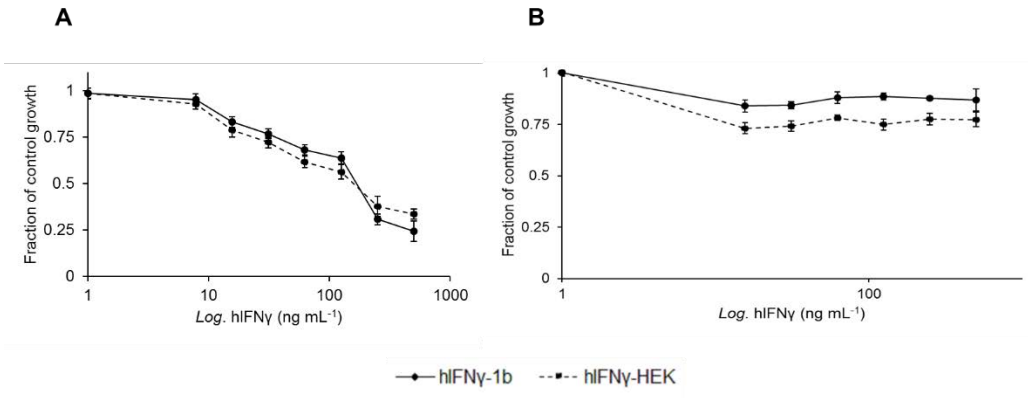

Figure 5.6. 48h-dose-response to treatment with hIFNγ-1b and hIFNγ-HEK on the growth of PEO1 (A) and SOKV3 (B). Growth is expressed as a fraction of control values. (Mean ± SD, n=3).

5.5 Discussion

Differences in cytotoxicity, cytostasis, IC_{50} and therapeutic efficacy of drugs, including hIFNγ, have been observed in cancer cells, including PEO1 and SKOV3, which has been documented to reflect high heterogeneity in cancer cells regarding genomic mutations, DNA copy number, oncogene bypass, and epigenetic alterations. (Hu & Zhang, 2016; Kim *et al*, 2012b).

5.5.1 hIFNγ efficacy in SKOV3

SKOV3 has been reported as insensitive to treatment with hIFNγ-1b ((Wall *et al*, 2003). However, this study showed a degree of sensitivity to mammalian expressed hIFNγ. Deglycosylation had a marginal impact on the cytotoxic efficacy but a significant impact on the cytostatic efficacy in CHO-, but not HEK-expressed hIFNγ. This implies that other parameters like the proper folding of the native protein in mammalian expression systems are as important as glycosylation for drug potency and pharmacodynamics (Frokjaer & Otzen, 2005; Vink *et al*, 2014).

Although just under 50% of dead cells were $TUNEL^+$, signalling molecules typically involved in apoptosis (cleaved PARP and caspase3) were not detected by Western blot analysis, ruling out apoptosis as the principal mechanism of cell death. This discrepancy might be explained by non-specificity of the TUNEL assay, which is a serious drawback as it fails to discriminate between apoptotic and necrotic cell death, or generally any mechanism which causes damage to the nucleic acid and generate free end DNA fragments (Charriaut-Marlangue & Ben-Ari, 1995). Although FADD was present in SKOV3 at detectable levels also in control cells, the possibility that FADD acts as an initiator of the extrinsic apoptotic pathway can be ruled out, as no cleaved PARP and caspase 3 were detected. Overall cell death was low in SKOV3, which together with the presence of FADD in control cells, may indicate that FADD inhibits apoptosis through the activation of NF-κB (see introduction) (Fig. 5.1) (Schinske *et al*, 2011). FADD may also contribute to necroptotic cell death via signalling leading to mitochondrial dysfunction, which requires further investigation on increased levels of proteins participating in the formation of complex II (Fig. 5.1) (Lee *et al*, 2012; Pasparakis & Vandenabeele, 2015). The occurrence of autophagy is also unlikely because expression of FADD inhibits the autophagic cell death mechanism (Bell *et al*, 2008) Of all cell death mechanisms, necroptosis is the most probable for observed cell death in SKOV 3, an interpretation supported by hIFNγ-induced cell death mechanisms in other cancer types (Pyo *et al*, 2005; Thapa *et al*, 2011). Further investigation is

required to prove the occurrence of necroptotic cell death by detection of receptor-interacting kinase 3 (RIPK3) which has been discovered to be a core component of this process (Pasparakis & Vandenabeele, 2015).

To the best knowledge of the authors, this is the first report on FADD levels in SKOV3 cells, which could potentially correlate with tumorigenesis, anti-apoptotic behaviour, and resistance against anticancer drugs, which has also been reported for lymphomas, lung, and colorectal carcinomas (see introduction) (Patel *et al*, 2014). Additionally, FADD can be a novel potential target to overcome drug resistance in this ovarian cancer cell line (Fig. 5.1) (Schinske *et al*, 2011).

In SKOV3; cytostasis caused by cell cycle arrest in S phase seems to be the major inhibitory effect of all three types of hIFNγ, and Western blot analysis showed a reduction of Histone H3 expression (as an indicator of M phase) in treatments in comparison to controls. This result is supported by previous studies showing hIFNγ-1b-induced elevated levels of p21 - and IRF-1 mRNA in SKOV3 (Burke *et al*, 1999). Other cancer types sensitive to hIFNγ-1b also showed a similar trend, *e.g.* the induction of cell cycle arrest in human mesothelioma with hIFNγ-1b seems to depend on cyclin regulation through $p21^{WAF1/CIP1}$ and $p27^{Kip1}$-independent mechanisms (Vivo *et al*, 2001) and relies on p53 and $p21^{WAF1/clp1/Sdl1}$ pathways in hepatocytes (Kano *et al*, 1997) (Fig. 5.1).

5.5.2 hIFNγ efficacy in PEO1

PEO1 showed a high degree of sensitivity and mortality after treatment with recombinant hIFNγ regardless of expression platform and glycosylation. Following treatment with recombinant hIFNγ, a significant reduction in the percentage of $TUNEL^+$ cells was observed, suggesting that cell death may not be a result of apoptosis. Key apoptotic signalling molecules (cleaved PARP and caspase-3) were also not detected by Western blot, although levels of procaspase-3 decreased slightly. These results oppose apoptotic signalling transduction as a consequence of hIFNγ treatment in PEO1, which is contrary to previous reports (Barton *et al*, 2005; Wall *et al*, 2003). Based on flow cytometric measurements of induced levels of caspase 8 and 9, Wall *et al* (2003) concluded apoptosis as a mechanism of cell death in PEO1. Levels of cleaved PARP or caspase-3 were, however, not reported and there were significant differences in cell densities (not given *vs.* 10,000 cells mL^{-1}), hIFNγ concentrations used (≈ 250 *vs.* 100 ng mL^{-1}), and treatment duration (96 h *vs.* 72 h) in their and our

study, which limits comparability. , however, confirmed the presence of cleaved PARP, caspase-8 and 9 in PEO1 using Western blotting after 48-96 h treatment with ~170 ng mL^{-1} of hIFNγ-, but again, cell densities used were not given. Thus different outcomes in our studies could be due to different experimental conditions and difference in cell density/ confluence status of the culture (100% *vs.* 40% used here). Apoptosis *in vitro* culture condition has been reported to be strongly cell density-dependent *e.g*. leukaemia HL-60 cells release an unknown low molecular weight peptide-containing factor in response to an increase in cell density to induce apoptosis in an autocrine manner (Saeki *et al*, 1997). Another possible explanation may be the high passage number of the cell lines at the time of purchase, particularly for PEO1 (not specified by (Barton *et al*, 2005)), which has been implicated to cause resistance to apoptosis (Pronsato *et al*, 2013).

The lack of FADD expression also makes necroptotic cell death in PEO1 unlikely, since activation of FADD is essential for induction of necroptosis (Lee *et al*, 2012; Pasparakis & Vandenabeele, 2015). A remaining possible hIFNγ-induced cell death mechanism in this high passage number PEO1 cell line is autophagy, as hIFNγ has been shown to induce autophagy signalling pathways with growth inhibition and cell death in other cancer cell lines like hepatocellular carcinoma (Li *et al*, 2012). Thus, it is recommended to investigate the presence of key autophagic cell death proteins *e.g.* LC3 (microtubule-associated protein 1 light chain 3), Beclin-1 or Atg5 (Autophagy protein 5) proteins (Li *et al*, 2012; Pyo *et al*, 2005).

In PEO1, treatment with recombinant hIFNγ led to cytostasis caused by cell cycle arrest in G_2 phase, which correlates well with previous reports that hIFNγ induced elevated levels of p21 mRNA and cytostasis in PEO1 following treatment with hIFNγ-1b (Burke *et al*, 1999). The assay used in this study for cell cycle analysis is not capable of detecting cells in M phase, but Western blot analysis showed decreased levels of the Cdk2 protein in treatments, indicative of lower cell numbers in G_1/S phases in comparison to controls (Liu *et al*, 2013). Histone H3 levels were low in controls and treatments, indicative perhaps of a very short M phase, as there were no significant differences between controls and treatments.

hIFNγ-1b dose response experiments on ovarian cancers primarily report dose-dependency of growth or cell death responses, but show high variability depending on cell lines used (Wall *et al*, 2003), For example, the IC_{50} reported for OVCAR4 was 10 units mL^{-1} (= 0.5 ng mL^{-1}), whereas it was >5000 units mL (>250 ng mL^{-1}) for SW626. The experiment was conducted using 5,000 cells per 96-well tissue plate for a

treatment time of 96 h (Wall *et al*, 2003). In our study, dose-response relationships were investigated for the first time for SKOV3 and PEO1, and results were “dose-independent” and “dose-dependent,” respectively. Growth inhibition of SKOV3 was higher in cells treated with hIFNγ-HEK compared to hIFNγ-1b, but no statistical differences were observed in PEO1. Comparisons of IC_{50s} between our study and previous studies is hampered due to significant differences in experimental conditions (*e.g.* cell density, the difference in cell lines, and duration of treatment, see above).

5.5.3 Differences in responses of SKOV3 and PEO1 to treatment with hIFNγ

Only in SKOV3 did mammalian expressed hIFNγ treatment result in higher levels of cell death compared to untreated controls and hIFNγ-1b treatments. It has been shown that glycosylation affects the three-dimensional structure (3D) and binding affinity of glycoproteins in general (Huang *et al*, 1997). It may be possible, since the N-glycosylation sites are on the external surface of the hIFNγ homodimer, that deglycosylation did not affect the 3D structure. This would explain why deglycosylation of hIFNγ expressed in HEK293 did not change its efficacy in SKOV3 cells. This contrasts observation of hIFNγ induced cell death in PEO1, where source and glycosylation did not result in different outcomes. This seems to indicate that the hIFNγ receptor (hIFNγ-R) in PEO1 and SKOV3 may be different in their ability to bind hIFNγ. The SKOV3 hIFNγ-R could bind de-glycosylated/glycosylated hIFNγ better than bacterial unglycosylated hIFNγ-1b, if the latter has a different 3D structure, while the hIFNγ-R interaction in PEO1 cells could be more tolerant of differences in 3D structure. This hypothesis is supported by studies that show mutations in hIFNγ-Rs that affect the capacity of the receptor to bind hIFNγ (Boselli *et al*, 2007; Jean *et al*, 1999; Rosner *et al*, 2006; Xu *et al*, 1998). Future detailed studies on the amino acid sequence differences in the receptors and crystallography to unravel changes in the 3D structure of hIFNγ forms and binding sites of the receptor are also required. Furthermore, induction of FADD in SKOV3, but not PEO1, could indicate hIFNγ-initiated Fas-signalling by the mammalian forms, especially the CHO-derived glycosylated form of hIFNγ, as shown in hIFNγ-producing human $CD4^+$ T-lymphocytes (Boselli *et al*, 2007).

5.5.4. Conclusion

hIFNγ expressed in mammalian expression platforms showed marginally significantly higher cytostatic and cytotoxic efficacy for SKOV3 but did not lead to large differences

in PEO1 compared to hIFNγ-1b. Additionally, this study is the first to show the presence of FADD even in untreated SKOV3, which might be the reason for the anti-apoptotic behaviour and drug resistance in this cell line. Furthermore, these levels positively responded to treatments with mammalian-expressed hIFNγ. Cytostatic effects and mechanisms of cell death of hIFNγ were not comparable with previous publications on PEO1, which emphasises that there is an urgent need for standardisation of toxicity assays (*e.g.* confluency, passage number, duration of treatment and use of bioactivity units), especially when aiming to unravel signalling cascades and treatment-induced cell death mechanisms. In addition to this and similar studies, a continuum of preclinical research is required to investigate responsivity of more ovarian cancer cell lines, other cancer types, and recombinant glycoproteins to generalise the idea that mammalian/human expression platforms can enhance the therapeutic efficacy of anti-cancer biotherapeutics.

Chapter 6. General discussion & conclusion

As outlined in Chapter 1 and throughout the thesis, hIFNγ has a range of medical application with increasing prospects to be used as an immunotherapeutic. However, cost-effective production and the impact of expression system and glycosylation are to date underexplored. To make informed decisions on cost-effectiveness and quality of recombinant expression of hIFNγ, new approaches should integrate productivity data, glycan analysis and cost of production. Before commencement of the present research, several knowledge gaps existed pertaining to cost-effective production and impact of expression system and glycosylation on productivity and therapeutic efficacy of recombinant hIFNγ.

To address these knowledge gaps, a comprehensive series of studies were undertaken that evaluated the possibility of using red yeast, *R. glutinis* as a eukaryotic expression system using cheap C1 carbon sources, with a particular emphasis on using methane, a GHG present in large amounts in point sources from agricultural activities *e.g.* intensive dairies, piggeries, *etc.* Later the productivity of recombinant hIFNγ in *P. pastoris* was evaluated, and the enhancement of expression was investigated. Finally, the effect of expression system and glycosylation of recombinant hIFNγ on the therapeutic efficacy of this glycoprotein was explored.

This research has contributed towards improving our knowledge about methane utilisation in *R. glutinis*, establishing that the yeast is neither methanotrophic nor methylotrophic and therefore unsuitable for achieving the first aim of this research The productivity of *P. pastoris* for large-scale production of recombinant hIFNγ also yielded results that contradicted published yields for this cytokine by *P. pastoris*. Enhancement of expression of recombinant proteins was achieved using selective pressure on the adjacent genes, and the research showed that expression system impacts on the therapeutic efficacy of recombinant hIFNγ on ovarian cancer cell lines.

The following discussion first summarises in more detail the main conclusions and outcomes obtained in the previous chapters, followed by synthesis of results and a discussion of the potential applications of the present research. Lastly, the discussion concludes by addressing future research directions.

6.1 Synopsis of major conclusions and outcomes

Chapter 1 reviewed the expression of recombinant hIFNγ, an important cytokine in the innate and adaptive immune system and described currently produced commercial recombinant hIFNγ in a prokaryotic expression system, *E. coli*. A short half-life,

formation of hIFNγ inclusion bodies in the bacterium and potential for endotoxin contamination of the product were known for this prokaryotic expression system, hurdles that do not exist in eukaryotic systems. In chapter 2., no methane utilisation was achieved with *R. glutinis* despite near identical experimental designs. Furthermore, no growth was observed on either methane or methanol as substrates, in contrast to previous reports (Wolf & Hanson, 1980; Wolf *et al*, 1980; Wolf & Hanson, 1979), who curiously reported that *R. glutinis* could not be grown on C1 carbon intermediates (methanol, formaldehyde, formate) commonly derived from bacterial methane oxidation. As supported by an abiotic methane dissipation control, it is concluded that *R. glutinis* is neither a methanotrophic nor methylotrophic yeast and that prior reports are likely a misinterpretation of either methane dissipation into the medium or that the culture harboured methanotrophic bacteria, with the yeast being saprophytic, utilising complex carbon exudates for growth. For this reason, the primary goal to use *R. glutinis*, as a potential expression system for recombinant hIFNγ while using cheap and abundant C1 carbon sources was compromised, resulting in a change of organism.
Chapter 3 investigated the use of the methylotrophic yeast, *P. pastoris* for expression of recombinant hIFNγ while feeding another cheap C1 carbon source, methanol. Efficient expression of hIFNγ had been reported once for *P. pastoris*. Based on this, we expanded the study of hIFNγ expression in *P. pastoris* using four different strains (X33: wild type; GS115: HIS-Mut+; KM71H: Arg+, Mut- and CBS7435: Mut^S) and three different vectors (pPICZαA, pPIC9, and pPpT4αS). In addition, transformations included using the natural sequence (NS) and two codon-optimised sequences (COS1 and COS2) for *P. pastoris*. Following methanol induction, no expression/ secretion of hIFNγ was detected in X33 with highest levels recorded for CBS7435: Mut^S (~16 μg L^{-1}). The low expression might be due to the low abundance of mRNA, based on mRNA copy number.
Simultaneously with chapter 3, in chapter 4. the transformed *P. pastoris* (strain GS115-pPIC9-COS1) was cultured under continuous amino acid starvation in the amino acid-free minimal medium for ten days, with five inoculations into unspent medium every second day. Under these conditions, only successfully transformed cells (*hIFNγ* – *HIS4*+) are able to synthesise histidine and therefore thrive. As shown by ELISA, amino acid starvation-induced selective pressure on *HIS4* improved expression and secretion of the adjacent hIFNγ by 55% compared to unchallenged cells. It is suggested that these adjacent genes (*hIFNγ* and *HIS4*) in the transformed *P. pastoris* are transcriptionally co-regulated and their expression is synchronised. To the best of the knowledge of the authors; this is the first study demonstrating that amino acid starvation-induced selective pressure on *HIS4* can alter the regulation pattern of

adjacent genes in *P. pastoris*. In contrast to the previous report (Wang *et al*, 2014), it is concluded that this expression platform is not an economically viable for commercial production of low-cost, high-quality eukaryotic recombinant hIFNγ, which is endorsed by another recent study by Prabhu *et al* (2016).

In chapter 5, the effect of glycosylation and expression system of recombinant hIFNγ on the growth of ovarian carcinoma cell lines is investigated. PEO1 cells were more sensitive to hIFNγ (~70% cell death, ~60% cytostasis arrest in G2-phase) than SKOV3 (~30% cell death, ~20-45% cytostasis arrest in S-phase). Responses were dose-dependent (IC_{50} = 200 ng mL^{-1}) and expression platform/glycosylation status-independent in PEO1, whereas the SKOV3 cell line was only affected by mammalian-expressed hIFNγ in a dose-independent manner. Cleaved PARP and caspase-3 were not detected for either cell line, but FADD was expressed in SKOV3 with levels increasing following treatment. hIFNγ did not induce apoptosis in either cell line. Mammalian- expressed hIFNγ increased cell death and cytostasis in the drug-resistant SKOV3. The presence of FADD in SKOV3, which may inhibit apoptosis through activation of NF-κB, could serve as a novel therapeutic target.

6.2 Synthesis of research outcomes

IFNs are crucial for effective non-specific host defence against many viruses and their anti-viral, immuno-modulatory, and anti-tumour effects make them successful therapeutics for clinical use. However, future research is required to expand the knowledge about the mechanisms of their effects and side-effects with the purpose of taking full advantage of their therapeutic potential (Fensterl & Sen, 2009). To date, the most used and efficient expression system for production of recombinant hIFNγ is *E. coli* due to the ease of recombination techniques and high productivity. However, bacterial expression systems have many disadvantages.

To overcome the inadequacies of the bacterial expression systems, the hIFNγ gene has also been expressed in other host cells (Table 1.4) (Bagis *et al*, 2011; Chen *et al*, 2004; Derynck *et al*, 1983; Ebrahimi *et al*, 2012; Haynes & Weissman, 1983; Lagutin *et al*, 1999; Mory *et al*, 1986). Only some of these expression systems provided satisfactory results in terms of yield, physico-chemical stability and biological activity (Leister *et al*, 2014). However, improvements achieved to date do not provide a viable replacement for *E. coli*. For these reasons, further attempts for exploring more efficient and adequate expression systems are necessary. This research needs to report on

crucial commercial aspects such as yields and system productivity, biological activity, glycosylation patterns, dimerisation and molecular size of the protein, which have been neglected in most of the previous studies (Table 1.3). Similarly, the efficiency of purification has not been considered in eukaryotic expression systems which require more attention in future studies.

6.2.1 Expression comparison of hIFNγ to other interferons achieved in *P. pastoris*

Despite dissimilarity of IFNγ to other interferons, *e.g.* IFNα and IFNβ in terms of sequence and functionality (Samuel, 2001), the comparison below is provided to depict a bigger picture for future investigations.

In the context of *P. pastoris* as a general expression system, it is noteworthy that universal application of *P. pastoris* is to some degree hampered by its unpredictable yields for different heterologous proteins, which is now assumed to be caused by varied efficiencies of recombinant proteins to traffic through the host secretion machinery (Yang *et al*, 2013).

Comparison to other human interferons
Successful expression of recombinant IFNα in *P. pastoris* has repeatedly been reported to yield 200-300 mg L^{-1} (Ghosalkar *et al*, 2008; Salunkhe *et al*, 2010; Shi *et al*, 2007), which is substantially higher than achieved for hIFNγ in the presented research (Razaghi *et al*, 2017), but identical to those reported by (Wang *et al*, 2014). However, the expression of recombinant IFNβ in *P. pastoris* was less productive ranging only between 2-12 mg L^{-1} (Skoko *et al*, 2003; Yu *et al*, 2003), which is in the same range as yields reported for hIFNγ in the patent (Thill & Davis, 1989) and still 3-orders of magnitude higher than achieved in this research.

Comparison to Interferon gammas originating from other species
Reported secreted yields of porcine IFNγ in *P. pastoris* yielded 108-125 mg L^{-1} (Huang *et al*, 2005; Yao *et al*, 2008). However, reported secreted yields of bovine IFNγ was even higher with 1 g L^{-1} (Shi *et al*, 2006).

There is an apparent mismatch between the reported exceptional yields (Huang *et al*, 2005; Yao *et al*, 2008) and the ranking of the journal in which the research was published. It might be well worth to revisit these studies to explore reproducibility. This hesitation in accepting this one of results as routinely achievable is informed by the

similarity of approach to expression (all studies used the methanol-inducible AOX promoter and α-mating secretion signal). Alternatively, it is perhaps possible that expression and secretion could be strongly sequence-dependant in *P. pastoris*, *i.e.,* even a small difference in sequence (either gene or amino acid) could result in a very different expression/ secretion levels which potentially can be due to the higher stability of mRNA or the protein. As shown in chapter 3, decreased MFE of COS2 in comparison to COS1 enhanced the expression/secretion of recombinant hIFNγ by 10-100 fold. Therefore, in order to improve the expression of recombinant hIFNγ in *P. pastoris*, it is necessary to examine DNA and amino acid sequence of hIFNγ and possibly modify it to remove any potential cleavage sites both in mRNA and protein. For instance, the importance of KEX2 cleavage to the production of recombinant secretory proteins in *P. pastoris* was determined by improvement of secretory yield after genomic integration of additional KEX2 copies to the secretion signal (Yang *et al*, 2013). This finding supports conclusions reached in section 3.5, that a difference in restriction sites in my hIFNγ construct could have caused incomplete cleavage of the secretion signal sequence. It would be very worthwhile to explore a hIFNγ expression and secretion in *P. pastoris* using a construct with additional KEX2 cleavage sites to determine, whether secretion could be improved to reach commercial outcomes.

6.2.2 Productivity and cost-effectiveness comparison of *P. pastoris* to other expression systems

Comparison of the three most commonly used expression systems in terms of economic viability and production costs of a typical recombinant protein expressed in three expression systems: *E. coli*, *P. pastoris*, and mammalian cells (*viz.* CHO) is as follows (Table 6.1). In evaluating Cost of Goods (CoG) for all three expression systems using the same bioreactor size and product titre, the model evaluation indicates that for a 2,000 L bioreactor and 3 $g.L^{-1}$ product, the *P. pastoris* system is the most cost-effective at US$148 per gram product, whereas the mammalian system, CHO, is more expensive at US$206 per gram product and finally, the *E. coli* system has the highest CoG of US$588 per gram product (Janice *et al*, 2010). In addition, recombinant protein expression in *E. coli* is in the form of insoluble inclusion bodies, whereas the two other systems express and secrete soluble proteins which lower the final cost of purification (Table 6.1) (Janice *et al*, 2010).

Taking all these points about the cost of production, protein folding and similarity of glycosylation into account, we conclude that mammalian expression systems are the systems of choice, particularly the CHO platform. Noteworthy improvement of yields (>10 g L^{-1}) was recently achieved for recombinant proteins in this most popular mammalian host, getting this system a significant step closer to the economic commercial production of therapeutic glycoproteins. (Kim *et al*, 2012a). Future research on the production of hIFNγ in this system using optimised conditions explored for other recombinant proteins could pave the way for the application of recombinant hIFNγ as an immunotherapeutic agent to win the "War on Cancer". Despite the proven pivotal role of hIFNγ in anti-tumour immunity, the success of this biopharmaceutical in cancer immunotherapy, however, will largely depend on tackling obstacles in clinical trials including the inability to deliver hIFNγ locally and tumour insensitivity to hIFNγ (Dunn *et al*, 2006).

Table 6.1 Summary of yield, economic viability (modelling bioprocess costs) and glycosylation similarity of different expression systems

	Syllogistic transitive order	Ref.
Yield	*E. coli* > TM > *Bacillus* sp. > CHO > Others	Chapter 1
Economic viability	*P. pastoris* > CHO > *E. coli*	(Janice *et al*, 2010)
Glycosylation similarity to native hIFNγ	CHO > TM > BIIC > yeast > *E. coli* (unglycosylated)	Chapter 1

Our study also showed that deglycosylation did not alter the efficacy of hIFNγ expressed in HEK293, though the efficacy of hIFNγ expressed in CHO was reduced. This suggests an advantageous replacement for commercially available hIFNγ-1b rendering the fact that human protein expression platform like HEK293 cells are cultured easily in a serum-free suspension culture, reproduce rapidly and have efficient protein production lowering the cost of the product. However, the most significant advantage of using this protein expression platform is that the resulting recombinant glycoprotein will display post-translational modifications (PTMs), such as, protein folding, the structure, number, and location of N-glycans that are consistent with those seen in endogenous human proteins. Even though other mammalian expression platforms can produce PTMs similar to human cells, they also produce non-human sialyations, such as galactose-α1,3-galactose and N-glycolylneuraminic acid, which due to their potential immunogenicity are a major risk of applying any biotherapeutic

causing concern regarding patient safety and therapeutic efficacy (Dumont *et al*, 2016; Maas *et al*, 2007).

6.3 Future research directions

During this research and as highlighted throughout this thesis, a number of areas were recognised that require further investigation. These are concisely summarised here:

1) A wide range of approaches (including using a variety of vectors, strains, codon optimised sequences, lowering the mRNA MFE and deactivation of extracellular protease activity) were trialled to improve expression/ secretion of recombinant hIFNγ in *P. pastoris*. None of these resulted in sufficient yield for protein purification and direct trials of pharmaceutical efficacy. One of the remaining possibility for low expression/ secretion might be intracellular degradation of hIFNγ in *P. pastoris* cells. Future research should aim to identify potential protease cleavage sites and optimise the sequence to eliminate them. For example, it was showed by Tsygankov *et al* (2014) that expression of modified versions of bovine and chicken IFNγ genes lacking predicted protease cleavage sites at the C-terminus in *P. pastoris*, increased the stability of the recombinant proteins in comparison to wild-type sequence while retaining biological activity.

2) Based on the research results, industrial production of hIFNγ in *P. pastoris* is economically unrealistic, unless transcription/translation can be significantly increased. It is therefore recommended that commercial production focuses on other eukaryotic expression systems *e.g.* CHO, mammary gland expression in transgenic mice, PER.C6, CAP/CAP-T, and HEK293 cell lines. In addition, research has to focus on unravelling the cause of low expression of hIFNγ in *P. pastoris* to overcome low yield hurdles to make the system competitive economically.

3) In relevance to the selective pressure on the adjacent gene *HIS4* to enhance the expression of hIFNγ, the involvement of Gcn4p as a “master regulator” in the regulation of both *HIS4* and *hIFNγ* was hypothesised as a probable scenario explaining the increased level of *hIFNγ* under amino acid starvation. Thus, it is interesting to study the expression of this protein and its relevance with co-transcription of *HIS4* and *hIFNγ.*

4) Future detailed studies on the amino acid sequence differences in the hIFNγ receptors and crystallography to unravel changes in the 3D structure of hIFNγ forms and binding sites of the receptor are also required.

5) Furthermore, mechanisms of cell death of hIFNγ were not comparable with previous publications on PEO1, which emphasises that there is an urgent need for standardisation of toxicity assays (*e.g.* confluency, passage number, duration of treatment and use of bioactivity units), especially when aiming to unravel signalling cascades and treatment-induced cell death mechanisms. In addition to this and similar studies, a continuum of preclinical research is required to investigate responsivity of more ovarian cancer cell lines, other cancer types, and recombinant glycoproteins to generalise the idea that mammalian/human expression platforms can enhance the therapeutic efficacy of anti-cancer biotherapeutics.

6) To the best knowledge of the authors, this is the first report on FADD levels in SKOV3 cells, which could potentially correlate with tumorigenesis, anti-apoptotic behaviour, and resistance against anti-cancer drugs, which has also been reported for lymphomas, lung, and colorectal carcinomas (Patel *et al*, 2014). Additionally, FADD can be a novel potential target to overcome drug resistance in this ovarian cancer cell line (Fig. 5.1) (Schinske *et al*, 2011). Other recent studies have demonstrated that high levels of phosphorylated FADD in lung adenocarcinoma correlates with increased activation of the anti-apoptotic transcription factor NF-κB and is a biomarker for aggressive disease and poor clinical outcome. These findings suggest that inhibition of FADD phosphorylation is a viable target for cancer therapy.

7) Cancer drug-development pre-clinical data were confirmed to be reproducible in only ~11% of cases. The use of small numbers of poorly characterised tumour cell lines, a poor appreciation of pharmacokinetics and pharmacodynamics, and the use of problematic endpoints, and erroneous experimental methods and testing strategies are prevailing challenges, resulting in erroneous use and misinterpretation (Begley & Ellis, 2012). For example, comparing the pharma-therapeutic anti-cancer results and potential mechanism of this study with previous reports revealed that non-conformity in experimental conditions could be a contributing cause for the different outcomes. This highlights an urgent need for stricter standardisation of experimental designs and approaches in pre-clinical cancer research.

6.4. Conclusion

The recombinant hIFNγ, is an effective biopharmaceutical, against a wide range of viral, immuno-suppressive diseases with promising prospects to being used in cancer immunotherapy resulting in a strongly increasing demand and price. The current production of this recombinant protein is in *E. coli* which has major disadvantages in functionality and required costly purification. We, therefore, recommend exploring

different mammalian expression systems *e.g.* CHO, HEK293, PER.C6, and CAP/CAP-T cell lines for the production of this biopharmaceutical because these expression systems are highly productive, cost-efficient, possess human-like post-translation glycosylation outcomes which increase biological activity and half-life in the bloodstream of the protein. The milestone of improving the quality and lowering the cost can also facilitate uptake of mammalian-expressed recombinant hIFNγ for clinical trials particularly due to a strong potential in cancer immunotherapy.

Bibliography

Ahmad M, Hirz M, Pichler H, Schwab H (2014) Protein expression in *Pichia pastoris*: recent achievements and perspectives for heterologous protein production. *Appl Microbiol Biotechnol* **98** (12)**:** 5301-5317

Aksu Z, Eren AT (2007) Production of carotenoids by the isolated yeast of *Rhodotorula glutinis*. *Biochem Eng J* **35** (2)**:** 107-113

Alappat EC, Feig C, Boyerinas B, Volkland J, Samuels M, Murmann AE, Thorburn A, Kidd VJ, Slaughter CA, Osborn SL, Winoto A, Tang WJ, Peter ME (2005) Phosphorylation of FADD at serine 194 by CKIalpha regulates its nonapoptotic activities. *Mol Cell* **19** (3)**:** 321-32

Alberts B, Johnson A, Lewis A, Morgan D, Raff M, Roberts K, Walter P (2014) *Molecular biology of the cell*, Sixth edn. New York Garland Publishing

Alberts DS, Marth C, Alvarez RD, Johnson G, Bidzinski M, Kardatzke DR, Bradford WZ, Loutit J, Kirn DH, Clouser MC, Markman M, Consortium GCT (2008) Randomized phase 3 trial of interferon gamma-1b plus standard carboplatin/paclitaxel versus carboplatin/paclitaxel alone for first-line treatment of advanced ovarian and primary peritoneal carcinomas: results from a prospectively designed analysis of progression-free survival. *Gynecol Oncol* **109** (2)**:** 174-81

Alfa MJ, Dembinski JJ, Jay FT (1987) Production of monoclonal antibodies against recombinant human interferon-gamma: screening of hybridomas without purified antigen. *Hybridoma* **6** (5)**:** 509-20

Ank N, West H, Bartholdy C, Eriksson K, Thomsen AR, Paludan SR (2006) Lambda interferon (IFN-lambda), a type III IFN, is induced by viruses and IFNs and displays potent antiviral activity against select virus infections *in vivo*. *J Virol* **80** (9)**:** 4501-9

Arakawa T, Alton NK, Hsu YR (1985) Preparation and characterization of recombinant DNA-derived human interferon-gamma. *J Biol Chem* **260** (27)**:** 14435-9

Arbabi M, Sanati MH, Hosseini S, Deldar A, Maghsoudi N (2003) Cloning and expression of human gamma-interferon on cDNA in *E. coli*. *Iran J Biotechnol* **1** (2)**:** 87-94

Armstrong-James D, Teo IA, Shrivastava S, Petrou MA, Taube D, Dorling A, Shaunak S (2010) Exogenous interferon-gamma immunotherapy for invasive fungal infections in kidney transplant patients. *Am J Transplant* **10** (8)**:** 1796-803

Arnone JT, McAlear MA (2011) Adjacent gene pairing plays a role in the coordinated expression of ribosome biogenesis genes MPP10 and YJR003C in *Saccharomyces cerevisiae*. *Eukaryot Cell* **10** (1)**:** 43-53

Arnone JT, Robbins-Pianka A, Arace JR, Kass-Gergi S, McAlear MA (2012) The adjacent positioning of co-regulated gene pairs is widely conserved across eukaryotes. *BMC Genomics* **13:** 546

Arora D, Khanna N (1996) Method for increasing the yield of properly folded recombinant human gamma interferon from inclusion bodies. *J Biotechnol* **52** (2)**:** 127-133

Averhoff FM, Glass N, Holtzman D (2012) Global burden of hepatitis C: considerations for healthcare providers in the United States. *Clin Infect Dis* **55 Suppl 1:** S10-5

Babaeipour V, Shojaosadati S, Khalilzadeh R, Maghsoudi N, Farnoud A (2010) Enhancement of human γ-Interferon production in recombinant *E. coli* using batch cultivation. *Appl Biochem Biotechnol* **160** (8)**:** 2366-2376

Babaeipour V, Shojaosadati SA, Maghsoudi N (2013) Maximizing production of human interferon-gamma in HCDC of recombinant *E. coli*. *Iran J Pharm Res* **12** (3)**:** 563-72

Babaeipour V, Shojaosadati SA, Robatjazi SM, Khalilzadeh R, Maghsoudi N (2007) Over-production of human interferon-γ by HCDC of recombinant *Escherichia coli*. *Process Biochemistry* **42** (1)**:** 112-117

Babu MM, Luscombe NM, Aravind L, Gerstein M, Teichmann SA (2004) Structure and evolution of transcriptional regulatory networks. *Curr Opin Struct Biol* **14** (3)**:** 283-91

Bach EA, Aguet M, Schreiber RD (1997) The IFN gamma receptor: a paradigm for cytokine receptor signaling. *Annu Rev Immunol* **15** (1)**:** 563-91

Bagis H, Aktoprakligil D, Gunes C, Arat S, Akkoc T, Cetinkaya G, Kankavi O, Taskin A, Arslan K, Dundar M, Tsoncheva V, Ivanov I (2011) Expression of biologically active human interferon gamma in the milk of transgenic mice under the control of the murine whey acidic protein gene promoter. *Biochem Genet* **49** (3-4)**:** 251-257

Balderas Hernández V, Paz Maldonado LT, Medina Rivero E, Barba de la Rosa A, Ordoñez Acevedo L, León Rodríguez A (2008) Optimization of human interferon gamma production in *Escherichia coli* by response surface methodology. *Biotechnol Bioproc E* **13** (1)**:** 7-13

Baldridge MT, King KY, Goodell MA (2011) Inflammatory signals regulate hematopoietic stem cells. *Trends Immunol* **32** (2)**:** 57-65

Barton C, Davies D, Balkwill F, Burke F (2005) Involvement of both intrinsic and extrinsic pathways in IFN-γ-induced apoptosis that are enhanced with cisplatin. *Eur J Cancer* **41** (10)**:** 1474-1486

Begley CG, Ellis LM (2012) Drug development: Raise standards for preclinical cancer research. *Nature* **483** (7391)**:** 531-3

Beilharz MW (2000) Therapeutic potential for orally administered type 1 interferons. *Pharm Sci Tech Today* **3** (6)**:** 193-197

Bell BD, Leverrier S, Weist BM, Newton RH, Arechiga AF, Luhrs KA, Morrissette NS, Walsh CM (2008) FADD and caspase-8 control the outcome of autophagic signaling in proliferating T cells. *Proc Natl Acad Sci* **105** (43)**:** 16677-82

Bento F, Gaylarde C (2001) Biodeterioration of stored diesel oil: studies in Brazil. *Int Biodeterior Biodegrad* **47** (2)**:** 107-112

Berger AB, Cabal GG, Fabre E, Duong T, Buc H, Nehrbass U, Olivo-Marin JC, Gadal O, Zimmer C (2008) High-resolution statistical mapping reveals gene territories in live yeast. *Nat Methods* **5** (12)**:** 1031-7

Bhosale P, Gadre RV (2001a) Beta-carotene production in sugarcane molasses by a *Rhodotorula glutinis* mutant. *J Ind Microbiol Biotechnol* **26** (6)**:** 327-32

Bhosale PB, Gadre RV (2001b) Production of β-carotene by a mutant of *Rhodotorula glutini*s. *Appl Microbiol Biotechnol* **55** (4)**:** 423-427

Bocci V, Pacini A, Pessina GP, Paulesu L, Muscettola M, Lunghetti G (1985) Catabolic sites of human interferon-gamma. *J Gen Virol* **66 (Pt 4)** (APR)**:** 887-91

Borden EC, Sen GC, Uze G, Silverman RH, Ransohoff RM, Foster GR, Stark GR (2007) Interferons at age 50: past, current and future impact on biomedicine. *Nat Rev Drug Discov* **6** (12)**:** 975-90

Boselli D, Losana G, Bernabei P, Bosisio D, Drysdale P, Kiessling R, Gaston JS, Lammas D, Casanova JL, Kumararatne DS, Novelli F (2007) IFN-gamma regulates Fas ligand expression in human CD4+ T lymphocytes and controls their anti-mycobacterial cytotoxic functions. *Eur J Immunol* **37** (8)**:** 2196-204

Bouros D, Antoniou KM, Tzouvelekis A, Siafakas NM (2006) Interferon-γ1b for the treatment of idiopathic pulmonary fibrosis. *Exp Opin Biol Ther* **6** (10)**:** 1051-1060

Boutanaev AM, Kalmykova AI, Shevelyov YY, Nurminsky DI (2002) Large clusters of co-expressed genes in the Drosophila genome. *Nature* **420** (6916)**:** 666-9

Bozinovic G, Sit TL, Di Giulio R, Wills LF, Oleksiak MF (2013) Genomic and physiological responses to strong selective pressure during late organogenesis: few

gene expression changes found despite striking morphological differences. *BMC Genomics* **14:** 779

Burke F, Smith PD, Crompton MR, Upton C, Balkwill FR (1999) Cytotoxic response of ovarian cancer cell lines to IFN-γ is associated with sustained induction of IRF-1 and p21 mRNA. *Brit J Cancer* **80** (8)**:** 1236-1244

Buzzini P (2001) Batch and fed-batch carotenoid production by *Rhodotorula glutinis-Debaryomyces castellii* co-cultures in corn syrup. *J Appl Microbiol* **90** (5)**:** 843-7

Buzzini P, Martini A (2000) Production of carotenoids by strains of *Rhodotorula glutinis* cultured in raw materials of agro-industrial origin. *Bioresour Technol* **71** (1)**:** 41-44

Cereghino JL, Cregg JM (2000) Heterologous protein expression in the methylotrophic yeast *Pichia pastoris*. *FEMS Microbiol Rev* **24** (1)**:** 45-66

Charriaut-Marlangue C, Ben-Ari Y (1995) A cautionary note on the use of the TUNEL stain to determine apoptosis. *Neuroreport* **7** (1)**:** 61-4

Chelikani P, Fita I, Loewen PC (2004) Diversity of structures and properties among catalases. *Cell Mol Life Sci* **61** (2)**:** 192-208

Chen TL, Lin YL, Lee YL, Yang NS, Chan MT (2004) Expression of bioactive human interferon-gamma in transgenic rice cell suspension cultures. *Transgenic Res* **13** (5)**:** 499-510

Chen WS, Villaflores OB, Jinn TR, Chan MT, Chang YC, Wu TY (2011) Expression of recombinant human interferon-gamma with antiviral activity in the bi-cistronic baculovirus-insect/larval system. *Biosci Biotechnol Biochem* **75** (7)**:** 1342-8

Chevillard C, Henri S, Stefani F, Parzy D, Dessein A (2002) Two new polymorphisms in the human interferon gamma (IFN-gamma) promoter. *Eur J Immunogenet* **29** (1)**:** 53-6

Chidambarampadmavathy K, Karthikeyan OP, Huerlimann R, Maes GE, Heimann K (2016) Response of mixed methanotrophic consortia to different methane to oxygen ratios. *Waste Manag*

Choi JH, Keum KC, Lee SY (2006) Production of recombinant proteins by high cell density culture of *Escherichia coli*. *Chem Eng Sci* **61** (3)**:** 876-885

Chung BK, Yusufi FN, Mariati, Yang Y, Lee DY (2013) Enhanced expression of codon optimized interferon gamma in CHO cells. *J Biotechnol* **167** (3)**:** 326-33

Couderc R, Baratti J (2014) Oxidation of methanol by the yeast,*Pichia pastoris*. Purification and properties of the Alcohol Oxidase. *Agr Biol Chem* **44** (10)**:** 2279-2289

Crisafulli S, Pandya Y, Moolchan K, Lavoie T (2008) Interferon gamma: activity and ELISA detection comparisons. *Biotechniques* **45** (1)**:** 101-2

Dai CC, Tao J, Xie F, Dai YJ, Zhao M (2007) Biodiesel generation from oleaginous yeast *Rhodotorula glutinis* with xylose assimilating capacity. *Afr J Biotechnol* **6** (18)**:** 2130-2134

Dai MS, Lu H (2008) Crosstalk between c-Myc and ribosome in ribosomal biogenesis and cancer. *J Cell Biochem* **105** (3)**:** 670-7

Dalgard O, Bjoro K, Hellum KB, Myrvang B, Ritland S, Skaug K, Raknerud N, Bell H (2004) Treatment with pegylated interferon and ribavarin in HCV infection with genotype 2 or 3 for 14 weeks: a pilot study. *Hepatology* **40** (6)**:** 1260-5

Davoudi N, Hemmati A, Khodayari Z, Adeli A, Hemayatkar M (2011) Cloning and expression of human IFN-γ in *Leishmania tarentolae*. *World J Microbiol Biotechnol* **27** (8)**:** 1893-1899

Daxinger L, Whitelaw E (2010) Transgenerational epigenetic inheritance: more questions than answers. *Genome Res* **20** (12)**:** 1623-8

De Hoog GS, Guarro J, Gené J, Figueras MJ (2000) *Atlas of clinical fungi*. Vol. 8

Deng Y, Dai X, Xiang Q, Dai Z, He C, Wang J, Feng J (2010) Genome-wide analysis of the effect of histone modifications on the coexpression of neighboring genes in Saccharomyces cerevisiae. *BMC Genomics* **11:** 550

Derynck R, Singh A, Goeddel DV (1983) Expression of the human interferon-gamma cDNA in yeast. *Nucleic Acids Res* **11** (6)**:** 1819-37

Detjen KM, Farwig K, Welzel M, Wiedenmann B, Rosewicz S (2001) Interferon gamma inhibits growth of human pancreatic carcinoma cells via caspase-1 dependent induction of apoptosis. *Gut* **49** (2)**:** 251-62

Duan Z, Andronescu M, Schutz K, McIlwain S, Kim YJ, Lee C, Shendure J, Fields S, Blau CA, Noble WS (2010) A three-dimensional model of the yeast genome. *Nature* **465** (7296)**:** 363-7

Dummer R, Hassel JC, Fellenberg F, Eichmuller S, Maier T, Slos P, Acres B, Bleuzen P, Bataille V, Squiban P, Burg G, Urosevic M (2004) Adenovirus-mediated intralesional interferon-gamma gene transfer induces tumor regressions in cutaneous lymphomas. *Blood* **104** (6)**:** 1631-8

Dumont J, Euwart D, Mei B, Estes S, Kshirsagar R (2016) Human cell lines for biopharmaceutical manufacturing: history, status, and future perspectives. *Crit Rev Biotechnol* **36** (6)**:** 1110-1122

Dunn GP, Koebel CM, Schreiber RD (2006) Interferons, immunity and cancer immunoediting. *Nat Rev Immunol* **6** (11)**:** 836-48

Ealick SE, Cook WJ, Vijay-Kumar S, Carson M, Nagabhushan TL, Trotta PP, Bugg CE (1991) Three-dimensional structure of recombinant human interferon-gamma. *Science* **252** (5006)**:** 698-702

Ebisuya M, Yamamoto T, Nakajima M, Nishida E (2008) Ripples from neighbouring transcription. *Nat Cell Biol* **10** (9)**:** 1106-13

Ebrahimi N, Memari HR, Ebrahimi MA, Ardakani MR (2012) Cloning, transformation and expression of human gamma interferon gene in tomato (*Lycopersicon Esculentum* Mill.). *Biotechnol Biotechnologic Equip* **26** (2)**:** 2925-2929

Eggermont AM, Schraffordt Koops H, Lienard D, Kroon BB, van Geel AN, Hoekstra HJ, Lejeune FJ (1996) Isolated limb perfusion with high-dose tumor necrosis factor-alpha in combination with interferon-gamma and melphalan for nonresectable extremity soft tissue sarcomas: a multicenter trial. *J Clin Oncol* **14** (10)**:** 2653-65

El-Batal AI (2002) Continuous production of L-phenylalanine by *Rhodotorula glutinis* immobilized cells using a column reactor. *Acta Microbiologica Polonica* **51** (2)**:** 153

Farrar MA, Schreiber RD (1993) The molecular cell biology of interferon-gamma and its receptor. *Annu Rev Immunol* **11** (1)**:** 571-611

Fensterl V, Sen GC (2009) Interferons and viral infections. *Biofactors* **35** (1)**:** 14-20

Fox SR, Patel UA, Yap MG, Wang DI (2004) Maximizing interferon-gamma production by Chinese hamster ovary cells through temperature shift optimization: experimental and modeling. *Biotechnol Bioeng* **85** (2)**:** 177-184

Fraser HB (2013) Gene expression drives local adaptation in humans. *Genome Res* **23** (7)**:** 1089-96

Frokjaer S, Otzen DE (2005) Protein drug stability: a formulation challenge. *Nat Rev Drug Discov* **4** (4)**:** 298-306

Frucht DM, Fukao T, Bogdan C, Schindler H, O'Shea JJ, Koyasu S (2001) IFN-gamma production by antigen-presenting cells: mechanisms emerge. *Trends Immunol* **22** (10)**:** 556-60

Gaspar P, Moura G, Santos MAS, Oliveira JL (2013) mRNA secondary structure optimization using a correlated stem–loop prediction. *Nucleic Acids Res***:** 1-5

Geng X, Bai Q, Zhang Y, Li X, Wu D (2004) Refolding and purification of interferon-gamma in industry by hydrophobic interaction chromatography. *J Biotechnol* **113** (1-3)**:** 137-49

Ghosalkar A, Sahai V, Srivastava A (2008) Secretory expression of interferon-alpha 2b in recombinant *Pichia pastoris* using three different secretion signals. *Protein Expr Purif* **60** (2)**:** 103-9

Giannopoulos A, Constantinides C, Fokaeas E, Stravodimos C, Giannopoulou M, Kyroudi A, Gounaris A (2003) The immunomodulating effect of interferon-gamma intravesical instillations in preventing bladder cancer recurrence. *Clin Cancer Res* **9** (15)**:** 5550-8

Gilad Y, Oshlack A, Rifkin SA (2006) Natural selection on gene expression. *Trends Genet* **22** (8)**:** 456-61

Gleave ME, Elhilali M, Fradet Y, Davis I, Venner P, Saad F, Klotz LH, Moore MJ, Paton V, Bajamonde A, Bell D, Ernst S, Ramsey E, Chin J, Morales A, Martins H, Sanders C (1998) Interferon Gamma-1b Compared with Placebo in Metastatic Renal-Cell Carcinoma. *N Engl J Med* **338** (18)**:** 1265-1271

Gohil K (2014) Huge growth seen in hepatitis C market. *Pharmacy and Therapeutics* **39** (7)**:** 517-517

Gonzalez-Garcia Y, Hernandez R, Zhang G, Escalante FME, Holmes W, French WT (2013) Lipids accumulation in *Rhodotorula glutinis* and *Cryptococcus curvatus* growing on distillery wastewater as culture medium. *Environ Prog Sustain Energy* **32** (1)**:** 69-74

Gray PW, Leung DW, Pennica D, Yelverton E, Najarian R, Simonsen CC, Derynck R, Sherwood PJ, Wallace DM, Berger SL, Levinson AD, Goeddel DV (1982) Expression of human immune interferon cDNA in *E. coli* and monkey cells. *Nature* **295** (5849)**:** 503-8

Grewal SS, Li L, Orian A, Eisenman RN, Edgar BA (2005) Myc-dependent regulation of ribosomal RNA synthesis during Drosophila development. *Nat Cell Biol* **7** (3)**:** 295-302

Gruber AR, Lorenz R, Bernhart SH, Neuböck R, Hofacker IL (2008) The Vienna RNA Websuite. *Nucleic Acids Res* **36** (suppl 2)**:** W70-W74

Grunstein M (1997) Molecular model for telomeric heterochromatin in yeast. *Curr Opin Cell Biol* **9** (3)**:** 383-387

Guan Y-Q, Zheng Z, Liang L, Li Z, Zhang L, Du J, Liu J-M (2012) The apoptosis of OVCAR-3 induced by TNF-α plus IFN-γ co-immobilized polylactic acid copolymers. *J Mat Chem* **22** (29)**:** 14746

Guan Y-X, Pan H-X, Gao Y-G, Yao S-J, Cho M-G (2005) Refolding and purification of recombinant human interferon-γ expressed as inclusion bodies in *Escherichia coli* using size exclusion chromatography. *Biotechnol Bioproc E* **10** (2)**:** 122-127

Gustafsson C, Govindarajan S, Minshull J (2004) Codon bias and heterologous protein expression. *Trends Biotechnol* **22** (7)**:** 346-353

Haelewyn J, De Ley M (1995) A rapid single-step purification method for human interferon-gamma from isolated *Escherichia coli* inclusion bodies. *Biochem Mol Biol Int* **37** (6)**:** 1163-71

Hanson RS, Hanson TE (1996) Methanotrophic bacteria. *Microbiol Rev* **60** (2)**:** 439-71

Harnois DM (2012) Hepatitis C virus infection and the rising incidence of hepatocellular carcinoma. *Mayo Clin Proc* **87** (1)**:** 7-8

Hawkyard S, James K, Prescott S, Jackson AM, Ritchie AW, Smyth JF, Chisholm GD (1991) The effects of recombinant human interferon-gamma on a panel of human bladder cancer cell lines. *J Urol* **145** (5)**:** 1078-81

Haynes J, Weissman C (1983) Constitutive, long-term production of human interferons by hamster cells contalning multiple copies of a cloned interferon gene. *Nucleic Acids Res* **11** (3)**:** 687-706

Higgins IJ, Best DJ, Hammond RC, Scott D (1981) Methane-oxidizing microorganisms. *Microbiol Rev* **45** (4)**:** 556-90

Hinnebusch AG (2005) Translational regulation of GCN4 and the general amino acid control of yeast. *Annu Rev Microbiol* **59:** 407-50

Hinnebusch AG, Natarajan K (2002) Gcn4p, a master regulator of gene xxpression, is controlled at multiple levels by diverse signals of starvation and stress. *Eukaryot Cell* **1** (1)**:** 22-32

Honda S, Asano T, Kajio T, Nakagawa S, Ikeyama S, Ichimori Y, Sugino H, Nara K, Kakinuma A, Kung HF (1987) Differential purification by immunoaffinity chromatography of two carboxy-terminal portion-deleted derivatives of recombinant human interferon-gamma from *Escherichia coli*. *J Interferon Res* **7** (2)**:** 145-54

Hooker A, James D (1998) The glycosylation heterogeneity of recombinant human IFN-gamma. *J Interferon Cytokine Res* **18** (5)**:** 287-95

Hu X, Ivashkiv LB (2009) Cross-regulation of signaling pathways by interferon-gamma: implications for immune responses and autoimmune diseases. *Immunity* **31** (4)**:** 539-50

Hu X, Zhang Z (2016) Understanding the genetic mechanisms of cancer drug resistance using genomic approaches. *Trends Genet* **32** (2)**:** 127-37

Huang S-K, Jin J-Y, Guan Y-X, Yao Z, Cao K, Yao S-J (2013) Refolding of recombinant human interferon gamma inclusion bodies *in vitro* assisted by colloidal thermo-sensitive poly(N-isopropylacrylamide) brushes grafted onto the surface of uniform polystyrene cores. *Biochem Eng J* **74:** 20-26

Huang X, Barchi JJ, Jr., Lung FD, Roller PP, Nara PL, Muschik J, Garrity RR (1997) Glycosylation affects both the three-dimensional structure and antibody binding properties of the HIV-1IIIB GP120 peptide RP135. *Biochemistry* **36** (36)**:** 10846-56

Huang ZQ, Hu HY, Chen XL, Ren LM, Lin AX, Chen YF (2005) Secreted expression of porcine interferon-gamma gene in *Pichia pastoris*. *Sheng wu gong cheng xue bao = Chinese journal of biotechnology* **21** (5)**:** 731-6

Hurst LD, Pal C, Lercher MJ (2004) The evolutionary dynamics of eukaryotic gene order. *Nat Rev Genet* **5** (4)**:** 299-310

James DC, Freedman RB, Hoare M, Ogonah OW, Rooney BC, Larionov OA, Dobrovolsky VN, Lagutin OV, Jenkins N (1995) N-glycosylation of recombinant human interferon-gamma produced in different animal expression systems. *Biotechnology (N Y)* **13** (6)**:** 592-6

Janice A, Patkar A, McDonagh G, Sinclair A, Lucy P (2010) Modeling bioprocess cost: economic benefits of expression technology based on *Pseudomonas fluorescens*. *Bioprocess Int* **8:** 62-70

Jean MDS, Brignole Fi, Feldmann G, Goguel A, Baudouin C (1999) Interferon-γ induces apoptosis and expression of inflammation-related proteins in Chang conjunctival cells. *Invest Ophthalmol Vis Sci* **40** (10)**:** 2199-2212

Jiang H, Chen Y, Jiang P, Zhang C, Smith TJ, Murrell JC, Xing X-H (2010) Methanotrophs: multifunctional bacteria with promising applications in environmental bioengineering. *Biochem Eng J* **49** (3)**:** 277-288

Jin T, Guan YX, Yao SJ, Lin DQ, Cho MG (2006) On-column refolding of recombinant human interferon-gamma inclusion bodies by expanded bed adsorption chromatography. *Biotechnol Bioeng* **93** (4)**:** 755-60

Jonasch E, Haluska FG (2001) Interferon in oncological practice: review of interferon biology, clinical applications, and toxicities. *Oncologist* **6** (1)**:** 34-55

Kano A, Watanabe Y, Takeda N, Aizawa TS-i (1997) Analysis of IFN-γ-induced cell cycle arrest and cell death in hepatocytes. *J Biochem* **121** (4)**:** 677-683

Karthikeyan OP, Saravanan N, Cires S, Alvarez-Roa C, Razaghi A, Chidambarampadmavathy K, Velu C, Subashchandrabose G, Heimann K (2017) Culture scale-up and immobilisation of a mixed methanotrophic consortium for methane remediation in pilot-scale bio-filters. *Environ Technol* **38** (4)**:** 474-482

Kelker HC, Yip YK, Anderson P, Vilcek J (1983) Effects of glycosidase treatment on the physicochemical properties and biological activity of human interferon-gamma. *J Biol Chem* **258** (13)**:** 8010-3

Khalilzadeh R, Shojaosadati SA, Bahrami A, Maghsoudi N (2003) Over-expression of recombinant human interferon-gamma in high cell density fermentation of *Escherichia coli*. *Biotechnology letters* **25** (23)**:** 1989-92

Khalilzadeh R, Shojaosadati SA, Maghsoudi N, Mohammadian-Mosaabadi J, Mohammadi MR, Bahrami A, Maleksabet N, Nassiri-Khalilli MA, Ebrahimi M, Naderimanesh H (2004) Process development for production of recombinant human interferon-gamma expressed in *Escherichia coli*. *J Ind Microbiol Biotechnol* **31** (2)**:** 63-9

Kim EJ, Lee JM, Namkoong SE, Um SJ, Park JS (2002) Interferon regulatory factor-1 mediates interferon-gamma-induced apoptosis in ovarian carcinoma cells. *J Cell Biochem* **85** (2)**:** 369-80

Kim JY, Kim YG, Lee GM (2012a) CHO cells in biotechnology for production of recombinant proteins: current state and further potential. *Appl Microbiol Biotechnol* **93** (3)**:** 917-30

Kim N, He N, Kim C, Zhang F, Lu Y, Yu Q, Stemke-Hale K, Greshock J, Wooster R, Yoon S, Mills GB (2012b) Systematic analysis of genotype-specific drug responses in cancer. *Int J Cancer* **131** (10)**:** 2456-64

Koh GC, Limmathurotsakul D (2010) Gamma interferon supplementation for melioidosis. *Antimicrob Agents Chemother* **54** (10)**:** 4520-1

Kokordelis P, Kramer B, Korner C, Boesecke C, Voigt E, Ingiliz P, Glassner A, Eisenhardt M, Wolter F, Kaczmarek D, Nischalke HD, Rockstroh JK, Spengler U, Nattermann J (2014) An effective interferon-gamma-mediated inhibition of hepatitis C virus replication by natural killer cells is associated with spontaneous clearance of acute hepatitis C in human immunodeficiency virus-positive patients. *Hepatology* **59** (3)**:** 814-27

Kortylewski M, Komyod W, Kauffmann ME, Bosserhoff A, Heinrich PC, Behrmann I (2004) Interferon-gamma-mediated growth regulation of melanoma cells: involvement

of STAT1-dependent and STAT1-independent signals. *J Invest Dermatol* **122** (2)**:** 414-22

Kruglyak S, Tang H (2000) Regulation of adjacent yeast genes. *Trends Genet* **16** (3)**:** 109-111

Lagutin OV, Dobrovolsky VN, Vinogradova TV, Kyndiakov BN, Khodarovich YM, Jenkins N, James D, Markham N, Larionov OA (1999) Efficient human IFN-gamma expression in the mammary gland of transgenic mice. *J Interferon Cytokine Res* **19** (2)**:** 137-44

Lamas-Maceiras M, Cerdán ME, Freire-Picos MA (1999) *Kluyveromyces lactis HIS4* transcriptional regulation: similarities and differences to *Saccharomyces cerevisiae HIS4* gene. *FEBS Letters* **458** (1)**:** 72-76

Lee EW, Seo J, Jeong M, Lee S, Song J (2012) The roles of FADD in extrinsic apoptosis and necroptosis. *BMB Rep* **45** (9)**:** 496-508

Lee S, Choi J, Lee S (2005) Secretory production of therapeutic proteins in *Escherichia coli*. In *Therapeutic Proteins*, Smales CM, James D (eds) Vol. 308, Chapter 3, pp 31-41. Humana Press

Leister P, Tileva M, Krachmarova E, Nacheva G (2014) Expression of human interferon-gamma gene in human tissue culture cells. *Biotechnol Biotechnologic Equip* **27** (1)**:** 3573-3576

Lercher MJ, Blumenthal T, Hurst LD (2003) Coexpression of neighboring genes in Caenorhabditis elegans is mostly due to operons and duplicate genes. *Genome Res* **13** (2)**:** 238-43

Li LC, Jayaram S, Ganesh L, Qian L, Rotmensch J, Maker AV, Prabhakar BS (2011) Knockdown of MADD and c-FLIP overcomes resistance to TRAIL-induced apoptosis in ovarian cancer cells. *Am J Obstet Gynecol* **205** (4)**:** 362 e12-25

Li P, Du Q, Cao Z, Guo Z, Evankovich J, Yan W, Chang Y, Shao L, Stolz DB, Tsung A, Geller DA (2012) Interferon-gamma induces autophagy with growth inhibition and cell death in human hepatocellular carcinoma (HCC) cells through interferon-regulatory factor-1 (IRF-1). *Cancer Lett* **314** (2)**:** 213-22

Li Y, Zhao Z, Bai F (2007) High-density cultivation of oleaginous yeast *Rhodosporidium toruloides* Y4 in fed-batch culture. *Enzym Microbial Technol* **41** (3)**:** 312-317

Lienard D, Eggermont AM, Kroon BB, Schraffordt Koops H, Lejeune FJ (1998) Isolated limb perfusion in primary and recurrent melanoma: indications and results. *Seminars in surgical oncology* **14** (3)**:** 202-9

Lin-Cereghino J, Wong WW, Giang W, Luong LT, Vu J, Johnson SD, Lin-Cereghino GP (2005) Condensed protocol for competent cell preparation and transformation of the methylotrophic yeast *Pichia pastoris*. *Biotechniques* **38** (1)**:** 44-48

Liu Q, Liu X, Gao J, Shi X, Hu X, Wang S, Luo Y (2013) Overexpression of DOC-1R inhibits cell cycle G1/S transition by repressing CDK2 expression and activation. *Int J Biol Sci* **9** (6)**:** 541-9

Lundell DL, Narula SK (1994) Structural elements required for receptor recognition of human interferon-gamma. *Pharmacol Ther* **64** (1)**:** 1-21

Lv H, Zhang H, Wu J, Guan Y (2011) Effect of plasmid-mediated stable interferon-gamma expression on proliferation and cell death in the SKOV-3 human ovarian cancer cell line. *Immunopharmacol immunotoxicol* **33** (3)**:** 498-503

Maas C, Hermeling S, Bouma B, Jiskoot W, Gebbink MF (2007) A role for protein misfolding in immunogenicity of biopharmaceuticals. *J Biol Chem* **282** (4)**:** 2229-36

Malek Sabet N, Masoumian MR, Nasiri-Khalili MA, Maghsoudi N, Sami H, Saeedinia A, Mohammadi R (2008) The structural characterization of recombinant human interferon gamma. *J Biol Sci* **8** (6)**:** 1087-1091

Marciano BE, Wesley R, De Carlo ES, Anderson VL, Barnhart LA, Darnell D, Malech HL, Gallin JI, Holland SM (2004) Long-term interferon-gamma therapy for patients with chronic granulomatous disease. *Clin Infect Dis* **39** (5)**:** 692-9

Marth C, Windbichler GH, Hausmaninger H, Petru E, Estermann K, Pelzer A, Mueller-Holzner E (2006) Interferon-gamma in combination with carboplatin and paclitaxel as a safe and effective first-line treatment option for advanced ovarian cancer: results of a phase I/II study. *Int J Gynecol Cancer* **16** (4)**:** 1522-8

Maylin S, Martinot-Peignoux M, Ripault MP, Moucari R, Cardoso AC, Boyer N, Giuily N, Castelnau C, Pouteau M, Asselah T (2009) Sustained virological response is associated with clearance of hepatitis C virus RNA and a decrease in hepatitis C virus antibody. *Liver Int* **29** (4)**:** 511-517

McClain DA. Increasing IFN-gamma productivity in CHO cells through CDK inhibition. Ph.D., Massachusetts Institute of Technology, MITlibraries, Boston, 2010

Meager A (2006) *The interferons: characterization and application*: Wiley-Blackwell

Michalak P (2008) Coexpression, coregulation, and cofunctionality of neighboring genes in eukaryotic genomes. *Genomics* **91** (3)**:** 243-8

Mikulecky P, Zahradnik J, Kolenko P, Cerny J, Charnavets T, Kolarova L, Necasova I, Pham PN, Schneider B (2016) Crystal structure of human interferon-gamma receptor 2 reveals the structural basis for receptor specificity. *Acta Crystallogr D Struct Biol* **72** (Pt 9)**:** 1017-25

Miller CH, Maher SG, Young HA (2009) Clinical use of interferon-gamma. *Ann N Y Acad Sci* **1182:** 69-79

Mironova R, Niwa T, Dimitrova R, Boyanova M, Ivanov I (2003) Glycation and post-translational processing of human interferon-gamma expressed in *Escherichia coli*. *J Biol Chem* **278** (51)**:** 51068-74

Miyakawa N, Nishikawa M, Takahashi Y, Ando M, Misaka M, Watanabe Y, Takakura Y (2011) Prolonged circulation half-life of interferon gamma activity by gene delivery of interferon gamma-serum albumin fusion protein in mice. *J Pharm Sci* **100** (6)**:** 2350-7

Miyata K, Yamamoto Y, Ueda M, Kawade Y, Matsumoto K, Kubota I (1986) Purification of natural human interferon-gamma by antibody affinity chromatography: analysis of constituent protein species in the dimers. *J Biochem* **99** (6)**:** 1681-8

Mohammadian-Mosaabadi J, Naderi-Manesh H, Maghsoudi N, Nassiri-Khalili MA, Masoumian MR, Malek-Sabet N (2007) Improving purification of recombinant human interferon gamma expressed in *Escherichia coli*; effect of removal of impurity on the process yield. *Protein Expr Purif* **51** (2)**:** 147-56

Moharir A, Peck SH, Budden T, Lee SY (2013) The role of N-glycosylation in folding, trafficking, and functionality of lysosomal protein CLN5. *PloS ONE* **8** (9)**:** e74299

Mols J, Peeters-Joris C, Wattiez R, Agathos SN, Schneider Y-J (2005) Recombinant interferon-γ secreted by chinese hamster ovary-320 cells cultivated in suspension in protein-free media is protected against extracellular proteolysis by the expression of natural protease inhibitors and by the addition of plant protein hydrolysates to the culture medium. *In Vitro Cellular & Developmental Biology - Animal* **41** (3)**:** 83-91

Mory Y, Ben-Barak J, Segev D, Cohen B, Novick D, Fischer DG, Rubinstein M, Kargman S, Zilberstein A, Vigneron M, et al. (1986) Efficient constitutive production of human IFN-gamma in Chinese hamster ovary cells. *DNA* **5** (3)**:** 181-93

Muir AJ, Sylvestre PB, Rockey DC (2006) Interferon gamma-1b for the treatment of fibrosis in chronic hepatitis C infection. *J Viral Hepat* **13** (5)**:** 322-8

Näätsaari L, Mistlberger B, Ruth C, Hajek T, Hartner FS, Glieder A (2012) Deletion of the *Pichia pastoris KU70* homologue facilitates platform strain generation for gene expression and synthetic biology. *PLoS ONE* **7** (6)**:** e39720

Nacheva G, Todorova K, Boyanova M, Berzal-Herranz A, Karshikoff A, Ivanov I (2003) Human interferon gamma: significance of the C-terminal flexible domain for its biological activity. *Arch Biochem Biophys* **413** (1)**:** 91-8

Nakajima T, Tsunoda S, Nakada S, Nagata S, Oda K (1992) Hyperproduction of human interferon gamma by rat cells maintained in low-serum medium using the fibronectin gene promoter. *J Biochem* **112** (5)**:** 590-7

Natarajan K, Meyer MR, Jackson BM, Slade D, Roberts C, Hinnebusch AG, Marton MJ (2001) Transcriptional profiling shows that Gcn4p is a master regulator of gene expression during amino acid starvation in yeast. *Mol Cell Biol* **21** (13)**:** 4347-68

Nathan CF (1983) Identification of interferon-gamma as the lymphokine that activates human macrophage oxidative metabolism and antimicrobial activity. *J Experiment Med* **158** (3)**:** 670-689

Ni C, Wu P, Zhu X, Ye J, Zhang Z, Chen Z, Zhang T, Zhang T, Wang K, Wu D, Qiu F, Huang J (2013) IFN-gamma selectively exerts pro-apoptotic effects on tumor-initiating label-retaining colon cancer cells. *Cancer Lett* **336** (1)**:** 174-84

Nielsen J (2003) *Metabolic engineering*, 1 edn: Springer Berlin Heidelberg

Noone C, Kihm A, English K, O'Dea S, Mahon BP (2013) IFN-gamma stimulated human umbilical-tissue-derived cells potently suppress NK activation and resist NK-mediated cytotoxicity *in vitro*. *Stem Cells Dev* **22** (22)**:** 3003-14

Novick D, Eshhar Z, Fischer DG, Friedlander J, Rubinstein M (1983) Monoclonal antibodies to human interferon-gamma: production, affinity purification and radioimmunoassay. *EMBO J* **2** (9)**:** 1527-30

Osborne CS, Chakalova L, Brown KE, Carter D, Horton A, Debrand E, Goyenechea B, Mitchell JA, Lopes S, Reik W, Fraser P (2004) Active genes dynamically colocalize to shared sites of ongoing transcription. *Nat Genet* **36** (10)**:** 1065-71

Pai M, Riley LW, Colford JM, Jr. (2004) Interferon-gamma assays in the immunodiagnosis of tuberculosis: a systematic review. *Lancet Infect Dis* **4** (12)**:** 761-76

Panahi Y, Davoudi SM, Madanchi N, Abolhasani E (2012) Recombinant human interferon gamma (Gamma Immunex) in treatment of atopic dermatitis. *Clin Experiment Med* **12** (4)**:** 241-245

Park SY, Seol JW, Lee YJ, Cho JH, Kang HS, Kim IS, Park SH, Kim TH, Yim JH, Kim M, Billiar TR, Seol DW (2004) IFN-gamma enhances TRAIL-induced apoptosis through IRF-1. *Eur J Biochem* **271** (21)**:** 4222-8

Pasparakis M, Vandenabeele P (2015) Necroptosis and its role in inflammation. *Nature* **517** (7534)**:** 311-20

Patel S, Murphy D, Haralambieva E, Abdulla ZA, Wong KK, Chen H, Gould E, Roncador G, Hatton C, Anderson AP, Banham AH, Pulford K (2014) Increased expression of phosphorylated FADD in anaplastic large cell and other T-Cell lymphomas. *Biomark Insights* **9:** 77-84

Perez L, Vega J, Chuay C, Menendez A, Ubieta R, Montero M, Padron G, Silva A, Santizo C, Besada V, et al. (1990) Production and characterization of human gamma interferon from *Escherichia coli*. *Appl Microbiol Biotechnol* **33** (4)**:** 429-34

Perrier V, Dubreucq E, Galzy P (1995) Fatty acid and carotenoid composition of *Rhodotorula* strains. *Arch Microbiol* **164** (3)**:** 173-9

Petrov S, Nacheva G, Ivanov I (2010) Purification and refolding of recombinant human interferon-gamma in urea-ammonium chloride solution. *Protein Expr Purif* **73** (1)**:** 70-3

Pla A, Damasceno M, Vannelli T, Ritter G, Batt A, Shuler M (2006) Evaluation of Mut^{+} and Mut^{S} *Pichia pastoris* phenotypes for high level extracellular scFv expression under feedback control of the methanol concentration. *Biotechnol Progress* **22** (3)**:** 881-888

Pm C, Ap I, Pm H, At B (1995) The macroheterogeneity of recombinant human interferon-gamma produced by Chinese-hamster ovary cells is affected by the protein and lipid content of the culture medium. *Biotechnol Appl Biochem* **21** (1)**:** 87-100

Prabhu AA, Veeranki VD, Dsilva SJ (2016) Improving the production of human interferon gamma (hIFN-γ) in *Pichia pastoris* cell factory: An approach of cell level. *Process Biochem* **51** (6)**:** 709-718

Proctor JR, Meyer IM (2013) CoFold: an RNA secondary structure prediction method that takes co-transcriptional folding into account. *Nucleic Acids Res* **41** (9)**:** e102

Pronsato L, La Colla A, Ronda AC, Milanesi L, Boland R, Vasconsuelo A (2013) High passage numbers induce resistance to apoptosis in C2C12 muscle cells. *Biocell : official journal of the Sociedades Latinoamericanas de Microscopia Electronica et al* **37** (1)**:** 1-9

Purmann A, Toedling J, Schueler M, Carninci P, Lehrach H, Hayashizaki Y, Huber W, Sperling S (2007) Genomic organization of transcriptomes in mammals: Coregulation and cofunctionality. *Genomics* **89** (5)**:** 580-7

Pyo JO, Jang MH, Kwon YK, Lee HJ, Jun JI, Woo HN, Cho DH, Choi B, Lee H, Kim JH, Mizushima N, Oshumi Y, Jung YK (2005) Essential roles of Atg5 and FADD in autophagic cell death: dissection of autophagic cell death into vacuole formation and cell death. *J Biol Chem* **280** (21)**:** 20722-9

Qi Z, Nie P, Secombes CJ, Zou J (2010) Intron-containing type I and type III IFN coexist in amphibians: refuting the concept that a retroposition event gave rise to type I IFNs. *J Immunol* **184** (9)**:** 5038-46

Rader RA (2013) FDA biopharmaceutical product approvals and trends in 2012. *BioProcess Int* **11** (3)**:** 18-27

Raghu G, Brown KK, Bradford WZ, Starko K, Noble PW, Schwartz DA, King TE, Jr., Idiopathic Pulmonary Fibrosis Study G (2004) A placebo-controlled trial of interferon gamma-1b in patients with idiopathic pulmonary fibrosis. *N Engl J Med* **350** (2)**:** 125-33

Razaghi A, Huerlimann R, Owens L, Heimann K (2015) Increased expression and secretion of recombinant *hIFNγ* through amino acid starvation-induced selective pressure on the adjacent *HIS4* gene in *Pichia pastoris*. *Eur Pharm J* **62** (2)**:** 43-50

Razaghi A, Karthikeyan OP, Hao HT, Heimann K (2016a) Hydrolysis treatments of fruit and vegetable waste for production of biofuel precursors. *Bioresour Technol* **217:** 100-3

Razaghi A, Owens L, Heimann K (2016b) Review of the recombinant human interferon gamma as an immunotherapeutic: Impacts of production platforms and glycosylation. *J Biotechnol* **240:** 48-60

Razaghi A, Tan E, Lua LH, Owens L, Karthikeyan OP, Heimann K (2017) Is *Pichia pastoris* a realistic platform for industrial production of recombinant human interferon gamma? *Biologicals* **45:** 52-60

Reddy PK, Reddy SG, Narala VR, Majee SS, Konda S, Gunwar S, Reddy RC (2007) Increased yield of high purity recombinant human interferon-gamma utilizing reversed phase column chromatography. *Protein Expr Purif* **52** (1)**:** 123-30

Rieder J, Jahnke R, Schloesser M, Seibel M, Czechowski M, Marth C, Hoffmann G (2001) Nitric Oxide-Dependent Apoptosis in Ovarian Carcinoma Cell Lines. *Gynecol Oncol* **82** (1)**:** 172-176

Rinderknecht E, O'Connor BH, Rodriguez H (1984) Natural human interferon-gamma. Complete amino acid sequence and determination of sites of glycosylation. *J Biol Chem* **259** (11)**:** 6790-7

Rodrigues ME, Costa AR, Henriques M, Cunnah P, Melton DW, Azeredo J, Oliveira R (2013) Advances and drawbacks of the adaptation to serum-free culture of CHO-K1 cells for monoclonal antibody production. *Appl Biochem Biotechnol* **169** (4)**:** 1279-91

Rojas Contreras JA, Pedraza-Reyes M, Ordonez LG, Estrada NU, Barba de la Rosa AP, De Leon-Rodriguez A (2010) Replicative and integrative plasmids for production of human interferon gamma in *Bacillus subtilis*. *Plasmid* **64** (3)**:** 170-6

Rosner D, Stoneman V, Littlewood T, McCarthy N, Figg N, Wang Y, Tellides G, Bennett M (2006) Interferon-gamma induces Fas trafficking and sensitization to apoptosis in vascular smooth muscle cells via a PI3K- and Akt-dependent mechanism. *Am J Pathol* **168** (6)**:** 2054-63

Rubio MaC, Runco R, Navarro AR (2002) Invertase from a strain of *Rhodotorula glutinis*. *Phytochemistry* **61** (6)**:** 605-609

Saeki K, Yuo A, Kato M, Miyazono K, Yazaki Y, Takaku F (1997) Cell density-dependent apoptosis in HL-60 cells, which is mediated by an unknown soluble factor, is inhibited by transforming growth factor 1 and overexpression of Bcl-2. *J Biol Chem* **272** (32)**:** 20003-20010

Saenge C, Cheirsilp B, Suksaroge TT, Bourtoom T (2011) Potential use of oleaginous red yeast *Rhodotorula glutinis* for the bioconversion of crude glycerol from biodiesel plant to lipids and carotenoids. *Process Biochem* **46** (1)**:** 210-218

Salunkhe S, Soorapaneni S, Prasad KS, Raiker VA, Padmanabhan S (2010) Strategies to maximize expression of rightly processed human interferon alpha2b in *Pichia pastoris*. *Protein Expr Purif* **71** (2)**:** 139-46

Samuel CE (2001) Antiviral actions of interferons. *Clin Microbiol Rev* **14** (4)**:** 778-809

Santín Cerezales M, Benítez JD (2011) Diagnosis of tuberculosis infection using interferon-γ-based assays. *Enfermedades Infecciosas y Microbiología Clínica* **29** (0)**:** 26-33

Sareneva T, Cantell K, Pyhala L, Pirhonen J, Julkunen I (1993) Effect of carbohydrates on the pharmacokinetics of human interferon-gamma. *J Interferon Res* **13** (4)**:** 267-9

Sareneva T, Mortz E, Tolo H, Roepstorff P, Julkunen I (1996) Biosynthesis and N-glycosylation of human interferon-gamma. Asn25 and Asn97 differ markedly in how efficiently they are glycosylated and in their oligosaccharide composition. *Eur J Biochem* **242** (2)**:** 191-200

Sareneva T, Pirhonen J, Cantell K, Julkunen I (1995) N-glycosylation of human interferon-γ: glycans at Asn-25 are critical for protease resistance. *Biochem J* **308:** 9-14

Satyanarayana T, Kunze G (2009) *Yeast biotechnology: diversity and applications*. Vol. 78: Springer

Scahill SJ, Devos R, Van der Heyden J, Fiers W (1983) Expression and characterization of the product of a human immune interferon cDNA gene in Chinese hamster ovary cells. *Proc Nat Acad Sci* **80** (15)**:** 4654-8

Schinske KA, Nyati S, Khan AP, Williams TM, Johnson TD, Ross BD, Tomas RP, Rehemtulla A (2011) A novel kinase inhibitor of FADD phosphorylation chemosensitizes through the inhibition of NF-kappaB. *Mol Cancer Ther* **10** (10)**:** 1807-17

Schneider T, Graeff-Hönninger S, French W, Hernandez R, Merkt N, Claupein W, Hetrick M, Pham P (2013a) Lipid and carotenoid production by oleaginous red yeast *Rhodotorula glutinis* cultivated on brewery effluents. *Energy*

Schneider T, Rempp T, Graeff-Hönninger S, French WT, Hernandez R, Claupein W (2013b) Utilization of soluble starch by oleaginous red yeast *Rhodotorula glutinis*. *J Sustainabl Bioenergy Syst* **3:** 57-63

Schroder K, Hertzog PJ, Ravasi T, Hume DA (2004) Interferon-gamma: an overview of signals, mechanisms and functions. *J Leukoc Biol* **75** (2)**:** 163-89

Schroeder SJ (2009) Advances in RNA structure prediction from sequence: new tools for generating hypotheses about viral RNA structure-function relationships. *J Virol* **83** (13)**:** 6326-34

Sheehan KB, McInnerney K, Purevdorj-Gage B, Altenburg SD, Hyman LE (2007) Yeast genomic expression patterns in response to low-shear modeled microgravity. *BMC Genomics* **8:** 3

Shi L, Wang D, Chan W, Cheng L (2007) Efficient expression and purification of human interferon alpha2b in the methylotrophic yeast, *Pichia pastoris*. *Protein Expr Purif* **54** (2)**:** 220-6

Shi XJ, Wang B, Zhang C, Wang M (2006) Expressions of bovine IFN-gamma and foot-and-mouth disease VP1 antigen in *P. pastoris* and their effects on mouse immune response to FMD antigens. *Vaccine* **24** (1)**:** 82-9

Siegel RL, Miller KD, Jemal A (2015) Cancer statistics, 2015. *CA Cancer J Clin* **65** (1)**:** 5-29

Sinha J, Plantz BA, Inan M, Meagher MM (2005) Causes of proteolytic degradation of secreted recombinant proteins produced in methylotrophic yeast *Pichia pastoris*: case study with recombinant ovine interferon-tau. *Biotechnol Bioeng* **89** (1)**:** 102-12

Skoko N, Argamante B, Grujicic NK, Tisminetzky SG, Glisin V, Ljubijankic G (2003) Expression and characterization of human interferon-beta1 in the methylotrophic yeast *Pichia pastoris*. *Biotechnol Appl Biochem* **38** (Pt 3)**:** 257-65

Sola RJ, Griebenow K (2010) Glycosylation of therapeutic proteins: an effective strategy to optimize efficacy. *BioDrugs* **24** (1)**:** 9-21

Sproul D, Gilbert N, Bickmore WA (2005) The role of chromatin structure in regulating the expression of clustered genes. *Nat Rev Genet* **6** (10)**:** 775-81

Takaoka A, Yanai H (2006) Interferon signalling network in innate defence. *Cell Microbiol* **8** (6)**:** 907-22

Tang D, Lotze MT, Kang R, Zeh HJ (2011) Apoptosis promotes early tumorigenesis. *Oncogene* **30** (16)**:** 1851-4

Thapa RJ, Basagoudanavar SH, Nogusa S, Irrinki K, Mallilankaraman K, Slifker MJ, Beg AA, Madesh M, Balachandran S (2011) NF-kappaB protects cells from gamma interferon-induced RIP1-dependent necroptosis. *Mol Cell Biol* **31** (14)**:** 2934-46

Thill GP, Davis GR (1989) Expression of interferon-gamma in methylotrophic yeasts: Google Patents

Topalian SL, Wolchok JD, Chan TA, Mellman I, Palucka K, Banchereau J, Rosenberg SA, Dane Wittrup K (2015) Immunotherapy: The path to win the war on cancer? *Cell* **161** (2)**:** 185-6

Tsiouris SJ, Coetzee D, Toro PL, Austin J, Stein Z, El-Sadr W (2006) Sensitivity analysis and potential uses of a novel gamma interferon release assay for diagnosis of tuberculosis. *J Clin Microbiol* **44** (8)**:** 2844-50

Tsygankov MA, Zobnina AE, Padkina MV (2014) Synthesis of recombinant gamma interferons resistant to proteolysis in the yeast *Pichia pastoris*. *Appl Biochem Microbiol* **50** (4)**:** 387-393

Vadrot N, Legrand A, Nello E, Bringuier AF, Guillot R, Feldmann G (2006) Inducible nitric oxide synthase (iNOS) activity could be responsible for resistance or sensitivity to IFN-gamma-induced apoptosis in several human hepatoma cell lines. *J Interferon Cytokine Res* **26** (12)**:** 901-13

Vaiphei ST, Pandey G, Mukherjee KJ (2009) Kinetic studies of recombinant human interferon-gamma expression in continuous cultures of *E. coli*. *J Ind Microbiol Biotechnol* **36** (12)**:** 1453-8

Valencia Jiménez A, Wang H, Siegfried BD (2014) Expression and characterization of a recombinant endoglucanase from western corn rootworm, in *Pichia pastoris*. *J Insect Sci* **14** (1)**:** 242

Valenzuela L, Dhillon N, Dubey RN, Gartenberg MR, Kamakaka RT (2008) Long-range communication between the silencers of HMR. *Mol Cell Biol* **28** (6)**:** 1924-35

Van Dijken JP, Harder W (1975) Growth yields of microorganisms on methanol and methane. A theoretical study. *Biotechnol Bioeng* **17** (1)**:** 15-30

Vandenbroeck K, Martens E, D'Andrea S, Billiau A (1993) Refolding and single-step purification of porcine interferon-gamma from *Escherichia coli* inclusion bodies. Conditions for reconstitution of dimeric IFN-gamma. *Eur J Biochem* **215** (2)**:** 481-6

Varedi S, Shojaosadati S, Babaeipour V, Ghaemi N (2006) Physiological and morphological changes of recombinant *E. coli* during over-expression of human interferon-g in HCDC. *Iran J Biotechnol* **4** (4)**:** 230-238

Varki A (1993) Biological roles of oligosaccharides: all of the theories are correct. *Glycobiology* **3** (2)**:** 97-130

Varki A (2017) Biological roles of glycans. *Glycobiology* **27** (1)**:** 3-49

Vesenbeckh SM, Schonfeld N, Mauch H, Bergmann T, Wagner S, Bauer TT, Russmann H (2012) The use of interferon gamma release assays in the diagnosis of active tuberculosis. *Tuberc Res Treat* **2012:** 768723

Vial T, Descotes J (1994) Clinical toxicity of the interferons. *Drug-Safety* **10** (2)**:** 115-50

Vilcek J (2003) Novel interferons. *Nat immunol* **4** (1)**:** 8-9

Vink T, Oudshoorn-Dickmann M, Roza M, Reitsma JJ, de Jong RN (2014) A simple, robust and highly efficient transient expression system for producing antibodies. *Methods* **65** (1)**:** 5-10

Vivo C, Levy F, Pilatte Y, Fleury-Feith J, Chretien P, Monnet I, Kheuang L, Jaurand MC (2001) Control of cell cycle progression in human mesothelioma cells treated with gamma interferon. *Oncogene* **20** (9)**:** 1085-93

Wade CH, Umbarger MA, McAlear MA (2006) The budding yeast rRNA and ribosome biosynthesis (RRB) regulon contains over 200 genes. *Yeast* **23** (4)**:** 293-306

Wall L, Burke F, Barton C, Smyth J, Balkwill F (2003) IFN-gamma induces apoptosis in ovarian cancer cells *in vivo* and *in vitro*. *Clin Cancer Res* **9** (7)**:** 2487-96

Walter MR, Windsor WT, Nagabhushan TL, Lundell DJ, Lunn CA, Zauodny PJ, Narula SK (1995) Crystal structure of a complex between interferon-gamma and its soluble high-affinity receptor. *Nature* **376** (6537)**:** 230-5

Wang D, Ren H, Xu JW, Sun PD, Fang XD (2014) Expression, purification and characterization of human interferon-gamma in *Pichia pastoris*. *Mol Med Rep* **9** (2)**:** 715-9

Wang S, Xub H, Dengb Y (2009) The antiproliferative activity of combination treatment of IFN-γ and doxorubicin on H22 cells: *in vitro* and *in vivo*. *Cancer Ther* **9:** 10

Waschutza G, Li V, Schafer T, Schomburg D, Villmann C, Zakaria H, Otto B (1996) Engineered disulfide bonds in recombinant human interferon-gamma: the impact of the N-terminal helix A and the AB-loop on protein stability. *Protein engineering* **9** (10)**:** 905-12

Welander CE, Homesley HD, Reich SD, Levin EA (1988) A phase II study of the efficacy of recombinant interferon gamma in relapsing ovarian adenocarcinoma. *Am J Clin Oncol* **11** (4)**:** 465-469

Welch M, Villalobos A, Gustafsson C, Minshull J (2009) You're one in a googol: optimizing genes for protein expression. *J R Soc Interface* **6** (6 (Suppl 4))**:** S468-S476

Wiesenfeld M, O'Connell M, Wieand H, Gonchoroff N, Donohue J, Fitzgibbons R, Jr, Krook J, Mailliard J, Gerstner J, Pazdur R (1995) Controlled clinical trial of interferon-gamma as postoperative surgical adjuvant therapy for colon cancer. *J Clin Oncol* **13** (9)**:** 2324-2329

Williams EJ, Bowles DJ (2004) Coexpression of neighboring genes in the genome of Arabidopsis thaliana. *Genome Res* **14** (6)**:** 1060-7

Windbichler GH, Hausmaninger H, Stummvoll W, Graf AH, Kainz C, Lahodny J, Denison U, Muller-Holzner E, Marth C (2000) Interferon-gamma in the first-line therapy of ovarian cancer: a randomized phase III trial. *Brit J Cancer* **82** (6)**:** 1138-44

Wolf H, Hanson R (1980) Identification of methane-utilizing yeasts. *FEMS Microbiol Let* **7** (2)**:** 177-179

Wolf HJ, Christiansen M, Hanson RS (1980) Ultrastructure of methanotrophic yeasts. *J Bacteriol* **141** (3)**:** 1340-9

Wolf HJ, Hanson RS (1979) Isolation and characterization of methane-utilizing yeasts. *J General Microbiol* **114** (1)**:** 187-194

Xie FJ, Zhao P, Zhang YP, Liu FY, Nie XL, Zhu YH, Yu XM, Zheng QQ, Mao WM, Lu HY, Wei H, Huang W (2013) Adenovirus-mediated interferon-gamma gene therapy induced human pancreatic carcinoma Capan-2 cell apoptosis *in vitro* and *in vivo*. *Anat Rec (Hoboken)* **296** (4)**:** 604-10

Xu X, Fu XY, Plate J, Chong AS (1998) IFN-gamma induces cell growth inhibition by Fas-mediated apoptosis: requirement of STAT1 protein for up-regulation of Fas and FasL expression. *Cancer research* **58** (13)**:** 2832-7

Xue F, Miao J, Zhang X, Luo H, Tan T (2008) Studies on lipid production by *Rhodotorula glutinis* fermentation using monosodium glutamate wastewater as culture medium. *Bioresour Technol* **99** (13)**:** 5923-7

Yang S, Kuang Y, Li H, Liu Y, Hui X, Li P, Jiang Z, Zhou Y, Wang Y, Xu A, Li S, Liu P, Wu D (2013) Enhanced production of recombinant secretory proteins in *Pichia pastoris* by optimizing Kex2 P1' site. *PLoS One* **8** (9)**:** e75347

Yao Q, Huang Q, Cao Y, Si Y (2008) Secreting expression of porcine interferon-gamma in *Pichia pastoris* and its antiviral activity *Chinese Journal of Veterinary Science* **4:** 029

Yip YK, Barrowclough BS, Urban C, Vilcek J (1982) Purification of two subspecies of human gamma (immune) interferon. *Proc Nat Acad Sci* **79** (6)**:** 1820-4

Younes HM, Amsden BG (2002) Interferon-gamma therapy: evaluation of routes of administration and delivery systems. *J Pharm Sci* **91** (1)**:** 2-17

Young Ha, Hardy KJ (1995) Role of interferon-y in immune cell regulation. *J Leukocyte Biol* **58:** 373-381

Yphantis DA, Arakawa T (1987) Sedimentation equilibrium measurements of recombinant DNA derived human interferon gamma. *Biochemistry* **26** (17)**:** 5422-7

Yu QW, Li NL, Nie H, Ma AL, Xi B, Gong Y, Zhang DQ (2003) Purification and identification of human recombinant IFN-beta expressed in yeast *Pichia pastoris*. *Sheng wu hua xue yu sheng wu wu li xue bao Acta biochimica et biophysica Sinica* **35** (11)**:** 1035-9

Yurimoto H, Oku M, Sakai Y (2011) Yeast methylotrophy: metabolism, gene regulation and peroxisome homeostasis. *Int J Microbiol* **2011:** 101298

Zaidi MR, Merlino G (2011) The two faces of interferon-gamma in cancer. *Clin Cancer Res* **17** (19)**:** 6118-24

Zaman Z, Bowman SB, Kornfeld GD, Brown AJ, Dawes IW (1999) Transcription factor GCN4 for control of amino acid biosynthesis also regulates the expression of the gene for lipoamide dehydrogenase. *Biochemic J* **340** (Pt 3)**:** 855-862

Zhang Z, Tong KT, Belew M, Pettersson T, Janson JC (1992) Production, purification and characterization of recombinant human interferon gamma. *J Chromatogr* **604** (1)**:** 143-55

Zhao P, Zhu YH, Wu JX, Liu RY, Zhu XY, Xiao X, Li HL, Huang BJ, Xie FJ, Chen JM, Ke ML, Huang W (2007) Adenovirus-mediated delivery of human IFNgamma gene inhibits prostate cancer growth. *Life Sci* **81** (9)**:** 695-701

Zhong X, Somers W (2012) *Recent advances in glycosylation modifications in the context of therapeutic glycoproteins*. Shanghai: INTECH Open Access Publisher

Zuo Y, Wu J, Xu Z, Yang S, Yan H, Tan L, Meng X, Ying X, Liu R, Kang T, Huang W (2011) Minicircle-oriP-IFNgamma: a novel targeted gene therapeutic system for EBV positive human nasopharyngeal carcinoma. *PLoS ONE* **6** (5)**:** e19407

Zwerling A, van den Hof S, Scholten J, Cobelens F, Menzies D, Pai M (2012) Interferon-gamma release assays for tuberculosis screening of healthcare workers: a systematic review. *Thorax* **67** (1)**:** 62-70